

Technical University of Civil Engineering



124 Lacul Tei Blvd., sector 2, Bucharest, Romania

STUDY ON EARLY EARTHQUAKE DAMAGE EVALUATION
OF EXISTING BUILDINGS IN BUCHAREST, ROMANIA

Draft Report prepared by:

Technical University of Civil Engineering, Bucharest

Draft Report prepared for:

Building Research Institute

&

International Institute for Seismology and Earthquake Engineering,

Tsukuba, Japan

MARCH 2006



Table of Content

| | |
|--|-----------|
| 1. Vulnerability/Fragility Characteristics for Representative Building Types..... | 3 |
| 1.1 Description of Model Building Types..... | 3 |
| 1.2 Capacity Curves | 3 |
| 1.3 Fragility Curves..... | 10 |
| 1.3.1 Background | 10 |
| 1.3.2 Development of Damage State Medians | 11 |
| 1.3.3 Development of Damage State Variability | 11 |
| 1.3.4 Structural Damage..... | 14 |
| References Chapter 1..... | 17 |
| 2. Development of Seismic Risk Scenarios | 18 |
| 2.1 Introduction | 18 |
| 2.2 Direct physical losses estimation; debris..... | 19 |
| 2.3 Casualties and homeless estimation | 23 |
| 2.4 Direct economic losses | 28 |
| 2.5 Risk management | 30 |
| References Chapter 2..... | 36 |
| Annex A: Tables..... | 38 |
| Annex B: Case study | 44 |
| 3. Full Probabilistic Risk Assessment of Current Buildings..... | 57 |
| 3.1 Introduction | 57 |
| 3.2 Probabilistic seismic hazard assessment | 58 |
| 3.3 Probabilistic assessment of seismic structural response..... | 60 |
| 3.3.1 The structural model..... | 60 |
| 3.3.2 Ground motions..... | 61 |
| 3.3.3 Non-linear dynamic analyses | 61 |
| 3.3.4 Probabilistic assessment of seismic structural vulnerability | 63 |
| 3.3.5 Risk analysis..... | 66 |
| 3.4 Conclusions | 67 |
| References Chapter 3..... | 67 |



1. Vulnerability/Fragility Characteristics for Representative Building Types

1.1 Description of Model Building Types

Table 1.1 lists the model building types included in this study and considered to be representative for Bucharest building stock.

Table 1.1 Model Building Types

| No. | Label | Description | Height | | | |
|-----|-------|------------------------------|-----------|---------|---------|--------|
| | | | Range | | Typical | |
| | | | Name | Stories | Stories | Meters |
| 1 | RC1L | Concrete Moment Frame | Low-Rise | 1 - 3 | 2 | 5.7 |
| 2 | RC1M | | Mid-Rise | 4 - 7 | 6 | 17.1 |
| 3 | RC1H | | High-Rise | 8+ | 10 | 28.5 |
| 4 | RC2L | Concrete Shear Walls | Low-Rise | 1 - 3 | 2 | 5.7 |
| 5 | RC2M | | Mid-Rise | 4 - 7 | 6 | 17.1 |
| 6 | RC2H | | High-Rise | 8+ | 10 | 28.5 |

1.2 Capacity Curves

A building capacity curve (also known as a push-over curve) is a plot of a building's lateral load resistance as a function of a characteristic lateral displacement (i.e., a force-deflection plot). It is derived from a plot of static-equivalent base shear versus building (e.g., roof) displacement. In order to facilitate direct comparison with earthquake demand (i.e. overlaying the capacity curve with a response spectrum), the force (base shear) axis is converted to spectral acceleration and the displacement axis is converted to spectral displacement.

The building capacity curves developed are based on engineering design parameters and judgment. Three control points that define model building capacity describe each curve:

- Design Capacity
- Yield Capacity
- Ultimate Capacity

Design capacity represents the nominal building strength required by current model seismic code provisions or an estimate of the nominal strength for buildings not designed for earthquake loads.

Yield capacity represents the true lateral strength of the building considering redundancies in design, conservatism in code requirements and true (rather than nominal) strength of materials. Ultimate capacity represents the maximum strength of the building when the global structural system has reached a fully plastic state. Ultimate capacity implicitly accounts for loss of strength due to shear failure of brittle elements. Typically, buildings are assumed capable of deforming beyond their ultimate point without loss of stability, but their structural system provides no additional resistance to lateral earthquake force.

Up to the yield point, the building capacity curve is assumed to be linear with stiffness based on an estimate of the true period of the building. The true period is typically longer than the code-specified period of the building due to flexing of diaphragms of short, stiff buildings, flexural cracking of elements of concrete and masonry structures, flexibility of foundations and other factors observed to affect building stiffness. From the yield point to the ultimate point, the capacity curve transitions in slope from an essentially elastic state to a fully plastic state. The

capacity curve is assumed to remain plastic past the ultimate point. An example building capacity curve is shown in Figure 1.1.

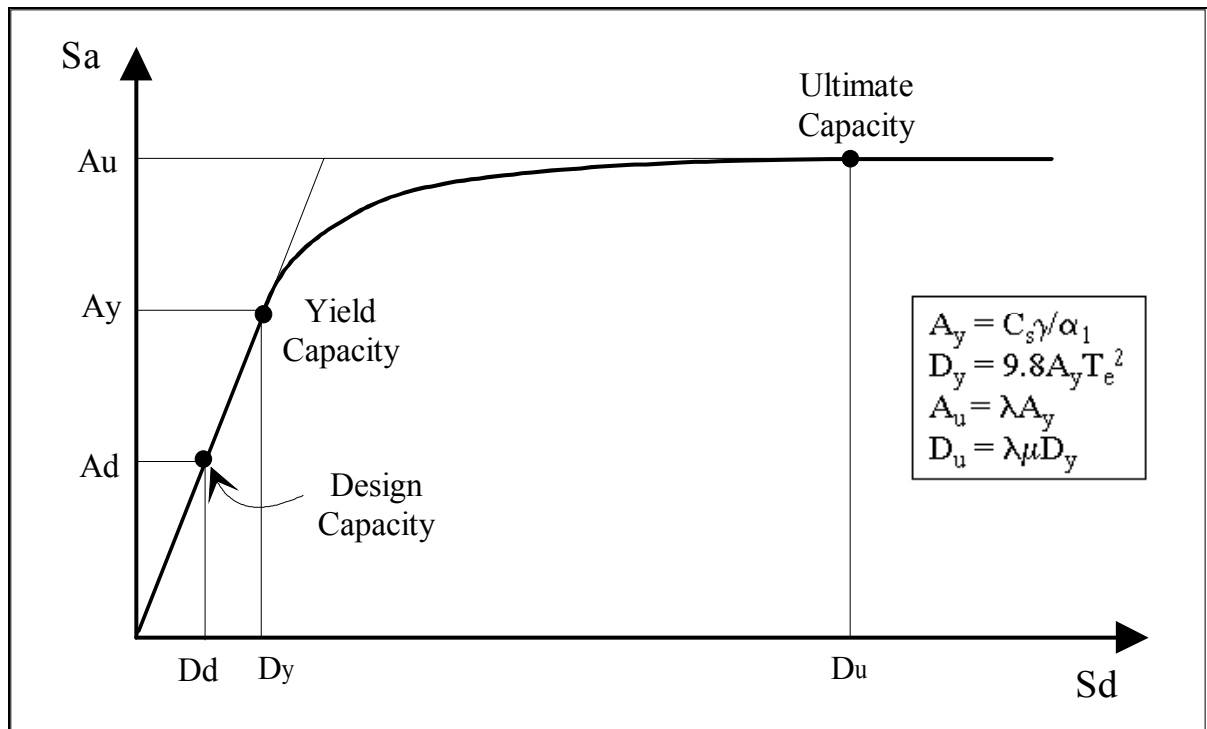


Figure 1.1 Example Building Capacity Curve

The building capacity curves are constructed based on estimates of engineering properties that affect the design, yield and ultimate capacities of each model building type. These properties are defined by the following parameters, Figure 1.1:

- C_s design strength coefficient (fraction of building's weight),
- T_e true "elastic" fundamental-mode period of building (seconds),
- α_1 fraction of building weight effective in push-over mode,
- α_2 fraction of building height at location of push-over mode displacement,
- γ "overstrength" factor relating "true" yield strength to design strength,
- λ "overstrength" factor relating ultimate strength to yield strength, and
- μ "ductility" factor relating ultimate displacement to λ times the yield displacement (i.e., assumed point of significant yielding of the structure)

The design strength, C_s is based on the lateral-force design requirements of seismic codes. These requirements are a function of the building's seismic zone location and other factors including type of lateral-force-resisting system and building period.

The major developments in four generations of seismic codes in Romania can be described as follows:

- | | |
|---|--|
| Pre-code period (prior to 1941/45): 1941 Draft Instructions 1945 Instructions | <ul style="list-style-type: none"> • Development of first national seismic code after the 1940 earthquake: lateral seismic force was 5% of building weight. |
|---|--|

Low-code period (1963- 1977):

- | | |
|--------|--|
| P13-63 | <ul style="list-style-type: none"> • Control period of response spectra $T_C=0.3$ s • Maximum dynamic amplification $DAF = \max SA/PGA = 3$ SA - structure absolute acceleration response spectra. |
| P13-70 | <ul style="list-style-type: none"> • Control period of response spectra $T_C=0.4$ s • Max. dynamic amplification $DAF = 2$ • Some ductility rules for RC frames. |

Moderate-code period (1978 - 1990):

- | | |
|---------|--|
| P100-78 | <ul style="list-style-type: none"> • Development of the first seismic code based on the unique strong ground motion recorded in soft soil of Bucharest during March 4, 1977 event: $PGA = 0.2g$ and the long predominant period of ground vibration was $T_p = 1.6s$. |
| P100-81 | <ul style="list-style-type: none"> • Control period of response spectra $T_C=1.5$ s • Maximum dynamic amplification $DAF = 2$ • Ductility rules for RC shear wall & frame structures. |

Moderate to High-code period (1990-present):

- | | |
|---------|---|
| P100-90 | <ul style="list-style-type: none"> • Control period of response spectra $T_C=1.5$ s |
| P100-92 | <ul style="list-style-type: none"> • Maximum dynamic amplification $DAF = 2.5$ • Advanced ductility rules for RC shear wall and frame structures and for steel structures. |

The history of overall seismic design coefficient, C_s for shear wall and frames structures in Bucharest, according to Romanian seismic codes during the time interval 1940-2002 is presented in Figure 1.2. The geometry of C_s is self explanatory. One may note the gap of the C_s for flexible buildings and structures during the period 1963-1978. However, even for rigid structures built during that period, the maximum C_s was about 2/3 of the present day C_s .

It is emphasised that after the 1977 event, new ductility rules for RC structures were imported from *US* practice and incorporated into Romanian seismic codes, *P100*. According to the *EUROCODE 8* requirements the rules were significantly improved after 1989.

Table 1.2 summarizes design capacity for each building type and design level. Building period, T_e , push-over mode parameters α_1 and α_2 , the ratio of yield to design strength, γ , and the ratio of ultimate to yield strength, λ , are assumed to be independent of design level. Values of these parameters are summarized in Tables 1.3a&b for each building type. Values of the “ductility” factor, μ , are given in Table 1.4 for each building type and design level. The values are given only for medium and high-rise RC buildings considered to be representative for Bucharest.

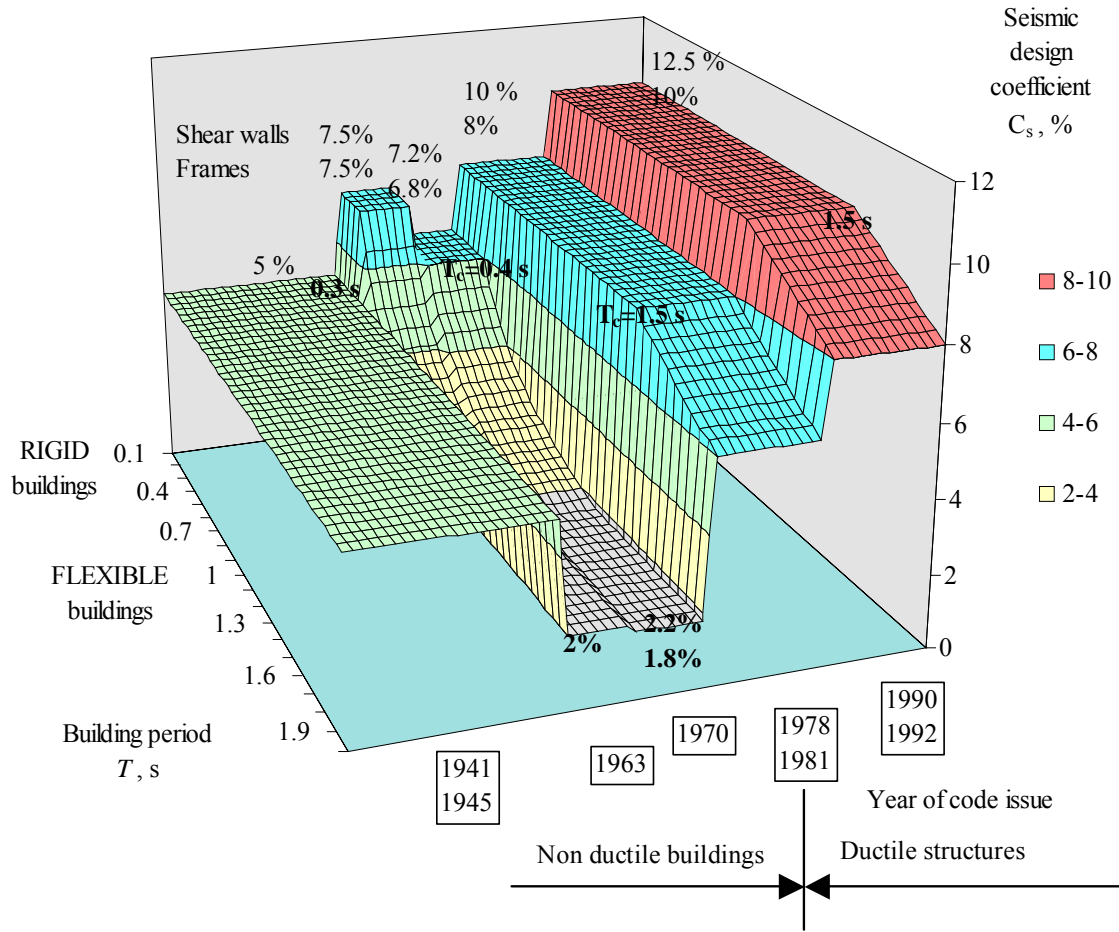


Figure 1.2 Evolution of seismic design coefficient in Bucharest during period 1940-2002

Table 1.2 Code Building Capacity Parameters - Design Strength (C_s)

| Building Type | Seismic Design Level (Percentage of Building Weight) | | | | |
|---------------|--|-----------|-----------|-----------|-----------|
| | 1941-1962 | 1963-1969 | 1970-1977 | 1978-1989 | 1990-2002 |
| RC1M | 5 | 3.21 | 3.4 | 8 | 10 |
| RC1H | 5 | 2.25 | 2.4 | 8 | 10 |
| RC2M | 5 | 7.71 | 7.2 | 10 | 12.5 |
| RC2H | 5 | 4.15 | 4.4 | 10 | 12.5 |

Table 1.3a Code Building Capacity Parameters - Period (T_e), Pushover Mode Response Factors (α_1, α_2) and Overstrength Ratios (γ, λ) - 1941-1977

| Building Type | Height to Roof (m) | Period, T_e (Sec) | Modal Factors | | Overstrength Ratios | |
|---------------|--------------------|---------------------|--------------------|--------------------|---------------------|---------------------|
| | | | Weight, α_1 | Height, α_2 | Yield, γ | Ultimate, λ |
| RC1M | 17.1 | 0.7 | 0.85 | 0.6 | 1.4 | 1.5 |
| RC1H | 28.5 | 1 | 0.75 | 0.6 | 1.4 | 1.5 |
| RC2M | 17.1 | 0.4 | 0.9 | 0.7 | 1.4 | 1.5 |
| RC2H | 28.5 | 0.7 | 0.8 | 0.7 | 1.4 | 1.5 |



Table 1.3b Code Building Capacity Parameters - Period (T_e), Pushover Mode Response Factors (α_1, α_2) and Overstrength Ratios (γ, λ) - 1978-2002

| Building Type | Height to Roof (m) | Period, T_e (Sec) | Modal Factors | | Overstrength Ratios | |
|---------------|--------------------|---------------------|--------------------|--------------------|---------------------|---------------------|
| | | | Weight, α_1 | Height, α_2 | Yield, γ | Ultimate, λ |
| RC1M | 17.1 | 0.6 | 0.85 | 0.6 | 1.5 | 2 |
| RC1H | 28.5 | 0.85 | 0.75 | 0.6 | 1.5 | 2 |
| RC2M | 17.1 | 0.35 | 0.9 | 0.7 | 1.5 | 2 |
| RC2H | 28.5 | 0.6 | 0.8 | 0.7 | 1.5 | 2 |

Table 1.4 Code Building Capacity Parameter - Ductility (μ)

| Building Type | Seismic Design Level (Percentage of Building Weight) | | | | |
|---------------|--|-----------|-----------|-----------|-----------|
| | 1941-1962 | 1963-1969 | 1970-1977 | 1978-1989 | 1990-2002 |
| RC1M | 2 | 3 | 3 | 5 | 5 |
| RC1H | 2 | 3 | 3 | 5 | 5 |
| RC2M | 2 | 3 | 3 | 4 | 4 |
| RC2H | 2 | 3 | 3 | 4 | 4 |

Building capacity curves are assumed to have a range of possible properties that are lognormally distributed. Capacity curves described by the values of parameters given in Tables 1.2, 1.3 and 1.4 represent median estimates of building capacity.

Tables 1.5a, 1.5b, 1.5c, 1.5d and 1.5e summarize yield capacity and ultimate capacity control points.

Table 1.5a Code Building Capacity Curves - 1941-1962

| Building Type | Yield Capacity Point | | Ultimate Capacity Point | |
|---------------|----------------------|-----------|-------------------------|-----------|
| | D_y (cm) | A_y (g) | D_u (cm) | A_u (g) |
| RC1M | 1.00 | 0.082 | 3.01 | 0.124 |
| RC1H | 2.32 | 0.093 | 6.96 | 0.140 |
| RC2M | 0.31 | 0.078 | 0.93 | 0.117 |
| RC2H | 1.07 | 0.088 | 3.20 | 0.131 |

Table 1.5b Code Building Capacity Curves - 1963-1969

| Building Type | Yield Capacity Point | | Ultimate Capacity Point | |
|---------------|----------------------|-----------|-------------------------|-----------|
| | D_y (cm) | A_y (g) | D_u (cm) | A_u (g) |
| RC1M | 0.64 | 0.053 | 2.90 | 0.079 |
| RC1H | 1.04 | 0.042 | 4.70 | 0.063 |
| RC2M | 0.48 | 0.120 | 2.15 | 0.180 |
| RC2H | 0.88 | 0.073 | 3.98 | 0.109 |



Table 1.5c Code Building Capacity Curves - 1970-1977

| Building Type | Yield Capacity Point | | Ultimate Capacity Point | |
|---------------|----------------------|-----------|-------------------------|-----------|
| | D_y (cm) | A_y (g) | D_u (cm) | A_u (g) |
| RC1M | 0.68 | 0.056 | 3.07 | 0.084 |
| RC1H | 1.11 | 0.045 | 5.01 | 0.067 |
| RC2M | 0.45 | 0.112 | 2.00 | 0.168 |
| RC2H | 0.94 | 0.077 | 4.22 | 0.116 |

Table 1.5d Code Building Capacity Curves - 1978-1989

| Building Type | Yield Capacity Point | | Ultimate Capacity Point | |
|---------------|----------------------|-----------|-------------------------|-----------|
| | D_y (cm) | A_y (g) | D_u (cm) | A_u (g) |
| RC1M | 1.26 | 0.141 | 12.63 | 0.282 |
| RC1H | 2.87 | 0.160 | 28.73 | 0.320 |
| RC2M | 0.51 | 0.167 | 4.06 | 0.333 |
| RC2H | 1.68 | 0.188 | 13.42 | 0.375 |

Table 1.5e Code Building Capacity Curves - 1990-2002

| Building Type | Yield Capacity Point | | Ultimate Capacity Point | |
|---------------|----------------------|-----------|-------------------------|-----------|
| | D_y (cm) | A_y (g) | D_u (cm) | A_u (g) |
| RC1M | 1.58 | 0.176 | 15.79 | 0.353 |
| RC1H | 3.59 | 0.200 | 35.91 | 0.400 |
| RC2M | 0.63 | 0.208 | 5.07 | 0.417 |
| RC2H | 2.10 | 0.234 | 16.77 | 0.469 |

The values of yielding and ultimate displacement and acceleration given in Tables 1.5a to 1.5e are represented in Figures 1.3, 1.4, 1.5 and 1.6 for building types *RC1H* and *RC2H*.

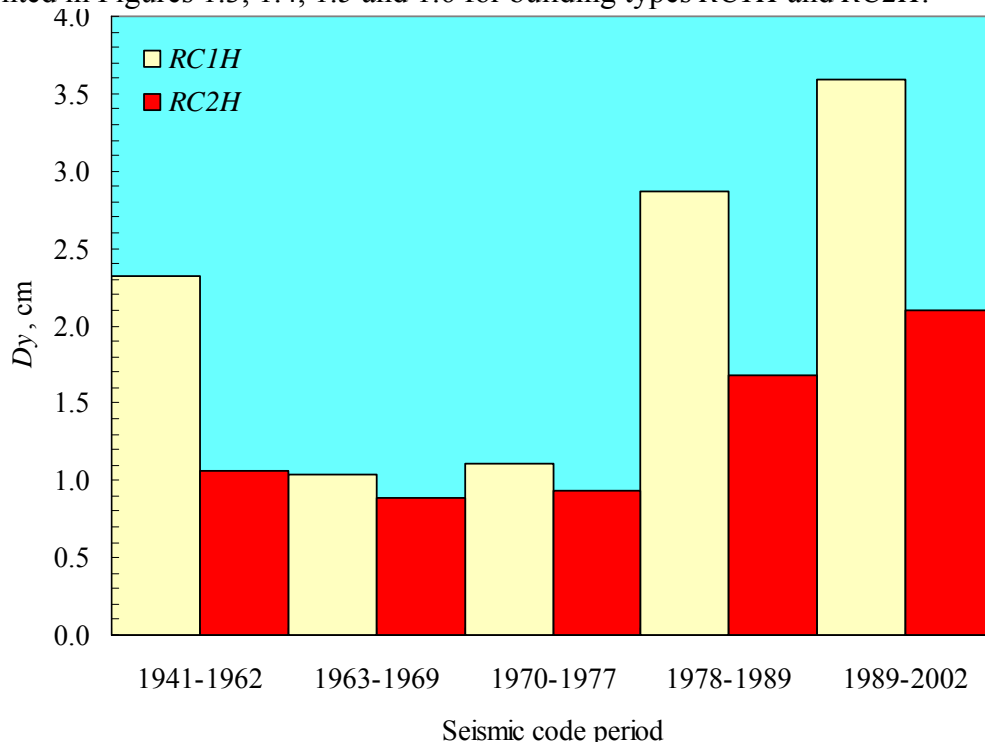


Figure 1.3. Yielding displacement according to seismic code period

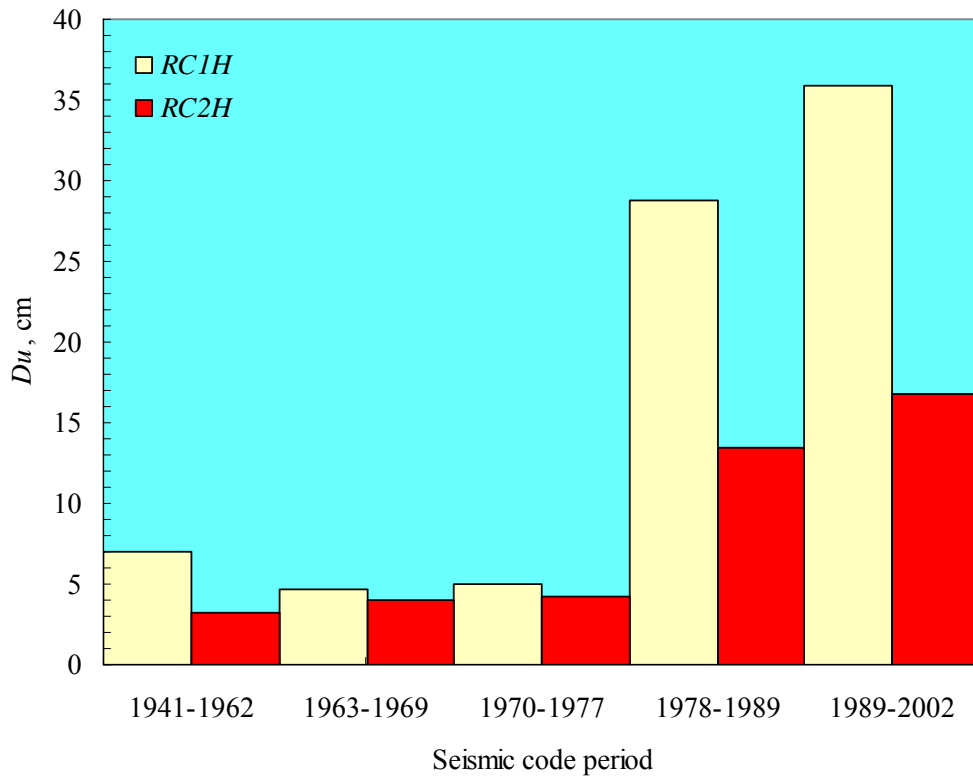


Figure 1.4. Ultimate displacement according to seismic code period

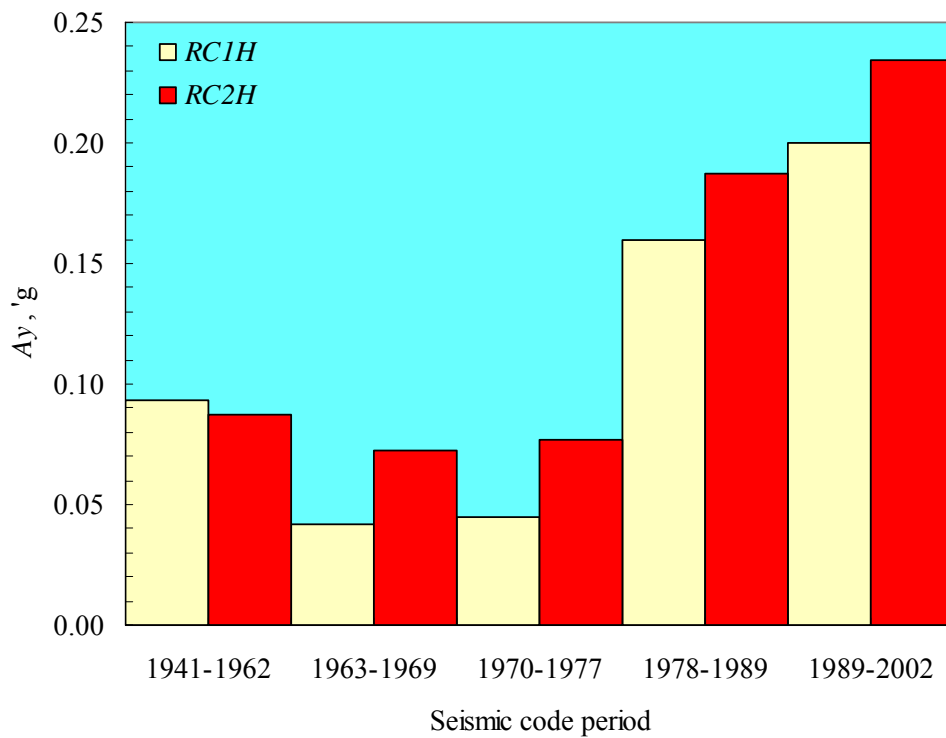


Figure 1.5. Yielding acceleration according to seismic code period

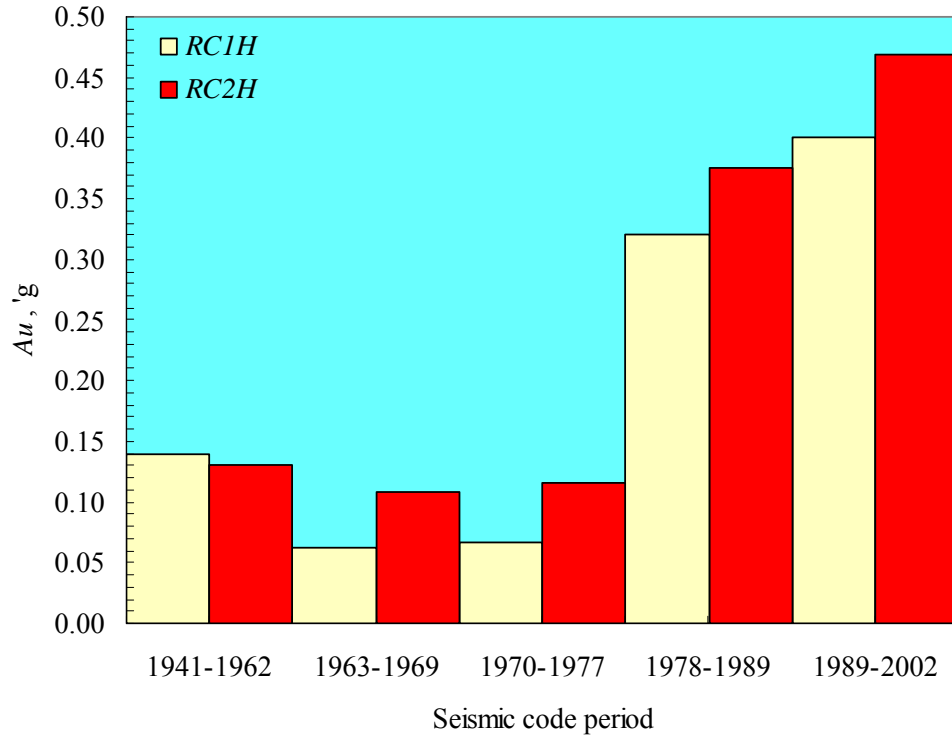


Figure 1.6. Ultimate acceleration according to seismic code period

1.3 Fragility Curves

This section describes building fragility curves for Slight, Moderate, Extensive and Complete structural damage states. Each fragility curve is characterized by median and lognormal standard deviation (β) values.

1.3.1 Background

The probability of being in or exceeding a given damage state is modeled as a cumulative lognormal distribution. For structural damage, given the spectral displacement, S_d , the probability of being in or exceeding a damage state, ds , is modeled as:

$$P[ds|S_d] = \Phi \left[\frac{1}{\beta_{ds}} \ln \left(\frac{S_d}{\bar{S}_{d,ds}} \right) \right] \quad (1-1)$$

where: $\bar{S}_{d,ds}$ is the median value of spectral displacement at which the building reaches the threshold of the damage state, ds ,
 β_{ds} is the standard deviation of the natural logarithm of spectral displacement of damage state, ds , and
 Φ is the standard normal cumulative distribution function.

1.3.2 Development of Damage State Medians

Median values of fragility curves are developed for each damage states (i.e., Slight, Moderate, Extensive and Complete). Structural fragility is characterized in terms of spectral displacement.

Median values of structural component fragility are based on building drift ratios that describe the threshold of damage states. Damage-state drift ratios are converted to spectral displacement using Equation (1-2):

$$\bar{S}_{d,Sds} = \delta_{R,Sds} \cdot \alpha_2 \cdot h \quad (1-2)$$

where: $\bar{S}_{d,Sds}$ is the median value of spectral displacement, in cm, of structural components for damage state, ds,
 $\delta_{R,Sds}$ is the drift ratio at the threshold of structural damage state, ds,
 α_2 is the fraction of the building (roof) height at the location of push-over mode displacement, as specified in Tables 1.6, and
 h is the typical roof height, in centimeters, of the model building type of interest (see Table 1.1 for typical building height).

For calibration of the drift ratio at the threshold of structural damage state one used a slightly modified version of the Park&Ang damage index, in which the recoverable deformation is removed from the first term, Eq. 1-3:

$$DI = \frac{D_m - D_y}{D_u - D_y} + \beta_\epsilon \cdot \frac{\int dE}{F_y \cdot D_u} \quad (1-3)$$

where D_m = maximum displacement attained during load history; D_u = ultimate displacement; D_y = yielding displacement; β_ϵ = strength degrading parameter; F_y = yielding force and E = dissipated hysteretic energy.

To obtain discrete damage states, ranges for the above-mentioned damage index need to be specified. In this respect the following classification suggested by Park, Ang & Wen was adapted:

| Range of damage index | Damage state |
|-----------------------|--------------|
| $DI \leq 0.1$ | None |
| $0.1 < DI \leq 0.25$ | Slight |
| $0.20 < DI \leq 0.40$ | Moderate |
| $0.40 < DI < 1.00$ | Extensive |
| $DI \geq 1.00$ | Complete |

The roof displacement at threshold of damage states is obtained using the values of the damage index at threshold of damage states and Equation 1-3. Finally, drift ratio at the threshold of structural damage state is computed by normalizing the roof displacement by the roof height.

1.3.3 Development of Damage State Variability

Lognormal standard deviation (β) values that describe the variability of fragility curves are developed for each damage states (i.e., Slight, Moderate, Extensive and Complete).

The total variability of each structural damage state, β_{Sds} , is modeled by the combination of three contributors to structural damage variability, β_C , β_D and $\beta_{M(Sds)}$, as described in Equation (1-4):

$$\beta_{Sds} = \sqrt{\beta_C^2 + \beta_D^2 + (\beta_{M(Sds)})^2} \quad (1-4)$$

where:

- β_{Sds} is the lognormal standard deviation that describes the total variability for structural damage state, ds,
- β_C is the lognormal standard deviation parameter that describes the variability of the capacity curve,
- β_D is the lognormal standard deviation parameter that describes the variability of the demand spectrum,
- $\beta_{M(Sds)}$ is the lognormal standard deviation parameter that describes the uncertainty in the estimate of the median value of the threshold of structural damage state, ds.

The variability of building response depends on demand and capacity (since capacity curves are nonlinear). Demand spectra and capacity curves are described probabilistically by median properties and variability parameters, β_D and β_C , respectively.

The variability in capacity properties of the model building type is increasing as the structure is undergoing larger inelastic deformations. This assumption is supported by the results given in Figure 1.7 and 1.8. The variability of the capacity properties is obtained through Monte-Carlo simulations.

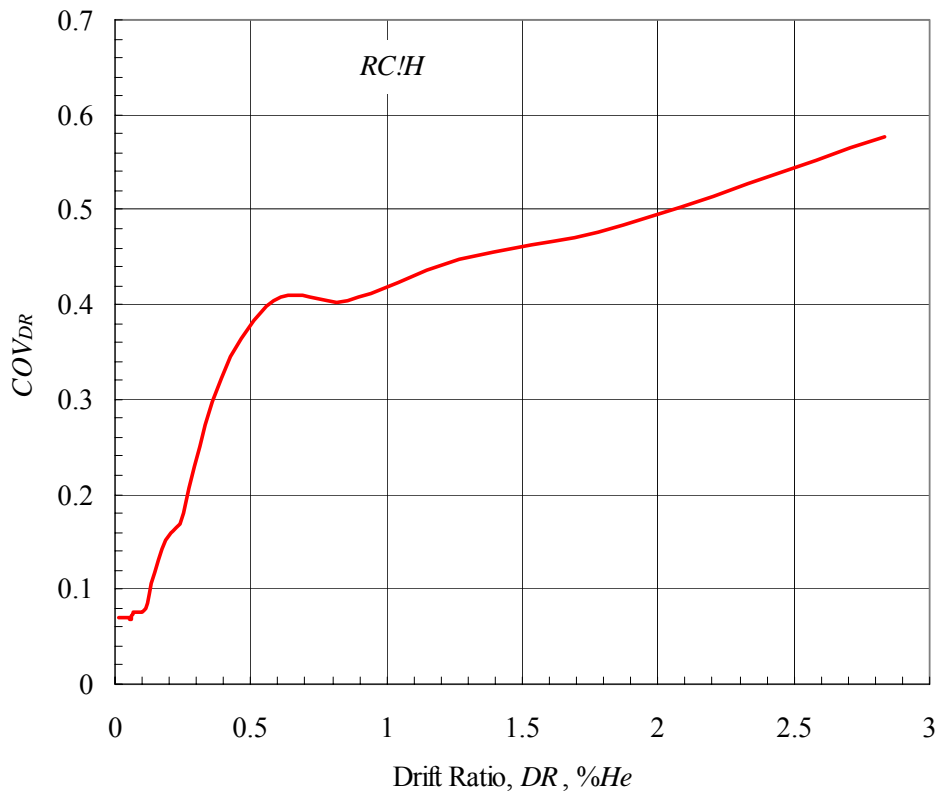


Figure 1.7 Variability of drift ratio for *RC/H* building type

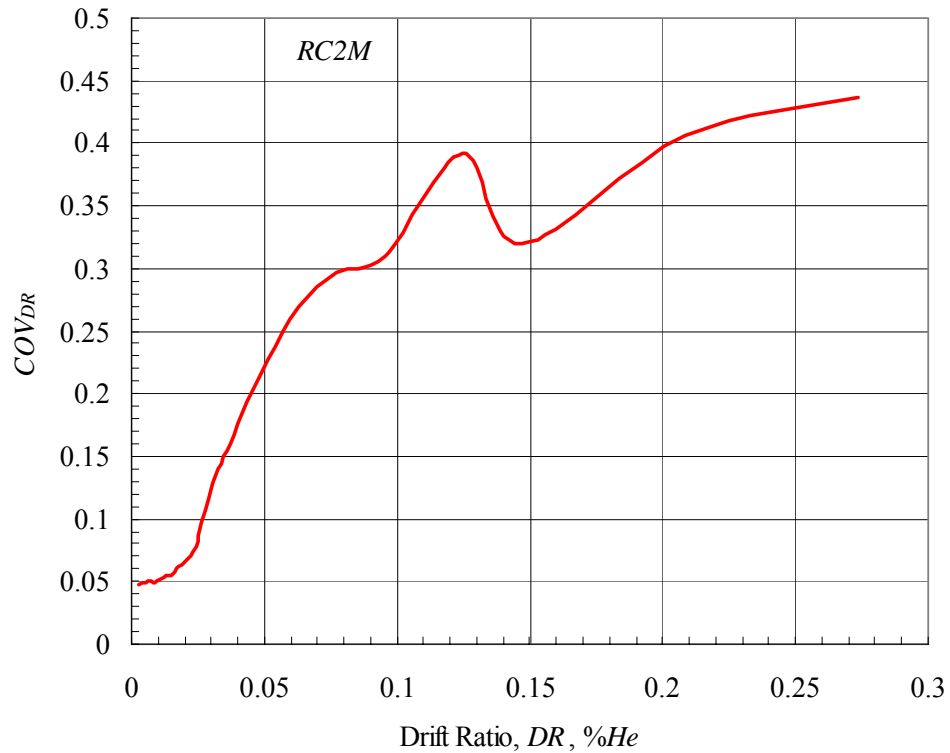


Figure 1.8 Variability of drift ratio for RC2M building type

Examples of the variability in response are given in Figure 1.9 for the relative displacement response spectra computed for the seismic motions recorded in Bucharest during 1986 and 1990 Vrancea earthquakes. One can notice an average COV of 0.5.

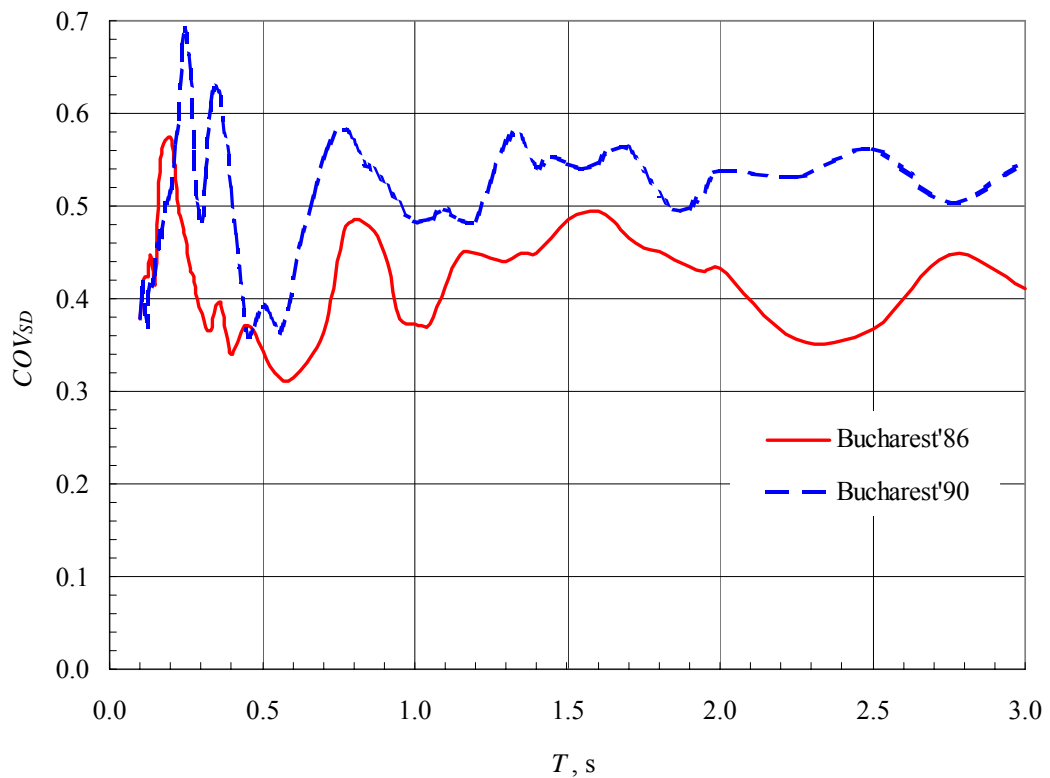


Figure 1.9 Variability of relative displacement response spectra

The lognormal standard deviation parameter that describes the uncertainty in the estimate of the median value of the threshold of structural damage state d_s , $\beta_{M(Sds)}$, is assumed to be independent of capacity and demand, and is added by the square-root-sum-of-the-squares (SRSS) method to the lognormal standard deviation parameters representing the demand and capacity variabilities. Uncertainty in the damage-state threshold of the structural system is assumed to be $\beta_{M(Sds)} = 0.4$, for all structural damage states and building types.

1.3.4 Structural Damage

Structural damage fragility curves for buildings are described by median values of drift that define the thresholds of Slight, Moderate, Extensive and Complete damage states. In general, these estimates of drift are different for each model building type (including height) and seismic design level. A complete listing of damage-state drift ratios for all building types and heights are provided for each seismic design level in Tables 1.6a, 1.6b, 1.6c, 1.6d and 1.6e, respectively.

Figure 1.10 provides an example of fragility curves for the four damage states used in this methodology.

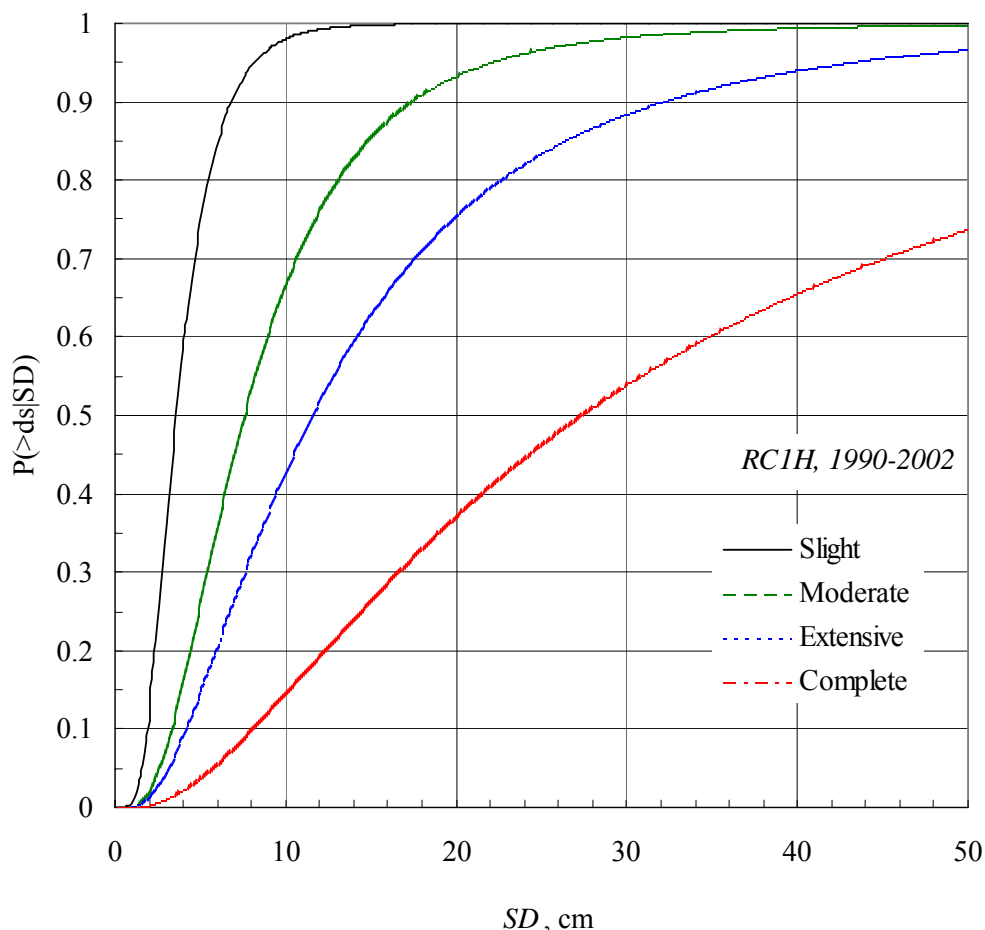


Figure 1.10 Example Fragility Curves for Slight, Moderate, Extensive and Complete Damage

Tables 1.6a, 1.6b, 1.6c, 1.6d and 1.6e summarize median and lognormal standard deviation (β_{Sds}) values for Slight, Moderate, Extensive and Complete structural damage states.



Table 1.6a Structural fragility curve parameters - 1941-1962

| Building properties | | | Interstory drift at threshold of damage state, % | | | | Spectral displacement, cm | | | | | | | |
|---------------------|-------------|-------|--|----------|-----------|----------|---------------------------|------|----------|------|-----------|------|----------|------|
| Type | Height (cm) | | | | | | Slight | | Moderate | | Extensive | | Complete | |
| | Roof | Modal | Slight | Moderate | Extensive | Complete | Median | Beta | Median | Beta | Median | Beta | Median | Beta |
| RC1L | 570 | 342 | 0.041 | 0.084 | 0.128 | 0.302 | 0.14 | 0.65 | 0.29 | 0.75 | 0.44 | 0.85 | 1.03 | 0.95 |
| RC1M | 1710 | 1026 | 0.037 | 0.076 | 0.115 | 0.272 | 0.38 | 0.65 | 0.78 | 0.75 | 1.18 | 0.85 | 2.79 | 0.95 |
| RC1H | 2850 | 1710 | 0.051 | 0.105 | 0.160 | 0.378 | 0.87 | 0.65 | 1.80 | 0.75 | 2.73 | 0.85 | 6.46 | 0.95 |
| RC2L | 570 | 399 | 0.004 | 0.008 | 0.012 | 0.027 | 0.01 | 0.65 | 0.03 | 0.75 | 0.05 | 0.85 | 0.11 | 0.95 |
| RC2M | 1710 | 1197 | 0.010 | 0.020 | 0.030 | 0.072 | 0.12 | 0.65 | 0.24 | 0.75 | 0.36 | 0.85 | 0.86 | 0.95 |
| RC2H | 2850 | 1995 | 0.020 | 0.041 | 0.063 | 0.149 | 0.40 | 0.65 | 0.83 | 0.75 | 1.26 | 0.85 | 2.97 | 0.95 |

Table 1.6b Structural fragility curve parameters - 1963-1969

| Building properties | | | Interstory drift at threshold of damage state, % | | | | Spectral displacement, cm | | | | | | | |
|---------------------|-------------|-------|--|----------|-----------|----------|---------------------------|------|----------|------|-----------|------|----------|------|
| Type | Height (cm) | | | | | | Slight | | Moderate | | Extensive | | Complete | |
| | Roof | Modal | Slight | Moderate | Extensive | Complete | Median | Beta | Median | Beta | Median | Beta | Median | Beta |
| RC1L | 570 | 342 | 0.058 | 0.120 | 0.182 | 0.430 | 0.20 | 0.65 | 0.41 | 0.75 | 0.62 | 0.85 | 1.47 | 0.95 |
| RC1M | 1710 | 1026 | 0.033 | 0.069 | 0.105 | 0.249 | 0.34 | 0.65 | 0.71 | 0.75 | 1.08 | 0.85 | 2.55 | 0.95 |
| RC1H | 2850 | 1710 | 0.033 | 0.067 | 0.102 | 0.242 | 0.56 | 0.65 | 1.15 | 0.75 | 1.75 | 0.85 | 4.14 | 0.95 |
| RC2L | 570 | 399 | 0.009 | 0.020 | 0.030 | 0.070 | 0.04 | 0.65 | 0.08 | 0.75 | 0.12 | 0.85 | 0.28 | 0.95 |
| RC2M | 1710 | 1197 | 0.021 | 0.044 | 0.067 | 0.158 | 0.25 | 0.65 | 0.53 | 0.75 | 0.80 | 0.85 | 1.89 | 0.95 |
| RC2H | 2850 | 1995 | 0.024 | 0.049 | 0.074 | 0.176 | 0.47 | 0.65 | 0.98 | 0.75 | 1.48 | 0.85 | 3.51 | 0.95 |

Table 1.6c Structural fragility curve parameters - 1970-1977

| Building properties | | | Interstory drift at threshold of damage state, % | | | | Spectral displacement, cm | | | | | | | |
|---------------------|-------------|-------|--|----------|-----------|----------|---------------------------|------|----------|------|-----------|------|----------|------|
| Type | Height (cm) | | | | | | Slight | | Moderate | | Extensive | | Complete | |
| | Roof | Modal | Slight | Moderate | Extensive | Complete | Median | Beta | Median | Beta | Median | Beta | Median | Beta |
| RC1L | 570 | 342 | 0.061 | 0.127 | 0.193 | 0.456 | 0.21 | 0.65 | 0.43 | 0.75 | 0.66 | 0.85 | 1.56 | 0.95 |
| RC1M | 1710 | 1026 | 0.035 | 0.073 | 0.112 | 0.264 | 0.36 | 0.65 | 0.75 | 0.75 | 1.14 | 0.85 | 2.70 | 0.95 |
| RC1H | 2850 | 1710 | 0.035 | 0.072 | 0.109 | 0.258 | 0.59 | 0.65 | 1.23 | 0.75 | 1.87 | 0.85 | 4.42 | 0.95 |
| RC2L | 570 | 399 | 0.008 | 0.016 | 0.024 | 0.056 | 0.03 | 0.65 | 0.06 | 0.75 | 0.09 | 0.85 | 0.22 | 0.95 |
| RC2M | 1710 | 1197 | 0.020 | 0.041 | 0.062 | 0.148 | 0.24 | 0.65 | 0.49 | 0.75 | 0.75 | 0.85 | 1.77 | 0.95 |
| RC2H | 2850 | 1995 | 0.025 | 0.052 | 0.079 | 0.186 | 0.50 | 0.65 | 1.04 | 0.75 | 1.57 | 0.85 | 3.72 | 0.95 |

Table 1.6d Structural fragility curve parameters - 1978-1989

| Building properties | | Interstory drift at threshold of damage state, % | | | | | Spectral displacement, cm | | | | | | | |
|---------------------|-------------|--|--------|----------|-----------|----------|---------------------------|------|----------|------|-----------|------|----------|------|
| Type | Height (cm) | | | | | | Slight | | Moderate | | Extensive | | Complete | |
| | Roof | Modal | Slight | Moderate | Extensive | Complete | Median | Beta | Median | Beta | Median | Beta | Median | Beta |
| RC1L | 570 | 342 | 0.147 | 0.324 | 0.502 | 1.213 | 0.50 | 0.65 | 1.11 | 0.75 | 1.72 | 0.85 | 4.15 | 0.95 |
| RC1M | 1710 | 1026 | 0.123 | 0.272 | 0.421 | 1.016 | 1.26 | 0.65 | 2.79 | 0.75 | 4.32 | 0.85 | 10.43 | 0.95 |
| RC1H | 2850 | 1710 | 0.168 | 0.371 | 0.574 | 1.387 | 2.87 | 0.65 | 6.35 | 0.75 | 9.82 | 0.85 | 23.72 | 0.95 |
| RC2L | 570 | 399 | 0.008 | 0.017 | 0.026 | 0.062 | 0.03 | 0.65 | 0.07 | 0.75 | 0.10 | 0.85 | 0.25 | 0.95 |
| RC2M | 1710 | 1197 | 0.036 | 0.077 | 0.118 | 0.282 | 0.43 | 0.65 | 0.92 | 0.75 | 1.41 | 0.85 | 3.37 | 0.95 |
| RC2H | 2850 | 1995 | 0.071 | 0.152 | 0.233 | 0.559 | 1.41 | 0.65 | 3.03 | 0.75 | 4.65 | 0.85 | 11.15 | 0.95 |

Table 1.6e Structural fragility curve parameters - 1990-2002

| Building properties | | Interstory drift at threshold of damage state, % | | | | | Spectral displacement, cm | | | | | | | |
|---------------------|-------------|--|--------|----------|-----------|----------|---------------------------|------|----------|------|-----------|------|----------|------|
| Type | Height (cm) | | | | | | Slight | | Moderate | | Extensive | | Complete | |
| | Roof | Modal | Slight | Moderate | Extensive | Complete | Median | Beta | Median | Beta | Median | Beta | Median | Beta |
| RC1L | 570 | 342 | 0.184 | 0.386 | 0.588 | 1.398 | 0.63 | 0.65 | 1.32 | 0.75 | 2.01 | 0.85 | 4.78 | 0.95 |
| RC1M | 1710 | 1026 | 0.154 | 0.324 | 0.493 | 1.172 | 1.58 | 0.65 | 3.32 | 0.75 | 5.06 | 0.85 | 12.03 | 0.95 |
| RC1H | 2850 | 1710 | 0.210 | 0.442 | 0.673 | 1.600 | 3.59 | 0.65 | 7.55 | 0.75 | 11.51 | 0.85 | 27.35 | 0.95 |
| RC2L | 570 | 399 | 0.010 | 0.020 | 0.031 | 0.072 | 0.04 | 0.65 | 0.08 | 0.75 | 0.12 | 0.85 | 0.29 | 0.95 |
| RC2M | 1710 | 1197 | 0.045 | 0.092 | 0.139 | 0.326 | 0.54 | 0.65 | 1.10 | 0.75 | 1.66 | 0.85 | 3.90 | 0.95 |
| RC2H | 2850 | 1995 | 0.090 | 0.182 | 0.275 | 0.646 | 1.79 | 0.65 | 3.64 | 0.75 | 5.49 | 0.85 | 12.89 | 0.95 |



References Chapter 1

Aldea, A., Lungu, D., Demetriu, S., Cornea, T., Vacareanu, R. May 2005. "City of Bucharest: Distinctive Features and Seismic Hazard", *Bulletin of the Technical University of Civil Engineering Bucharest*, 2/2003, p. 43-75

Ang A.H-S., 1987. Basis for earthquake-resistant design with tolerable structural damage, Proc. 5th International Conference on Applications of Statistics and Probability in Soil and Structural Engineering (ICASP5), Vancouver BC, Canada, Vol.1, 407-416

ATC 40, 1996. Seismic Evaluation and Retrofit of Concrete Buildings, Report ATC-40, Applied Technology Council, Redwood City CA.

HAZUS – Technical Manual 1997. Earthquake Loss Estimation Methodology, 3 Vol.

Lungu, D., Arion, C., Baur, M., Aldea, A., 2000. Vulnerability of existing building stock in Bucharest, 6ICSZ Sixth International Conference on Seismic Zonation, Palm Springs, California, USA, Nov.12-15, p.837-846

Lungu, D., Demetriu, S., Arion, C. 1998. Seismic vulnerability of buildings exposed to Vrancea earthquakes in Romania. In Vrancea Earthquakes. Tectonics, Hazard and Risk Mitigation, Kluwer Academic Publishers, Wenzel F., Lungu D., editors, Proc. of First International Workshop on Vrancea Earthquakes, p.215-224.

Park, Y.-J & Ang, A. H.-S.. Mechanistic seismic damage model for reinforced concrete. Journal of Structural Engineering. ASCE vol. 111 (4): 722-739, 1985

Reinhorn A. M., Valles-Mattox R. E., Kunnath S. K. – Seismic Damageability Evaluation of a Typical R/C Building in the Central U.S., NCEER Bulletin, Vol. 10, No. 4, October 1996

RISK-UE "An advanced approach to earthquake risk scenarios with applications to different European towns", financed by European Commission, Fifth Framework, 2000-2004

Rubinstein, R. Y. Simulation and the Monte Carlo method. John Wiley & Sons, New York, 1981

Văcăreanu R., 2000 - Monte Carlo Simulation Technique for Vulnerability Analysis of RC Frames – An Example – Scientific Bulletin on Technical University of Civil Engineering of Bucharest, pg. 9-18;

Văcăreanu R., 1998 - Seismic Risk Analysis for a High Rise Building - Proceedings of the 11th European Conference on Earthquake Engineering, Paris, Abstract Volume pg. 513

Văcăreanu R., Cornea T., Lungu D. Evaluation of seismic fragility of buildings, Earthquake Hazard and Countermeasures for Existing Fragile Buildings, Editors: Lungu D. & Saito T., Independent Film, Bucharest Romania, 315p

Williams, M. S. & Sexsmith, R. G. 1995. Seismic Damage Indices for Concrete Structures: A State-of-the-Art Review. Earthquake Spectra. Vol. 11(2): 319-345, 1997

2. Development of Seismic Risk Scenarios

2.1 Introduction

Human, economic and ecological costs and losses associated with earthquake disasters are increasing exponentially and these cost and losses pose a systemic risk to society's political and economic bases. It is correspondingly difficult, in some cases impossible, for local, national and global disaster management agencies to cope with the scope, magnitude and complexity of these disasters.

Even utilizing the most advanced technology, it is almost impossible, at the present state of knowledge, to predict exactly when and where an earthquake will occur and how big it will be. An earthquake suddenly hits an area where people are neither prepared nor alerted. Hence, the earthquake often causes huge damage to human society. On the other hand, the other natural disasters like floods and hurricanes are almost predictable, providing some lead time before they hit certain places. People could be alerted with a proper warning system and precautionary measures could be taken to protect lives and properties.

It is therefore urgent and crucial to make the physical environment resistant against earthquakes, strengthening buildings and infrastructure. Action should be taken for seismic risk reductions. Different strategies may be taken to mitigate earthquake disasters, based on appropriate risk assessment.

There is a tendency to think that disaster prevention would cost much more than relief activities. However, the reality is the reverse. Our society has been spending a lot of resources for response activities after disasters; these resources could have been drastically reduced if some had been spent for disaster prevention. There is also a tendency to look at disasters mainly from a humanitarian angle, bringing us into the position of giving priority to the response to disasters. However, relief activities can never save human lives that have already been lost. Response activities can never help immediately resume functions of an urban infrastructure that has already been destroyed. The bottom line is that buildings should not kill people by collapsing and infrastructure should not halt social and economic activities of the city for a long time.

The damage caused by an earthquake could be magnified in areas where:

- ✓ People are concentrated;
- ✓ Economic and political functions are concentrated;
- ✓ Buildings and infrastructure have been built to inadequate standards of design.

The larger an urban area is, the greater the damage would be. As the urban areas are growing rapidly, the seismic risk in the urban areas is also growing rapidly. Even an intermediate earthquake could cause destructive damage to a city.

Risk is the expectancy of losses or of other negative future happenings derived on the basis of present knowledge. The risk analysis recognizes basically the impossibility of deterministic prediction of events of interest, like future earthquakes, exposure of elements at risk, or chain effects occurring as a consequence of the earthquake-induced damage. Since the expectancy of losses represents the outcome of a more or less explicit and accurate

predictive analysis, a prediction must be made somehow in probabilistic terms, by extrapolating or projecting into the future the present experience.

The objective is to *develop earthquake-risk model scenarios* for physical and human loss estimation. The model should take into account the following components:

- *Direct physical losses*
- *Human losses*
- *Direct economic losses*
- *Problems due to homeless, debris*

The worst case earthquake scenario – constant hazard scenario - is selected on probabilistic basis, as uniform hazard acceleration spectra corresponding to a mean recurrence interval $MRI = 475$ yr (10 % probability of exceedance in 50 yr).

2.2 Direct physical losses estimation; debris

The expected response of the built systems to given earthquake scenarios expressed in terms of acceleration – displacement spectra of uniform hazard is obtained by capacity spectrum method, Figure 2.1. The expected spectral displacement S_d of an inelastic system is determined by the following steps:

1. The uniform hazard spectrum of absolute acceleration obtained in RISK-UE Project, Figure 2.2, is converted into acceleration-displacement response spectrum, *ADRS*, Figure 2.3. A demand constant-ductility spectrum is established by reducing the elastic acceleration-displacement spectrum by appropriate ductility-dependent factors that depend on T .
2. The capacity curve is plotted on the same graph.
3. The yielding branch of the capacity curve intersects the demand spectra for several μ values of ductility factor. One of these intersection points, which remains to be determined, will provide the expected spectral displacement. At the one relevant intersection point, the ductility factor calculated from the capacity curve should match the ductility value associated with the intersecting demand spectrum.
4. The building fragility functions are determined. The conditional probability of being in, or exceeding, a particular damage state, d_s , given the spectral displacement, S_d , is defined by the lognormal distribution of damage state conditional upon spectral displacement.

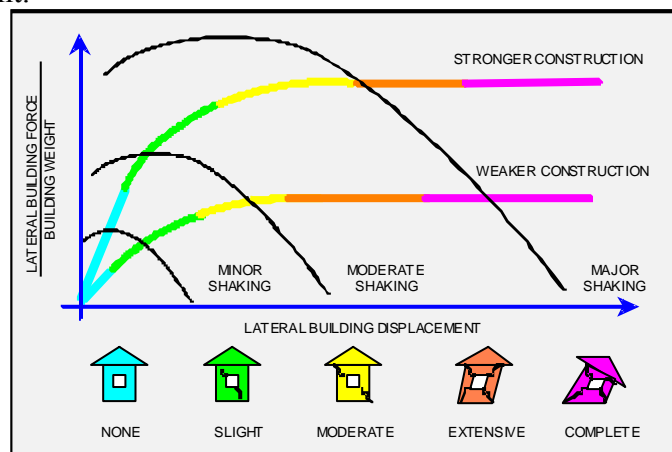


Figure 2.1. Capacity spectrum method (Source: www.fema.org)

An example of the application of the capacity spectrum method within *RISK-UE* Project is given in Figure 2.4 and the computation of the probabilities of being in or exceeding different damage states is presented for illustration in Figure 2.5.

Once the probabilities for being in various damage states are obtained (with Level I or Level II methodology) the general methodology presented hereinafter is evenly applicable.

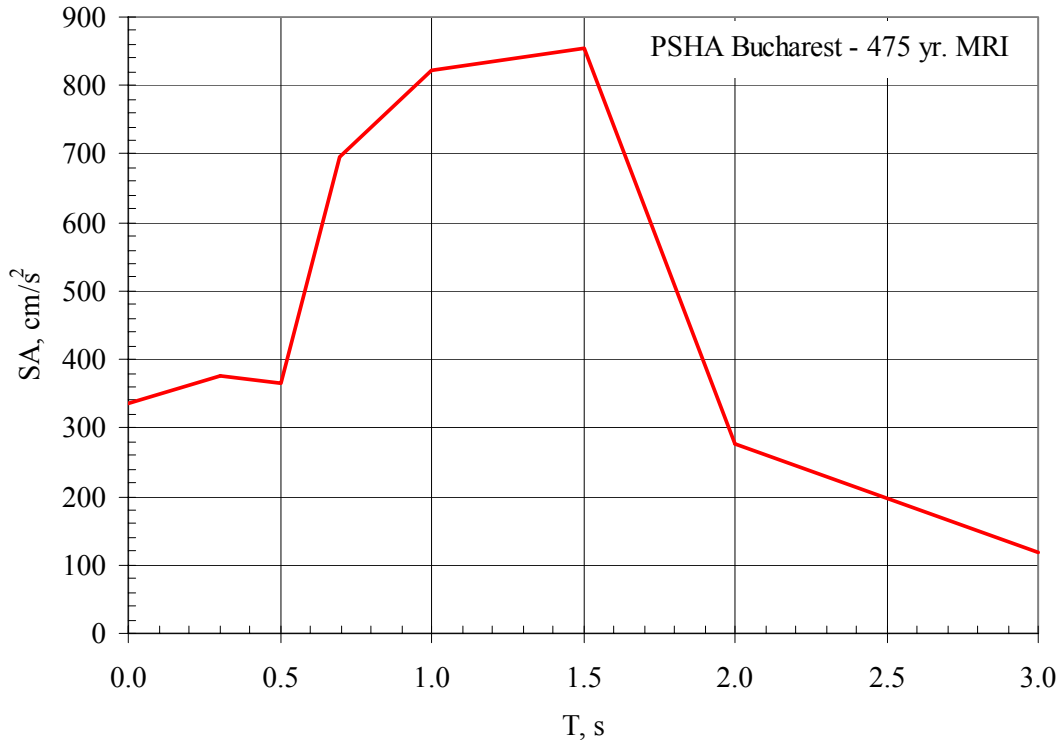


Figure 2.2. Uniform hazard spectrum of absolute acceleration

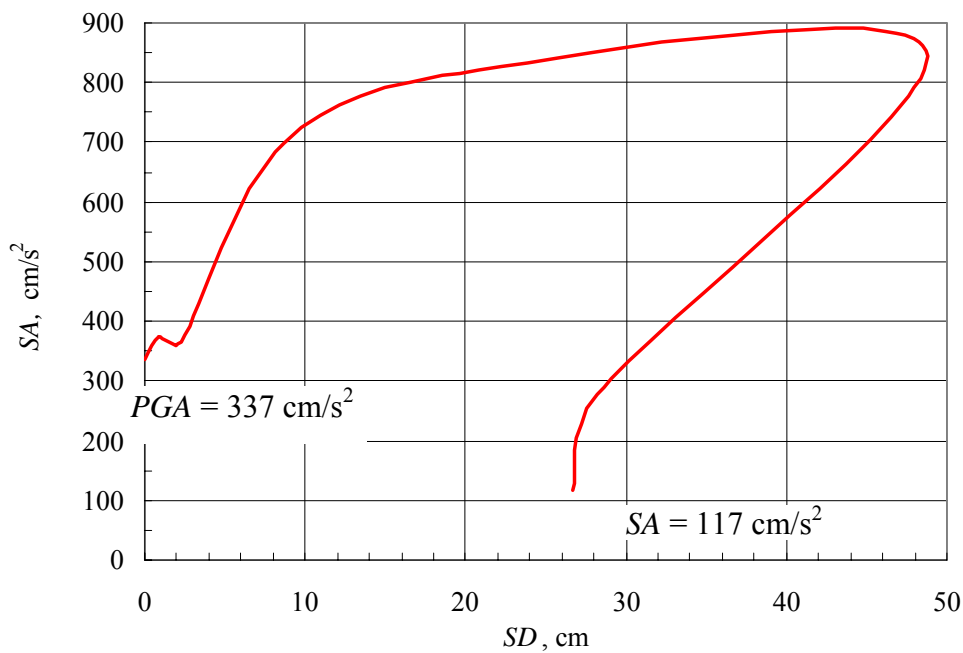


Figure 2.3. Acceleration – displacement spectrum of constant hazard

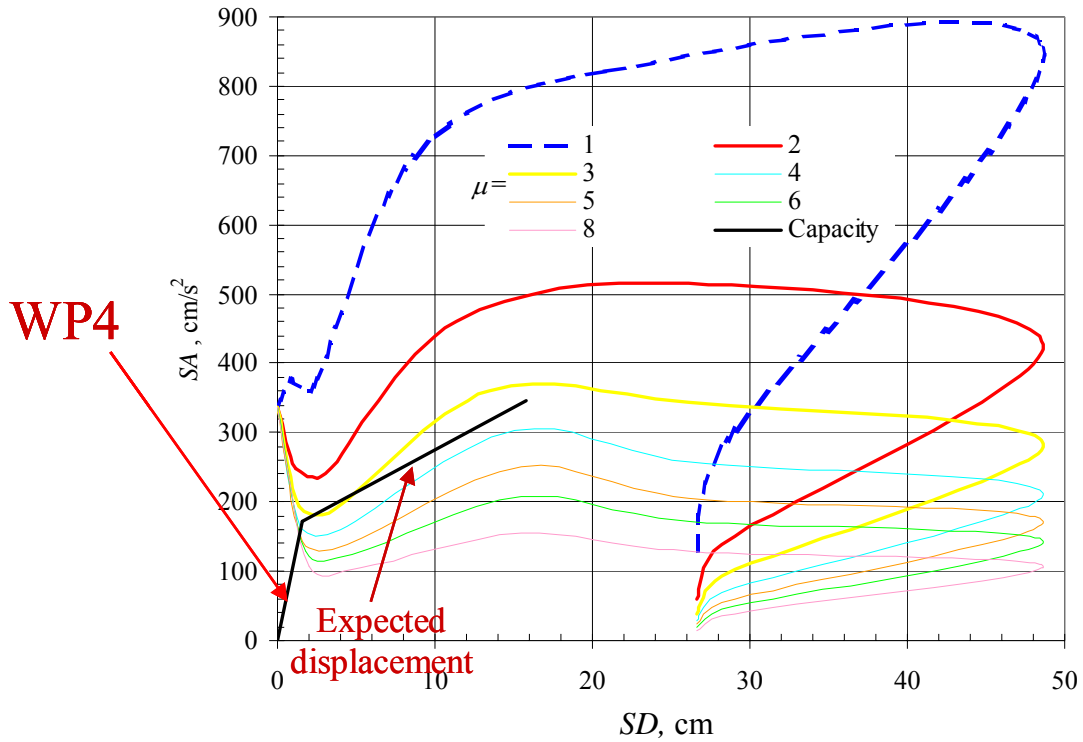


Figure 2.4. Application of capacity spectrum method

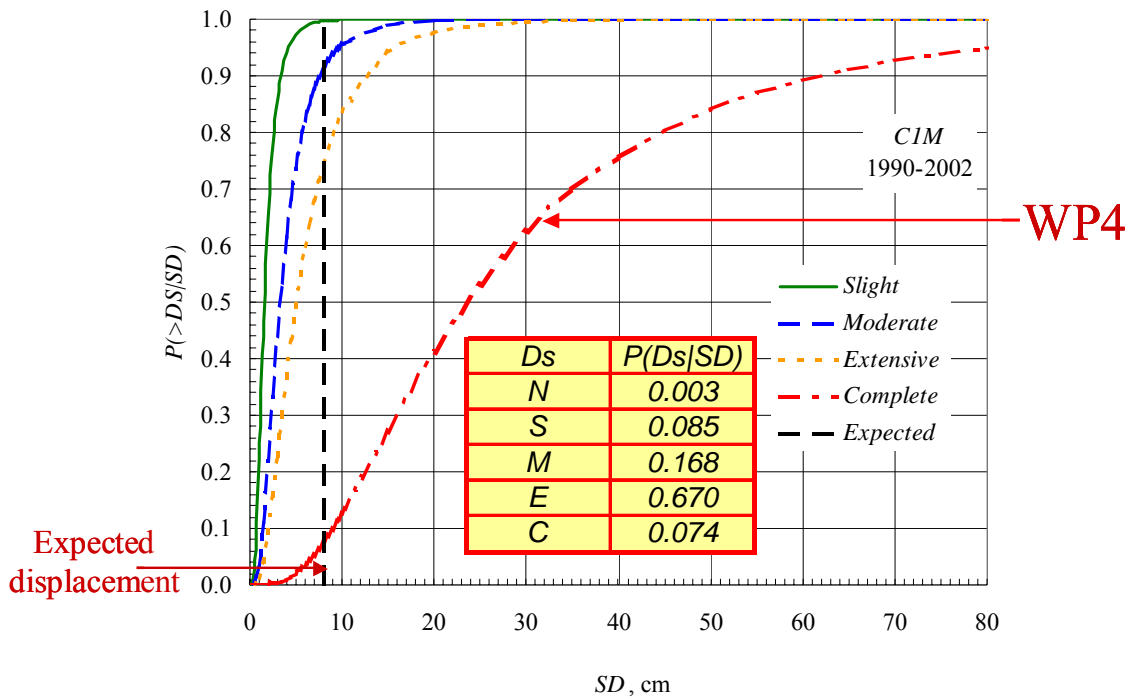


Figure 2.5. Fragility functions and damage states exceedance probabilities

Debris

An empirical approach that estimates two different types of debris is used (HAZUS, 1999):



- ✓ Debris that falls in large pieces, such as steel members or reinforced concrete elements - require special treatment to break into smaller pieces before they are hauled away;
- ✓ Debris that is smaller and more easily moved with bulldozers and other machinery and tools - includes brick, wood, glass, building contents and other materials.

The following input is required for the evaluation of debris amount:

- ✓ Probabilities of damage states for building typologies;
- ✓ Floor area of building typologies analyzed.

Given the damage states, the debris estimates are based on observations of damage that has occurred in past earthquakes and estimates of the weights of structural elements. Tables are compiled to estimate generated debris from different damage states for each building typology.

The debris generated from damaged buildings (in tons) is based on:

- ✓ Unit weight of structural elements (tons/1000m² of floor area) for each of the building typologies, Table A.1, Annex A;
- ✓ Probabilities of damage states;
- ✓ Floor area of each of the building typologies;
- ✓ Debris generated from different damage states (% of unit weight of element), Table A.2 and Table A.3, Annex A.

The following notation is used:

- i - the iteration variable for the types of debris, $i = 1$ to 2
 where: 1- brick, wood and other
 2- reinforced concrete and steel components
- j - the iteration variable for the damage states, $j=1$ to 5,
 where: 1- None, 2- Slight; 3- Moderate; 4- Extensive; 5- Complete
- k - the iteration variable for the building typology.

The input is the probabilities of different structural damage states. Thus, the first step in the debris calculation is to combine the debris fraction generated from the different damage states into the expected debris fraction for each building typology. The expected debris fraction for building typology k and debris type i due to structural damage is given by:

$$EDF_s(i,k) = \sum_{j=2}^5 P_s(j,k) * DF_s(i,j,k) \quad (2.1)$$

where:

- $EDF_s(i,k)$ - the expected debris fraction of debris type i due to structural damage for building typology k
- $P_s(j,k)$ - the probability of structural damage state j for building typology k
- $DF_s(i,j,k)$ - the debris fraction of debris type i for building typology k in structural damage state j (from Tables A.2 and A.3, Annex A)

These values indicate the expected percentage of debris type i generated due to structural damage to building typology k . If one knows the total floor area of each building typology



and weights of debris type i per 1000 m² of building, then the amount of debris for this particular location can be obtained by multiplying the expected debris fraction of debris type i due to structural damage for building typology k with the weight of debris type i per 1000 m² of floor area for structural elements of building typology k (From Table A.1, Annex A) and with the total floor area of each building typology and the summing for all k .

2.3 Casualties and homeless estimation

Direct Social Losses – Casualties

Earthquakes are devastating to people as individuals, to families, to social and economic organization of the region affected and the country as a whole. Unquestionably the most terrible consequence of earthquakes is the massive loss of human life that they cause.

The statistics recording the earthquake effects include a wide range of earthquake-induced cause of human casualty and deaths. Although the principal cause of human casualty and deaths is the collapse of the buildings, there are a wide range of other causes of death and injury officially attributed to the earthquake occurrence, ranging from medical conditions induced by the shock of experiencing ground motion, to accidents occurring during the disturbance, epidemics among the homeless and shootings during martial law.

About 70% of fatalities and nearly 100% of injuries attributed to earthquakes are caused by collapse of buildings (Spence et al., 1991). If a major earthquake occurs at night, catching most people asleep in their homes, *the mortality rate* - the percentage of the population killed - in the towns and villages of the epicentral area could be as high as 30% (Table 2.1). *The morbidity rate* - the percentage of the population injured and requiring some level of medical treatment - could be 60-80%.

Table 2.1. Breakdown of typical injury ratios for a population affected by a severe-case earthquake scenario, Coburn and Spence, 2002

| | |
|---|----------|
| Fatalities | 20 - 30% |
| Injuries requiring first aid/outpatient treatment | 50 - 70% |
| Injuries requiring hospitalization | 5 - 10% |
| Injuries requiring major surgery | 1 - 2% |

When building collapses, not all the occupants are killed, injured or trapped inside. Many are likely to escape just before the collapse and some, although even injured are able to free themselves shortly after. In a high rise buildings, escape from upper floors is unlikely before the collapse, and if it collapses completely about 70% of the its occupants are likely to be killed, at best injured and trapped. In low-rise buildings, that have apparently 20-30 seconds to collapse, more than three quarters of the occupants may be able to escape before the collapse, and only one quarter are to be considered as casualty toll.

A wide range of types and severity of injury are caused by earthquakes. A significant percentage of injuries are not only a direct consequence of building collapses and may be

result of many different earthquake-induced accidents. Some injuries are caused by non-structural building damage, such as broken glass or the fall of architectural ornament or collapse of parapet walls. But the majority of injuries in a mayor earthquake are caused by building damage.

Many more people tend to be injured in an earthquake than are killed. A ratio of three people requiring medical attention to every one person killed is typical (Ville de Goyet 1976; Alexander 1984), but this can vary very significantly with different types of construction affected and with the size of the earthquake. Similarly light injuries requiring outpatient hospitalization - typically there may be between 10 and 30 people requiring outpatient treatment for every person hospitalized.

The relationship between the number of people killed and the number of buildings that collapse, the lethality ratio, is the important parameter to determine. If this ratio is known, then human casualties can be estimated from estimates of the number of collapsed buildings.

The casualty model is stated as a series of these factors that are applied to building typologies. For a building typology, or corresponding building (apartment) area, the number of casualties due to collapse of building can be expressed as, Coburn and Spence, 2002:

$$Ks = C \times [M1 \times M2 \times M3 \times (M4 + M5 \times (1 - M4))] \quad (2.2)$$

where C is total number (or floor area) of collapsed buildings in that typology class.

$M1$ is the occupancy rate (number of people / built m^2). In low-rise residential building stock, the population per building (P/B) is equivalent to the average family size living in each house. In European cities, average residential P/B sizes are around 2 to 3. In cities with rapidly expanding populations, a large immigration of population or a shortage of building stock, P/B ratios can be much higher and can increase or decrease quite suddenly with changes of population movement.

Factor $M2$ is the occupancy at time of earthquake. The time of day that an earthquake occurs has long been known to affect the number of people killed, Figure 2.6. An earthquake occurring when a lot of the population is indoors kills more people in the buildings that collapse.

Factor $M3$ represents the percentage of occupants trapped by collapse. Although there is little detailed information or statistics to quantify it empirically, it is clear that not all the occupants that are inside a building when an earthquake occurs are trapped if it collapses. People escape before collapse, or the collapse of the structure is not total, or they are able to free themselves relatively easily by their own efforts.

In single story structures, there is evidence that many people are able to get out of a building before it collapses unless (as appears in the case for weak masonry buildings in the epicenter of strong earthquakes) collapse is instantaneous. In multi-story structures fewer people are able to leave the building once shaking has started. There is little documentation of the time taken for buildings to collapse. A large magnitude earthquake can have a minute or more of

strong ground motion but the strongest amplitude shaking - the ones most likely to exceed the strength of the structures - happen relatively early in the time history. A ductile building may collapse over a period of several tens of seconds. A brittle building may collapse more quickly. Tests of evacuation times show that people cannot get out of a building from anywhere above the first floor in less than thirty seconds, even if they are capable of walking during the violent shaking. A reasonable assumption is that a certain percentage of occupants of the ground floor - e.g. 50% for a building of fairly shallow plan depth, will be capable of escape, all other occupants of the building will remain inside.

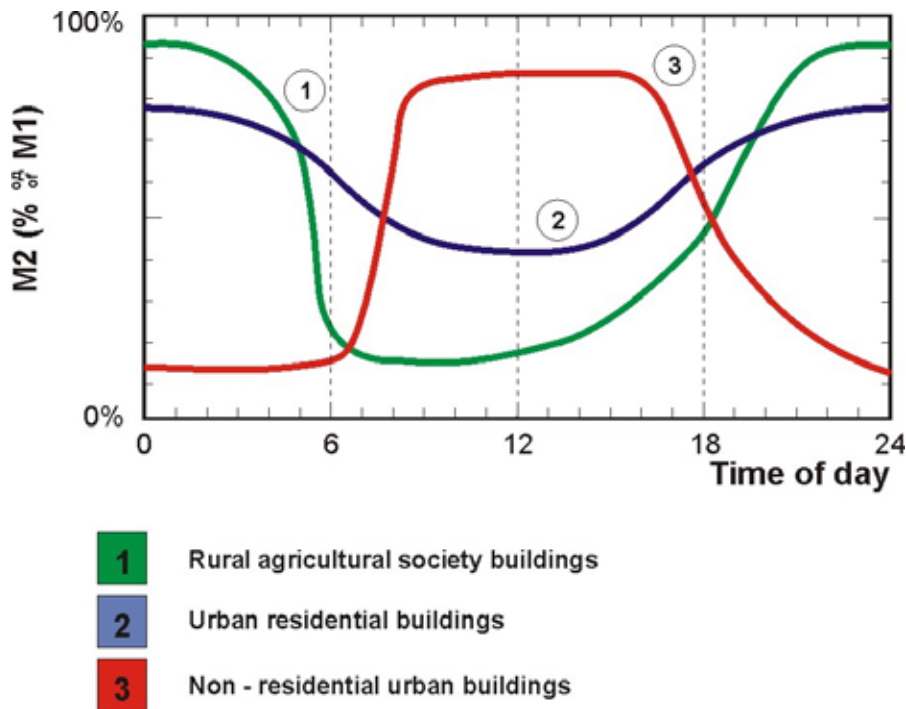


Figure 2.6. $M2$ - occupancy at time of earthquake, Coburn and Spence, 2002

Table 2.2. Factor $M3$ - Estimated average percentage of occupants trapped by collapse, Coburn and Spence, 2002

| Building type | Seismic Intensity (MSK Scale) | | | |
|---|----------------------------------|------|----|----|
| | VII | VIII | IX | X |
| Masonry buildings (up to 3 stories) | | | | |
| Non earthquake resistant | 5 | 30 | 60 | 70 |
| Earthquake resistant | - | 10 | 30 | 60 |
| RC structures | | | | |
| Near-field high frequency ground motion | | | 70 | |
| Distant, long-period ground motion | | | 50 | |

Factor $M4$ gives the injury distribution at collapse. People caught in building collapses suffer a range of types of injury (Table 2.3). A proportion of the buildings occupants are killed outright when collapse occurs. This proportion (deaths at time 0 or T after the earthquake) is taken as the $M4$ factor in the casualty model. Others are injured to various degrees of severity.



A number of injury severity scales have been proposed for quantifying earthquake injury epidemiological studies. One of the simplest and most useful to emergency managers is the four-point standard triage categorization of injuries. There is very little data to indicate the distribution of severity of injury to occupants when a building collapses. However, studies back-figuring injury types and survival times from mortality data of people retrieved from building collapses several days later suggest that in reinforced concrete structures, the *M4* injury distribution is bi-modal, with most people being either killed or only slightly injured, with very few people badly injured in-between. By contrast, injury distributions in masonry buildings appear more uniform, with high percentages of trapped victims having serious injuries.

Table 2.3. Factor *M4* - Estimated injury distribution at collapses, in % of trapped occupants, Coburn and Spence, 2002

| Triage injury category | Low strength masonry | Masonry | RC |
|--|----------------------|---------|----|
| Dead or unsavable | 10 | 20 | 40 |
| Life threatening cases needing immediate medical attention | 20 | 30 | 10 |
| Injury requiring hospital treatment | 30 | 30 | 40 |
| Light injury not necessitating hospitalization | 40 | 20 | 10 |

Factor *M5* represents the mortality post-collapse. Those trapped in the rubble will die if they are not rescued and given medical treatment. Those who have serious injuries will die quickly. Less severely injured people can survive for longer. The unaffected community usually rallies to the collapsed buildings and set to work to extricate trapped victims. Effective emergency activities will save the lives of many of those trapped in building collapses that would otherwise have died.

Time is critical and death rates increase with every hour that passes. The *M5* factor - the additional mortality of trapped victims after collapse - is a measure of the effectiveness of post-collapse activities (Table 2.4). It is clear that in cases of extreme destruction, where high percentages of the total population of a community are trapped in collapses (i.e. $M2 \times M3 > 50\%$) the *M5* factor becomes very high. The community itself loses its capability of rescuing its own victims, both because its manpower is greatly reduced and because it is psychologically and socially incapacitated by the disaster. In very high casualty earthquakes ('hyper-fatality events') this appears to be a major factor in the escalation of casualty figures.

Table 2.4. Factor *M5* - percentage of trapped survivors in collapsed buildings that subsequently die, Coburn and Spence, 2002

| Situation | Masonry | RC |
|---|---------|----|
| Community incapacitated | 95 | - |
| Community capable of organizing rescue activities | 60 | 90 |
| Community + emergency squads after 12 hours | 50 | 80 |
| Community emergency squads SAR experts after 36 hours | 45 | 70 |

The possible output of the presented methodology is presented in Figure 2.7 for different building typologies.

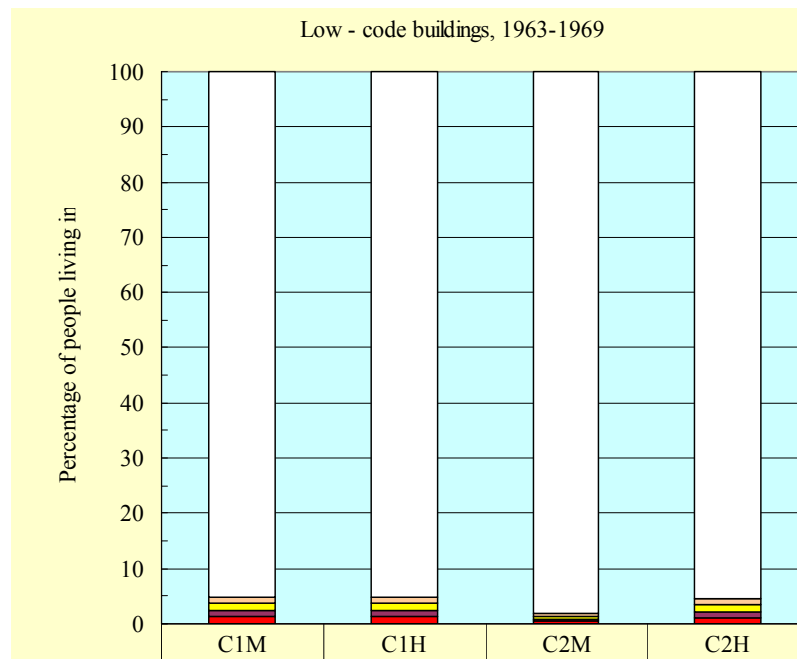


Figure 2.7. Casualties' distribution for the given scenario

Homeless estimation

The following inputs are required to compute the number of uninhabitable dwelling units and the number of displaced households, HAZUS, 1999:

- Total Number of Single-Family Dwelling Units (#SFU)
- Total Number of Multi-Family Dwelling Units (#MFU)
- Damage state probability for moderate structural damage in the single-family residential occupancy class (%SFM).
- Damage state probability for extensive structural damage state in the single-family residential occupancy class (%SFE).
- Damage state probability for complete structural damage state in the single-family residential occupancy class (%SFC).
- Damage state probability for moderate structural damage state in the multi-family residential occupancy class (%MFM).
- Damage state probability for extensive structural damage state in the multi-family residential occupancy class (%MFE).
- Damage state probability for complete structural damage state in the multi-family residential occupancy class (%MFC).

The number of uninhabitable dwelling units due to structural damage is determined by combining a) the number of uninhabitable dwelling units due to actual structural damage, and b) the number of damaged units that are perceived to be uninhabitable by their occupants.

Based on comparisons with previous work (Perkins, 1992), the methodology considers all dwelling units located in buildings that are in the complete damage state to be uninhabitable. In addition, dwelling units that are in moderately and extensively damaged multi-family structures are also considered to be uninhabitable due to the fact that renters perceive some moderately damaged rental property as uninhabitable. On the other hand, those living in single-family homes are much more likely to tolerate damage and continue to live in their home. Therefore, the total number of uninhabitable units ($\#UNU_{SD}$) due to structural damage is calculated by the following relationship:

$$\begin{aligned} \%SF &= w_{SFM} \times \%SFM + w_{SFE} \times \%SFE + w_{SFC} \times \%SFC \\ \%MF &= w_{MFM} \times \%MFM + w_{MFE} \times \%MFE + w_{MFC} \times \%MFC \\ \#UNU_{SD} &= \#SFU \times \%SF + \#MFU \times \%MF \end{aligned} \quad (2.3)$$

The values of weighting factors are 1.0 for w_{SFC} and w_{MFC} , 0.9 for w_{MFE} and 0.0 for w_{SFM} , w_{SFE} , w_{MFM} .

2.4 Direct economic losses

The methodology described in HAZUS, 1999 is used and provides estimates of the repair costs caused by building damage and the associated loss of building contents, Figure 2.8. These losses are calculated from the building damage estimates.

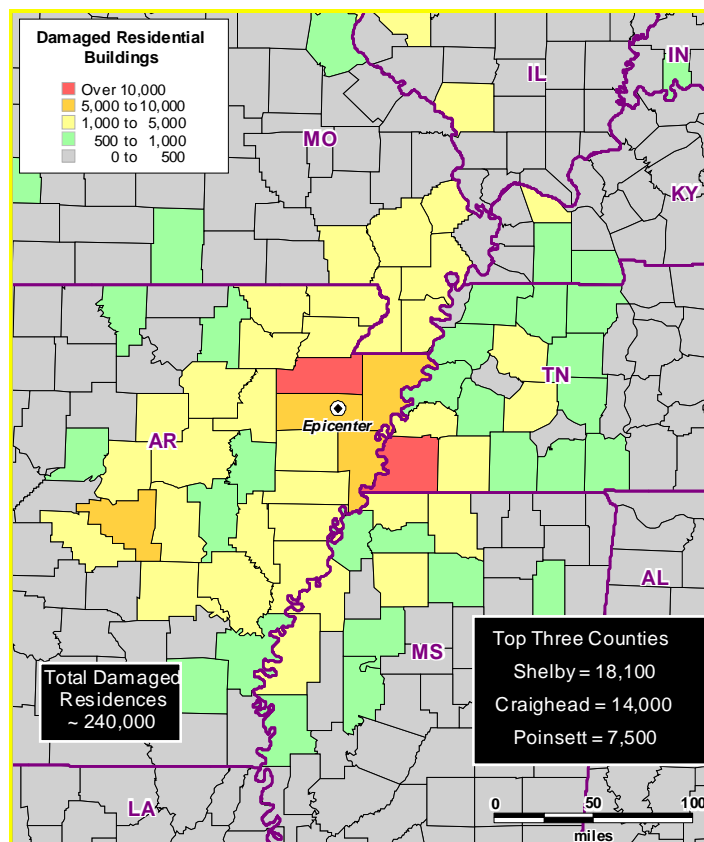


Figure 2.8. Number of damaged residences (HAZUS, 1999)

For building related items, methods for calculating the following monetary losses are provided for:

- ✓ Building Repair and Replacement Costs
- ✓ Building Contents Losses.

Building Repair and Replacement Costs

To establish monetary loss estimates, the damage state probabilities are converted to monetary loss equivalents. For a given occupancy and damage state, building repair and replacement costs are estimated as the product of the floor area of each building typology, the probability of the building typology being in the given damage state, and repair costs of the building typology per square meter for the given damage state, summed over all building typologies.

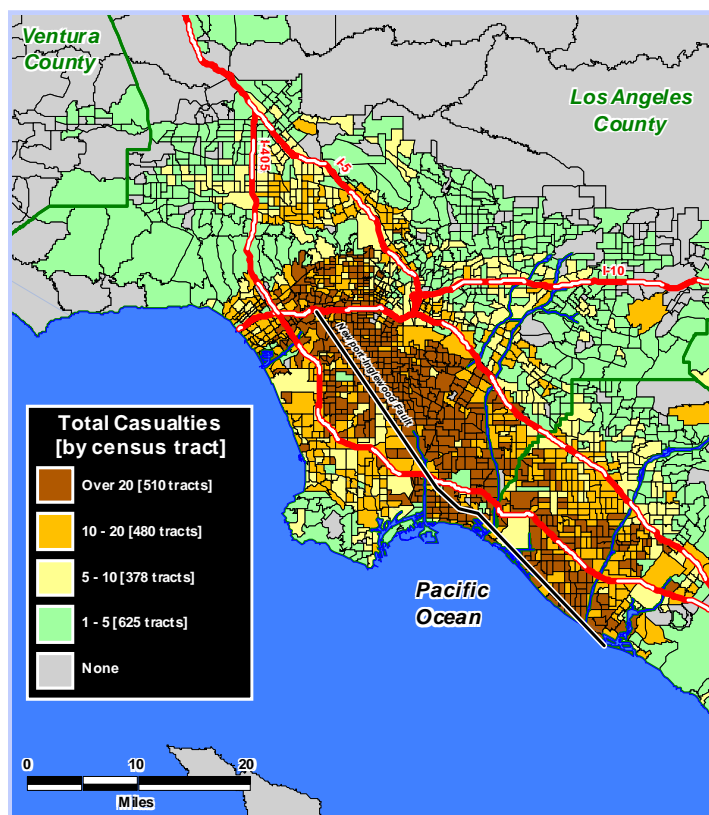


Figure 2.9. Expected casualties (HAZUS, 1999)

For structural damage, losses are calculated as follows:

$$CS_{ds} = \sum_j Fa_j \times PMBTSTR_{ds,j} \times RCS_{ds,j} \tag{2.4}$$

$$CS = \sum_{ds=2}^5 CS_{ds} \tag{2.5}$$

where:

CS_{ds} cost of structural damage (repair and replacement costs) for damage state ds



| | |
|------------------|---|
| CS | cost of structural damage (repair and replacement costs) |
| FA_j | floor area of building type j (in m^2) |
| $PMBTSTR_{ds,j}$ | probability of building type j being in structural damage state ds |
| $RCS_{ds,j}$ | structural repair and replacement costs (per m^2) for building type j in damage state ds |

Note that damage state "None" ($ds = 1$) does not contribute to the calculation of the cost of structural damage and thus the summation in Equation 2.5 is from $ds = 2$ to $ds = 5$.

The cost of damage is expressed as a percentage of the complete damage state. The assumed relationship between damage states and repair/replacement costs is as follows:

| | |
|-------------------|-----------------|
| Slight damage: | 2% of Complete |
| Moderate damage: | 10% of Complete |
| Extensive damage: | 50% of Complete |

These values are consistent with and in the range of the damage definitions and corresponding damage ratios presented in *ATC-13, 1985, Earthquake Damage Evaluation Data for California*.

Structural Repair Costs for Complete Damage (Euro/ m^2) should be considered according to the contractions and real estate markets in each region. For example, for Bucharest region it was considered an amount equivalent to 300 Euro/ m^2 as structural repair cost for complete damage.

Building Content Losses

Building content is defined as the furniture, equipment that is not integral with the structure, computers and other supplies. From Table 4.11 of *ATC-13, 1985* it is assumed that contents value of residential buildings represent 50 percent of building replacement value.

2.5 Risk management

Seismic risk is the outcome of the convolution of seismic hazard, exposure of elements at risk and vulnerability of the elements at risk. The 20th century witnessed a painful history of devastating earthquakes. A list of most deadly earthquakes worldwide starting with year 1900 is given in Table A.4, Annex A.

Economic losses are another important feature of earthquake-induced phenomena. Sometimes the economic burden and pressure induced by the consequences of an earthquake disaster caused irreparable economic crisis for poor countries. Table 2.5 presents a combination of human and economic losses for earthquakes where monetary evaluations were available.

Table 2.5. Human and economic losses produced by earthquakes in 20th century

| No. | Date UTC | Location | Deaths | Losses (\$bn) | Magnitude |
|-----|--------------|--------------------|---------|---------------|-----------|
| 1 | 1963 July 26 | FYROM, Skopje | 1,070 | 0.98 | 6.2 |
| 2 | 1972 Dec 23 | Nicaragua, Managua | 5,000 | 2 | 6.2 |
| 3 | 1976 Feb 4 | Guatemala | 23,000 | 1.1 | 7.5 |
| 4 | 1976 Jul 27 | China, Tangshan | 255,000 | 6 | 8 |
| 5 | 1977 Mar 4 | Romania, Vrancea | 1,500 | 2.0 | 7.2 |

| | | | | | |
|----|-------------|---|--------|------|-----|
| 6 | 1979 Apr 15 | Montenegro | 101 | 4.5 | 7 |
| 7 | 1980 Nov 23 | Italy, southern Campania | 4,680 | 45 | 7.2 |
| 8 | 1985 Sep 19 | Mexico, Michoacan | 9,500 | 5 | 8.1 |
| 9 | 1986 Oct 10 | El Salvador | 1,000 | 1.5 | 5.5 |
| 10 | 1988 Dec 7 | Turkey-USSR border region Spitak, Armenia | 25,000 | 17 | 7 |
| 11 | 1989 Oct 17 | Loma Prieta | 63 | 8 | 6.9 |
| 12 | 1990 Jun 21 | Western Iran, Gilan | 40,000 | 7.2 | 7.7 |
| 13 | 1990 Jul 16 | Luzon, Philippine Islands | 1,621 | 1.5 | 7.8 |
| 14 | 1994 Jan 17 | Northridge | 57 | 30 | 6.8 |
| 15 | 1995 Jan 16 | Japan, Kobe | 5,502 | 82.4 | 6.9 |
| 16 | 1999 Jan 25 | Colombia | 1,185 | 1.5 | 6.3 |
| 17 | 1999 Aug 17 | Turkey | 17,118 | 20 | 7.6 |
| 18 | 1999 Sep 20 | Taiwan | 2,297 | 0.8 | 7.6 |

Human losses in Table 2.5 are represented as a function of magnitude in Figure 2.10. In Figure 2.11 human losses are represented versus economic losses, also based on data in Table 2.5.

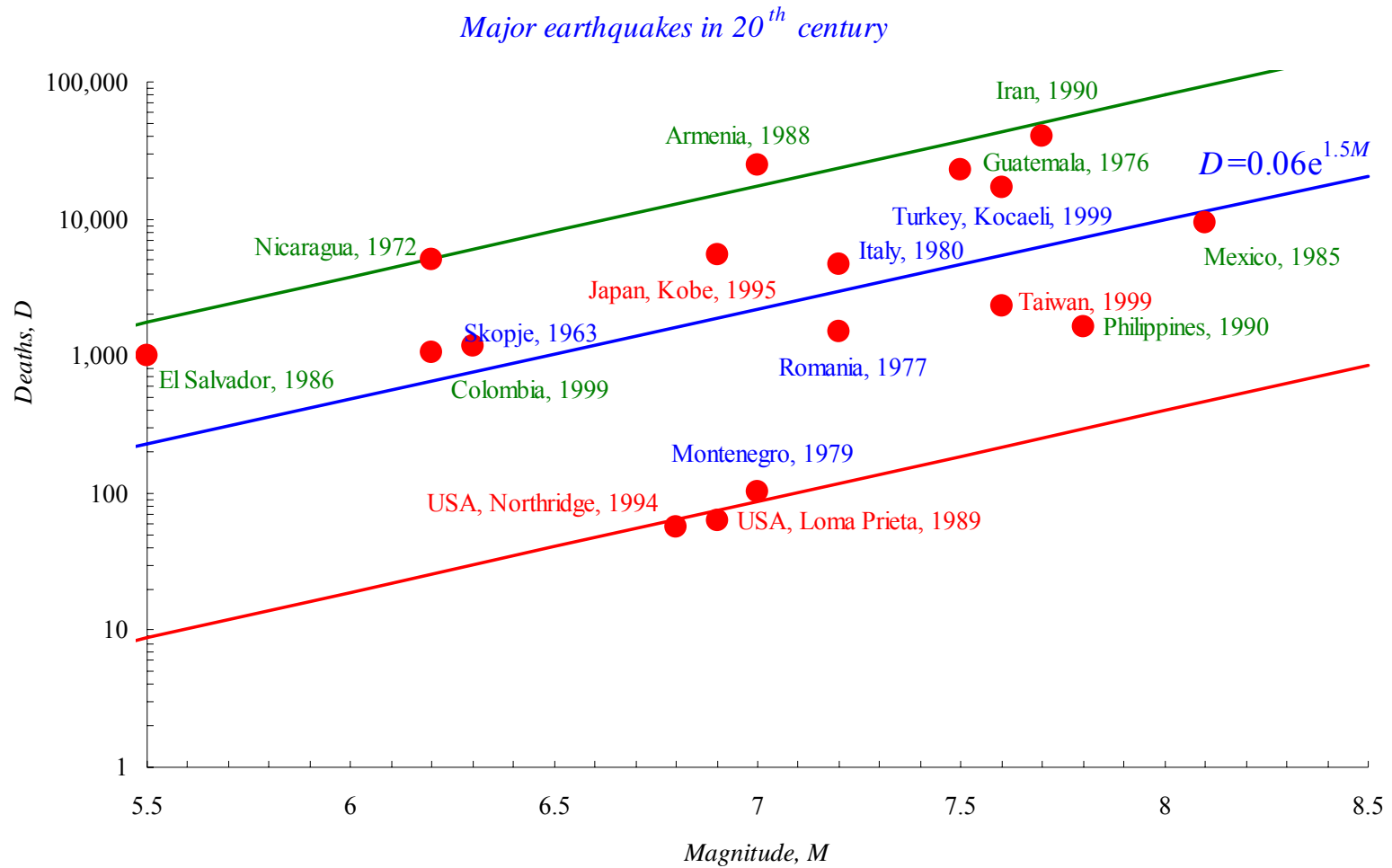


Figure 2.10. Human losses as a function of magnitude

Major earthquakes in 20th century

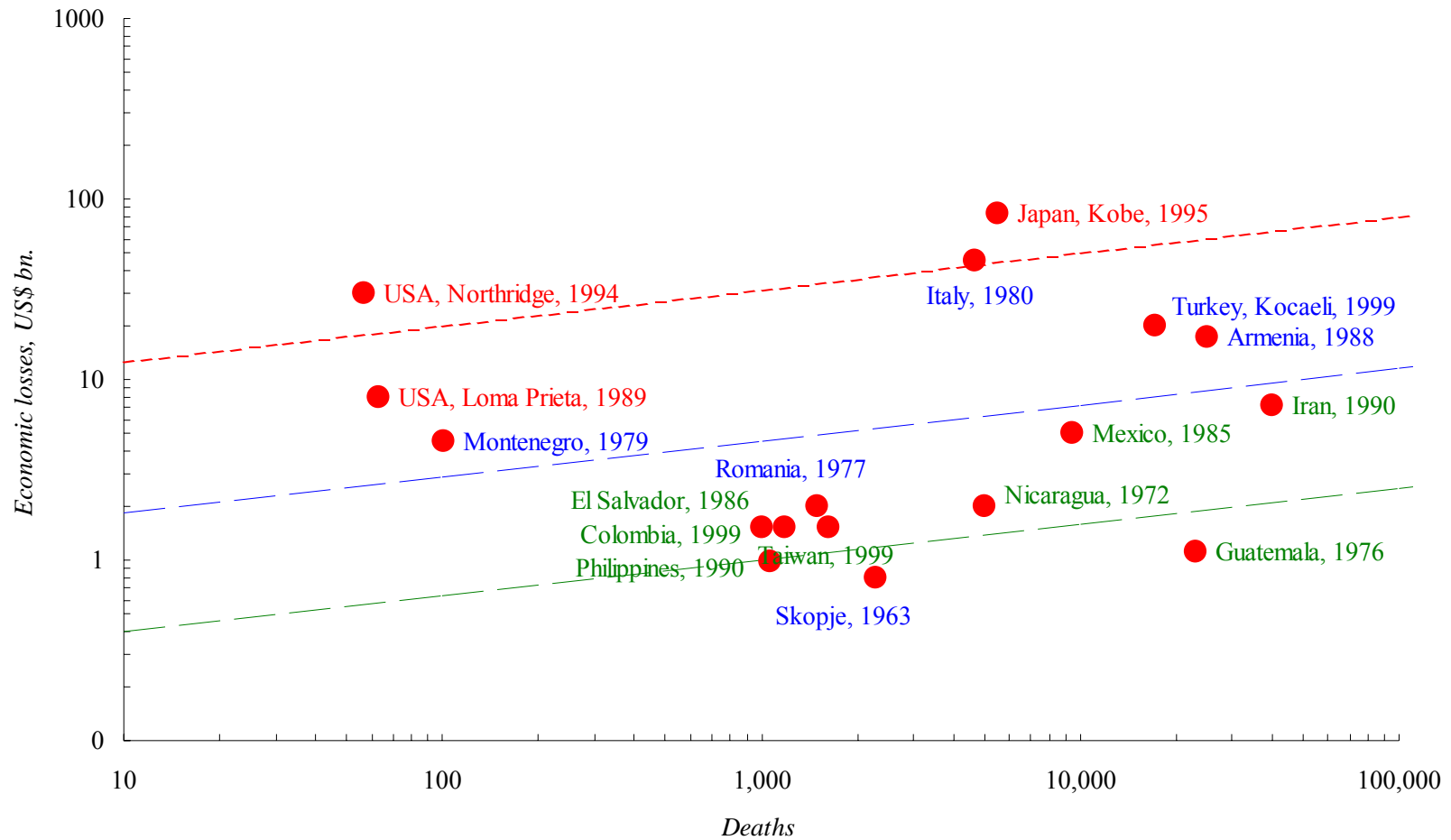


Figure 2.11. Human versus economic losses caused by earthquakes



Based on data in Table 2.5, the number of deaths from an earthquake can be related to the magnitude of the earthquake by the following relations:

$$\begin{aligned}
 D &= 0.002 \cdot e^{1.5M} && \text{--lower bound value} \\
 D &= 0.06 \cdot e^{1.5M} && \text{--median value} \\
 D &= 0.4 \cdot e^{1.5M} && \text{--upper bound value}
 \end{aligned}
 \tag{2.6}$$

where

D is the number of deaths, and
 M is the magnitude of the earthquake.

The economic losses can be related to the number of deaths from an earthquake by the following relations:

$$\begin{aligned}
 \lg L &= -0.6 + 0.2 \lg D && \text{--lower bound value} \\
 \lg L &= 0.06 + 0.2 \lg D && \text{--median value} \\
 \lg L &= 0.9 + 0.2 \lg D && \text{--upper bound value}
 \end{aligned}
 \tag{2.7}$$

where

L are the economic losses expressed in billion US\$, and
 D is the number of deaths.

The general characteristics of earthquake-induced disasters as well as the general countermeasures for emergency management are presented in Table 2.6.

Table 2.6. General characteristics of earthquake disasters, general countermeasures and special problem areas for emergency management

| <i>Characteristics</i> | <i>General counter measures</i> | <i>Special problem areas for emergency management</i> |
|---|---|--|
| <ul style="list-style-type: none"> ▪ Usually no warning, Following a major earthquake, secondary shocks may give warning of a further earthquake. ▪ Onset is sudden. ▪ Earthquake-prone areas are generally well identified and well known. ▪ Major effects arise mainly from violent ground shaking (vibration), fracture or slippage; especially they include damage (usually very severe) to | <ul style="list-style-type: none"> ▪ Development of possible warning indicators. ▪ Land-use regulations. ▪ Building regulations. ▪ Relocation of communities. ▪ Public awareness and education programs. | <ul style="list-style-type: none"> ▪ Severe and extensive damage, creating the need for urgent counter-measures, especially search and rescue, and medical assistance. ▪ Difficulty of access and movement. ▪ Widespread loss of or damage to infrastructure, essential services and life support systems. ▪ Recovery requirements (e.g. restoration and rebuilding) may be very extensive and |



| <i>Characteristics</i> | <i>General counter measures</i> | <i>Special problem areas for emergency management</i> |
|---|---------------------------------|--|
| structures and lifeline systems, plus considerable casualty due to lack of warning. | | <p>costly.</p> <ul style="list-style-type: none"> ▪ Rarity of occurrence in some areas may cause problems for economies of counter-measures and public awareness. ▪ Response problems may be severe, extensive and difficult (e.g. rescue from a high occupancy building collapses, or in a circumstances where additionally a chemical or radiation hazard exists, etc.). ▪ Victim identification may often be very difficult. |

Reduction of vulnerability to earthquakes is, clearly, an urgent goal for the coming decades. It is, moreover, one that is realizable as policy makers now have many earthquake mitigation options available. These include insurance, construction codes and standards, strengthening and retrofit, demolition of hazardous structures, relocations, siting and land-use criteria, training and exercises. The key to success will be to integrate risk assessment and risk management as an ongoing strategy aimed at avoidance of flaws in planning, design, siting, construction and use which create or increase vulnerability.

Mitigation strategies

- i. Regulating, strengthening, or removing unsafe structures
- ii. Enhancing critical utility networks and facilities [e.g., redundancy, backup power]
- iii. Improving land use planning

It is the local governments, first of all, that should recognize the risk of disasters within their domain. Decision makers and local government officials have the actual power to make the physical environment resistant against disasters through development policies such as urban planning, construction of infrastructure, land-use control, and building regulations. If urban infrastructures were to be destroyed by disasters, urban activities would be halted for a long time, severely damaging economic and social activities.

It is the communities and citizens that should recognize the risk of loss of their own houses and lives. They are supposed to build and maintain their houses in good physical condition, while local governments are not able to reinforce a huge number of inappropriately constructed buildings, most of which are owned privately, in developing countries. It is said



that earthquakes do not kill people but collapsed buildings and houses do. Unless people take action concerning their existing houses, casualties cannot be reduced by much.

Semi-public companies, which maintain basic urban infrastructures such as the telephone, and water supply, should be prepared for disasters as their disruption could cause serious damage to urban activities. Business leaders and related companies such as building owners, developers, real estate agents, and insurance/reinsurance companies should also understand the seismic risk to their properties, to avoid human loss caused by their collapse and to minimize the damage their businesses.

From experience, it can be said that even if scientists were to lay stress on such seismic risk to local governments, the officials would not take it into account. Only when the government officials can understand the possible damage through their own efforts, are they likely to take the necessary action.

Similarly, although most of the buildings seem highly vulnerable to earthquakes, and although it is obvious that certain houses would be easily destroyed, communities and residents are, in some instances, indifferent to the seismic risk. They will take appropriate action for the reinforcement of their houses only when they understand that they would be killed by their houses or lose their fortunes.

References Chapter 2

Ang A.H-S., 1987. Basis for earthquake-resistant design with tolerable structural damage, Proc. 5th International Conference on Applications of Statistics and Probability in Soil and Structural Engineering (ICASP5), Vancouver BC, Canada, Vol.1, 407-416

ATC-13, 1985. Earthquake Damage Evaluation Data for California, Applied Technology Council, Redwood City, CA.

ATC 40, 1996. Seismic Evaluation and Retrofit of Concrete Buildings, Report ATC-40, Applied Technology Council, Redwood City, CA.

Coburn, A., Spence, R., 2002. Earthquake Protection. Second Edition, John Wiley and Sons Ltd., Chichester, England

HAZUS – Technical Manual 1999. Earthquake Loss Estimation Methodology, 3 Vol.

Lungu, D., Arion, C., Baur, M., Aldea, A., 2000. Vulnerability of existing building stock in Bucharest, 6ICSZ Sixth International Conference on Seismic Zonation, Palm Springs, California, USA, Nov.12-15, p.837-846

Lungu, D., Demetriu, S., Arion, C. 1998. Seismic vulnerability of buildings exposed to Vrancea earthquakes in Romania. In Vrancea Earthquakes. Tectonics, Hazard and Risk Mitigation, Kluwer Academic Publishers, Wenzel F., Lungu D., editors, Proc. of First International Workshop on Vrancea Earthquakes, p.215-224.

Lungu, D. & Aldea, A., 1999. Understanding Urban Risk Around the World. United Nations RADIUS Project at Geohazards Int., Ca., USA. Documents for the City of Bucharest seismic profile, 29p.+25p.+8p.

National Institute of Statistics, Romanian Statistical Yearbook 2000.

Park, Y.-J & Ang, A. H.-S.. Mechanistic seismic damage model for reinforced concrete. Journal of Structural Engineering. ASCE vol. 111 (4): 722-739, 1985

Perkins, J. B. - Estimates of Uninhabitable Dwelling Units in Future Earthquakes Affecting the San Francisco Bay Region. ABAG: Oakland, California, 89 pp., 1992

Reinhorn A. M., Valles-Mattox R. E., Kunnath S. K. – Seismic Damageability Evaluation of a Typical R/C Building in the Central U.S., NCEER Bulletin, Vol. 10, No. 4, October 1996

RISK-UE "An advanced approach to earthquake risk scenarios with applications to different European towns", financed by European Commission, Fifth Framework, 2000-2004

Rubinstein, R. Y. Simulation and the Monte Carlo method. John Wiley & Sons, New York, 1981

Văcăreanu R., 2000 - Monte Carlo Simulation Technique for Vulnerability Analysis of RC Frames – An Example –Bulletin on Technical University of Civil Engineering Bucharest, pg. 9-18;

Văcăreanu, R., Lungu, D., Aldea, A., Arion, C. May 2005. "WP7 Handbook – Seismic Risk Scenarios", *Bulletin of the Technical University of Civil Engineering Bucharest*, 2/2003, p. 97-117

Văcăreanu R., 1998 - Seismic Risk Analysis for a High Rise Building - Proceedings of the 11th European



Conference on Earthquake Engineering, Paris, Abstract Volume pg. 513

Văcăreanu R., Cornea T., Lungu D. Evaluation of seismic fragility of buildings, Earthquake Hazard and Countermeasures for Existing Fragile Buildings, Editors: Lungu D. & Saito T., Independent Film, Bucharest Romania, 315p

Williams, M. S. & Sexsmith, R. G. 1995. Seismic Damage Indices for Concrete Structures: A State-of-the-Art Review. Earthquake Spectra. Vol. 11(2): 319-345, 1997

Annex A: Tables

Table A.1. Suggested unit weight for structural elements as building debris, adapted from HAZUS, 1999, in t/ m²

| <i>Building Typology</i> | <i>Brick, Wood and Other</i> | <i>Reinforced Concrete and Steel</i> |
|---|------------------------------|--------------------------------------|
| M1.1, M1.2, M1.3, M2, M3.1, M 3.2, M3.3, M3.4 | 0.38 | 0.45 – 0.6 t/m ² |
| M4, M5, RC3.1, RC3.2 | 0.2 – 0.25 | 0.85 – 1.05 t/m ² |
| RC1, RC2, RC4, RC6 | 0 | 1.05 – 1.3 t/m ² |
| RC5 | 0.1 | 0.45 t/m ² |
| S1, S2 | 0.45 – 0.5 | 0.5 t/m ² |
| S3 | 0.25 | 0.5 t/m ² |
| S4, S5 | 0 | 0.7 t/m ² |
| W | 0.1 | 0.17 t/m ² |

Table A.2. Suggested brick, wood, and other debris generated from damaged structural elements, adapted from HAZUS, 1999, in fraction of weight

| <i>Building Typology</i> | <i>Structural Damage State</i> | | | |
|---|--------------------------------|-----------------|------------------|-----------------|
| | <i>Slight</i> | <i>Moderate</i> | <i>Extensive</i> | <i>Complete</i> |
| M1.1, M1.2 M1.3, M2 M3.1, M 3.2 M3.3, M3.4 | 0.05 | 0.25 | 0.55 | 1 |
| M4, M5 RC3.1, RC3.2 | 0.05 | 0.25 | 0.6 | 1 |
| RC1, RC2, RC4, RC6, S1, S2, S4, S5 | 0 | 0 | 0 | 1 |
| RC5 | 0 | 0.06 | 0.32 | 1 |
| S3 | 0.05 | 0.25 | 0.6 | 1 |
| W | 0 | 0.05 | 0.34 | 1 |



Table A.3. Suggested reinforced concrete and wrecked steel generated from damaged structural elements, adapted from HAZUS, 1999, in fraction of weight

| Building Typology | Structural Damage State | | | |
|--|-------------------------|----------|-----------|----------|
| | Slight | Moderate | Extensive | Complete |
| M1.1, M1.2 M1.3, M2 M3.1, M 3.2, M3.3, M3.4 | 0 | 0.02 | 0.25 | 1 |
| M4, M5 | 0 | 0.03 | 0.305 | 1 |
| RC1 | 0 | 0.05 | 0.33 | 1 |
| RC2 | 0.01 | 0.08 | 0.35 | 1 |
| RC3.1, RC3.2 | 0 | 0.04 | 0.32 | 1 |
| RC4, RC5, RC6 | 0.02 | 0.1 | 0.35 | 1 |
| S1, S2, S3 | 0 | 0.04 | 0.3 | 1 |
| S4, S5 | 0.02 | 0.1 | 0.4 | 1 |
| W | 0 | 0.03 | 0.27 | 1 |

Table A.4. Earthquakes with 1,000 or More Deaths from 1900 (Source: USGS, www.usgs.gov)

| No. | Date UTC | Location | Deaths | Magnitude | Comments |
|-----|-------------|---|----------------------|-----------|-------------------------------------|
| 1 | 1902 Apr 19 | Guatemala, 14 N 91 W | 2,000 | 7.5 | |
| 2 | 1902 Dec 16 | Turkestan, 40.8 N 72.6 E | 4,500 | 6.4 | |
| 3 | 1903 Apr 19 | Turkey, 39.1 N 42.4 E | 1,700 | | |
| 4 | 1903 Apr 28 | Turkey, 39.1 N 42.5 E | 2,200 | 6.3 | |
| 5 | 1905 Apr 4 | India, Kangra, 33.0 N 76.0 E | 19,000 | 8.6 | |
| 6 | 1905 Sep 8 | Italy, Calabria, 39.4 N 16.4 E | 2,500 | 7.9 | |
| 7 | 1906 Jan 31 | Colombia, 1 N 81.5 W | 1,000 | 8.9 | |
| 8 | 1906 Mar 16 | Formosa, Kagi, (Taiwan), 23.6 N 120.5 E | 1,300 | 7.1 | |
| 9 | 1906 Aug 17 | Chile, Santiago, 33 S 72 W | 20,000 | 8.6 | |
| 10 | 1907 Jan 14 | Jamaica, Kingston, 18.2 N 76.7 W | 1,600 | 6.5 | |
| 11 | 1907 Oct 21 | Central Asia, 38 N 69 E | 12,000 | 8.1 | |
| 12 | 1908 Dec 28 | Italy, Messina, 38 N 15.5 E | 70,000 to 100,000 | 7.5 | Deaths from earthquake and tsunami. |
| 13 | 1909 Jan 23 | Iran, 33.4 N 49.1 E | 5,500 | 7.3 | |
| 14 | 1912 Aug 9 | Marmara Sea, 40.5 N 27 E | 1,950 | 7.8 | |
| 15 | 1915 Jan 13 | Italy, Avezzano, 42 N 13.5 E | 29,980 | 7.5 | |
| 16 | 1917 Jan 21 | Indonesia, Bali, 8.0 S 115.4 E | 15,000 | | |
| 17 | 1917 Jul 30 | China, 28.0 N 104.0 E | 1,800 | 6.5 | |
| 18 | 1918 Feb 13 | China, Kwangtung, (Guangdong) 23.5 N 117.0 E | 10,000 | 7.3 | |
| 19 | 1920 Dec 16 | China, Gansu, 35.8 N 105.7 E | 200,000 | 8.6 | Major fractures, landslides. |
| 20 | 1923 Mar 24 | China, 31.3 N 100.8 E | 5,000 | 7.3 | |
| 21 | 1923 May 25 | Iran, 35.3 N 59.2 E | 2,200 | 5.7 | |
| 22 | 1923 Sep 1 | Japan, Kanto, Tokyo-Yokohama 35.0 N 139.5 E | 143,000 | 8.3 | Great Tokyo fire. |
| 23 | 1925 Mar 16 | China, Yunnan, 25.5 N 100.3 E | 5,000 | 7.1 | Talifu almost completely destroyed. |
| 24 | 1927 Mar 7 | Japan, Tango, 35.8 N 134.8 E | 3,020 | 7.9 | |
| 25 | 1927 May 22 | China, near Xining, 36.8 N 102.8 E | 200,000 | 8.3 | Large fractures. |
| 26 | 1929 May 1 | Iran, 38 N 58 E | 3,300 | 7.4 | |
| 27 | 1930 May 6 | Iran, 38.0 N 44.5 E | 2,500 | 7.2 | |
| 28 | 1930 Jul 23 | Italy, 41.1 N 15.4 E | 1,430 | 6.5 | |
| 29 | 1931 Mar 31 | Nicaragua, 13.2 N 85.7 W | 2,400 | 5.6 | |
| 30 | 1932 Dec 25 | China, Gansu, 39.7 N 97.0 E | 70,000 | 7.6 | |
| 31 | 1933 Mar 2 | Japan, Sanriku, 39.0 N 143.0 E | 2,990 | 8.9 | |



| No. | Date UTC | Location | Deaths | Magnitude | Comments |
|-----|-------------|---|---------------------|-----------|---|
| 32 | 1933 Aug 25 | China, 32.0 N 103.7 E | 10,000 | 7.4 | |
| 33 | 1934 Jan 15 | India, Bihar-Nepal, 26.6 N 86.8 E | 10,700 | 8.4 | |
| 34 | 1935 Apr 20 | Formosa, 24.0 N 121.0 E | 3,280 | 7.1 | |
| 35 | 1935 May 30 | Pakistan, Quetta, 29.6 N 66.5 E | 30,000 to 60,000 | 7.5 | Quetta almost completely destroyed. |
| 36 | 1935 Jul 16 | Taiwan, 24.4 N 120.7 E | 2,700 | 6.5 | |
| 37 | 1939 Jan 25 | Chile, Chillan, 36.2 S 72.2 W | 28,000 | 8.3 | |
| 38 | 1939 Dec 26 | Turkey, Erzincan, 39.6 N 38 E | 30,000 | 8.0 | |
| 39 | 1940 Nov 10 | Romania, 45.8 N 26.8 E | 1,000 | 7.3 | |
| 40 | 1942 Nov 26 | Turkey, 40.5 N 34.0 E | 4,000 | 7.6 | |
| 41 | 1942 Dec 20 | Turkey, Erbaa, 40.9 N 36.5 E | 3,000 | 7.3 | Some reports of 1,000 killed. |
| 42 | 1943 Sep 10 | Japan, Tottori, 33.6 N 134.2 E | 1,190 | 7.4 | |
| 43 | 1943 Nov 26 | Turkey, 41.0 N 33.7 E | 4,000 | 7.6 | |
| 44 | 1944 Jan 15 | Argentina, San Juan, 31.6 S 68.5 W | 5,000 | 7.8 | Reports of as many as 8,000 killed. |
| 45 | 1944 Feb 1 | Turkey, 41.4 N 32.7 E | 2,800 | 7.4 | Reports of as many as 5,000 killed. |
| 46 | 1944 Dec 7 | Japan, Tonankai, 33.7 N 136.2 E | 1,000 | 8.3 | |
| 47 | 1945 Jan 12 | Japan, Mikawa, 34.8 N 137.0 E | 1,900 | 7.1 | |
| 48 | 1945 Nov 27 | Iran, 25.0 N 60.5 E | 4,000 | 8.2 | |
| 49 | 1946 May 31 | Turkey, 39.5 N 41.5 E | 1,300 | 6.0 | |
| 50 | 1946 Nov 10 | Peru, Ancash, 8.3 S 77.8 W | 1,400 | 7.3 | Landslides, great destruction. |
| 51 | 1946 Dec 20 | Japan, Tonankai, 32.5 N 134.5 E | 1,330 | 8.4 | |
| 52 | 1948 Jun 28 | Japan, Fukui, 36.1 N 136.2 E | 5,390 | 7.3 | |
| 53 | 1948 Oct 5 | USSR, (Turkmenistan, Ashgabat) 38.0 N 58.3 E | 110,000 | 7.3 | |
| 54 | 1949 Aug 5 | Ecuador, Ambato, 1.2 S 78.5 E | 6,000 | 6.8 | Large landslides, topographical changes. |
| 55 | 1950 Aug 15 | India, Assam, Tibet, 28.7 N 96.6 E | 1,530 | 8.7 | Great topographical changes, landslides, floods. |
| 56 | 1954 Sep 9 | Algeria, Orleansville, 36 N 1.6 E | 1,250 | 6.8 | |
| 57 | 1957 Jun 27 | USSR, (Russia), 56.3 N 116.5 E | 1,200 | | |
| 58 | 1957 Jul 2 | Iran, 36.2 N 52.7 E | 1,200 | 7.4 | |
| 59 | 1957 Dec 13 | Iran, 34.4 N 47.6 E | 1,130 | 7.3 | |
| 60 | 1960 Feb 29 | Morocco, Agadir, 30 N 9 W | 10,000 to 15,000 | 5.9 | Occurred at shallow depth just under city. |
| 61 | 1960 May 22 | Chile, 39.5 S 74.5 W | 4,000 to 5,000 | 9.5* | More than 2,000 killed, 3,000 injured, 2,000,000 homeless, and \$550 million damage in Hawaii; 138 deaths and \$50 million damage in Japan; 32 dead and missing in the Philippines; and \$500,000 damage to the west coast of the United States |
| 62 | 1962 Sep 1 | Iran, Qazvin, 35.6 N 49.9 E | 12,230 | 7.3 | |
| 63 | 1963 Jul 26 | Yugoslavia, Skopje, 42.1 N 21.4 E | 1,100 | 6.0 | Occurred at shallow depth just under city. |
| 64 | 1966 Aug 19 | Turkey, Varto, 39.2 N 41.7 E | 2,520 | 7.1 | |
| 65 | 1968 Aug 31 | Iran, 34.0 N 59.0 E | 12,000 to 20,000 | 7.3 | |
| 66 | 1969 Jul 25 | Eastern China, 21.6 N 111.9 E | 3,000 | 5.9 | |
| 67 | 1970 Jan 4 | Yunnan Province, China, 24.1 N 102.5 E | 10,000 | 7.5 | |
| 68 | 1970 Mar 28 | Turkey, Gediz, 39.2 N 29.5 E | 1,100 | 7.3 | |
| 69 | 1970 May 31 | Peru, 9.2 S 78.8 W | 66,000 | 7.8 | \$530,000 damage, great rock slide, floods. |
| 70 | 1972 Apr 10 | Southern Iran, 28.4 N 52.8 E | 5,054 | 7.1 | |



| No. | Date UTC | Location | Deaths | Magnitude | Comments |
|-----|---------------|--|--------------------|-----------|--|
| 71 | 1972 Dec 23 | Nicaragua, Managua, 12.4 N 86.1 W | 5,000 | 6.2 | |
| 72 | 1974 May 10 | China, 28.2 N 104.0 E | 20,000 | 6.8 | |
| 73 | 1974 Dec 28 | Pakistan, 35.0 N 72.8 E | 5,300 | 6.2 | |
| 74 | 1975 Feb 4 | China, 40.6 N 122.5 E | 10,000 | 7.4 | |
| 75 | 1975 Sep 6 | Turkey, 38.5 N 40.7 E | 2,300 | 6.7 | |
| 76 | 1976 Feb 4 | Guatemala, 15.3 N 89.1 W | 23,000 | 7.5 | |
| 77 | 1976 May 6 | Northeastern Italy, 46.4 N 13.3 E | 1,000 | 6.5 | |
| 78 | 1976 Jun 25 | West Irian, (New Guinea), 4.6 S 140.1 E | 422 | 7.1 | 5,000 to 9,000 missing and presumed dead. |
| 79 | 1976 Jul 27 | China, Tangshan, 39.6 N 118.0 E | 255,000 (official) | 8.0 | Estimated death toll as high as 655,000. |
| 80 | 1976 Aug 16 | Philippines, Mindanao, 6.3 N 124.0 E | 8,000 | 7.9 | |
| 81 | 1976 Nov 24 | Iran-USSR border, 39.1 N 44.0 E | 5,000 | 7.3 | Deaths estimated. |
| 82 | 1977 Mar 4 | Romania, 45.8 N 26.8 E | 1,500 | 7.2 | |
| 83 | 1978 Sep 16 | Iran, 33.2 N 57.4 E | 15,000 | 7.8 | |
| 84 | 1980 Oct 10 | Algeria, El Asnam, (formerly Orleansville), 36.1 N 1.4 E | 3,500 | 7.7 | |
| 85 | 1980 Nov 23 | Italy, southern Campania, 40.9 N 15.3 E | 4,680 | 7.2 | |
| 86 | 1981 Jun 11 | Southern Iran, 29.9 N 57.7 E | 3,000 | 6.9 | |
| 87 | 1981 Jul 28 | Southern Iran, 30.0 N 57.8 E | 1,500 | 7.3 | |
| 88 | 1982 Dec 13 | Western Arabian Peninsula, 14.7N 44.4 E | 2,800 | 6.0 | |
| 89 | 1983 Oct 30 | Turkey, 40.3 N 42.2 E | 1,342 | 6.9 | |
| 90 | 1985 Sep 19 | Mexico, Michoacan, 18.2 N 102.5 W | 9,500 (official) | 8.1 | Estimated death toll as high as 30,000. |
| 91 | 1986 Oct 10 | El Salvador, 13.8 N 89.2 W | 1,000+ | 5.5 | |
| 92 | 1987 Mar 6 | Colombia-Ecuador, 0.2 N 77.8 W | 1,000+ | 7.0 | |
| 93 | 1988 Aug 20 | Nepal-India border region, 26.8 N 86.6 E | 1,450 | 6.6 | |
| 94 | 1988 Dec 7 | Turkey-USSR border region Spitak, Armenia, 41.0 N 44.2 E | 25,000 | 7.0 | |
| 95 | 1989 Oct 17 | Loma Prieta | 63 | 6.9 | 3,757injuries 5,900Property Damage (\$ Million) |
| 96 | 1990 Jun 21 | Western Iran, Gilan, 37.0 N 49.4 E | 40,000 to 50,000 | 7.7 | Landslides. |
| 97 | 1990 Jul 16 | Luzon, Philippine Islands, 15.7 N 121.2 E | 1,621 (2,600) | 7.8 | Landslides, subsidence, and sand blows. |
| 98 | 1991 Oct 19 | Northern India, 30.8 N 78.8 E | 2,000 | 7.0 | |
| 99 | 1992 April 26 | Cape Mendocino | | 6.5 | 356 injuries 48.3 Property Damage (\$ Million) |
| 100 | 1992 June 28 | Big Bear | 1 | 6.6 | 402 injuries 91.1 Property Damage (\$ Million) |
| 101 | 1992 Dec 12 | Flores Region, Indonesia, 8.5 S 121.9 E | 2,500 | 7.5 | Tsunami ran inland 300 meters; wave height 25 meters. |
| 102 | 1993 Sep 29 | Southern India, 18.1 N 76.5 E | 9,748 | 6.3 | |
| 103 | 1994 Jan 17 | Northridge | 57 | 6.8 | 9,000 injuries 10,000 Property Damage (\$ Million) |
| 104 | 1995 Jan 16 | Japan, Kobe, Near S. Coast of Western Honshu, 34.6 N 135 E | 5,502 | 6.9 | Landslide, liquefaction. |
| 105 | 1995 May 27 | Sakhalin Island, 52.6 N 142.8 E | 1,989 | 7.5 | |
| 106 | 1997 May 10 | Northern Iran, 33.9 N 59.7 E | 1,560 | 7.5 | 4,460 injured, 60,000 homeless. |
| 107 | 1998 Feb 04 | Afghanistan-Tajikistan Border Region, 37.1 N 70.1 E | 2,323 | 6.1 | 818 injured, 8,094 houses destroyed, 6,725 livestock killed. |
| 108 | 1998 May 30 | Afghanistan-Tajikistan Border Region, | 4,000 | 6.9 | Many thousands injured and |



| No. | Date UTC | Location | Deaths | Magnitude | Comments |
|-----|-------------|--|--------|-----------|---|
| | | 37.1 N 70.1 E | | | homeless. |
| 109 | 1998 Jul 17 | Papua New Guinea, Near N. Coast, 2.96 S 141.9 E | 2,183 | 7.1 | Thousands injured, about 9,500 homeless and about 500 missing as a result of a tsunami with maximum wave heights estimated at 10 meters. |
| 110 | 1999 Jan 25 | Colombia, 4.46 N 75.82 W | 1,185 | 6.3 | At least 1,185 killed, over 700 missing and presumed killed, over 4,750 injured, and over 250,000 homeless. |
| 111 | 1999 Aug 17 | Turkey, 40.7 N 30.0 E | 17,118 | 7.6 | More than 17,000 killed, 50,000 injured, thousands missing, and about 600,000 homeless. Damage estimated at 3 to 6.5 billion U.S. dollars. |
| 112 | 1999 Sep 20 | Taiwan, 23.7 N 121.0 E | 2,297 | 7.6 | At least 2,400 killed, over 8,700 injured, 82,000 housing units damaged, and 600,000 left homeless. Damaged estimated at 14 billion U.S. dollars. |
| 113 | 2001 Jan 26 | India, 23.3 N 70.3 E | 20,023 | 7.7 | At least 20,005 people killed, 166,836 injured, approximately 339,000 buildings destroyed and 783,000 damaged in the Bhuj-Ahmadabad-Rajkot area and other parts of Gujarat. Many bridges and roads damaged in Gujarat. At least 18 people killed and some injured in southern Pakistan. Felt throughout northern India and much of Pakistan. Also felt in Bangladesh and western Nepal. The earthquake occurred along an approximately east-west trending thrust fault at shallow depth. The stress that caused this earthquake is due to the Indian plate pushing northward into the Eurasian plate. Complex earthquake. A small event is followed by a larger one about 2 seconds later.. |
| 114 | 2002 Mar 25 | Hindu Kush Region, Afghanistan, 35.9 N 69.2 E | 1,000 | 6.1 | 4,000 injured, 1,500 houses destroyed in the Nahrin area. Approximately 20,000 people homeless. |
| 115 | 2003 May 21 | Northern Algeria | 2000 | 6.8 | At least 2,000 people killed, 1,136 missing, 9,085 injured, 200,000 homeless and extensive damage (X) in the Algiers-Bourmerdes-Thenia area. A tsunami generated with an estimated wave height |



| No. | Date UTC | Location | Deaths | Magnitude | Comments |
|-----|----------|----------|--------|-----------|---|
| | | | | | of 2m caused damage to boats and underwater telephone cables off the Balearic Islands, Spain. Also felt in Monaco and southwestern Spain. |

Annex B: Case study

Case study on mid-rise and high-rise RC residential buildings built in Bucharest in-between 1978 and 1990 – corresponding to moderate earthquake resistant code period

The following categories of buildings were considered:

RC1M – mid rise RC frames

RC1H – high rise RC frames



Figure B.1. Typical RC frame apartment building, built in 80's

RC2M – mid rise RC shear walls

RC2H – high rise RC shear wall



Figure B.2. Typical RC shear wall apartment building

Seismic action

The seismic action is described by the acceleration spectrum with 475 yr. *MRI* defined in *RISK-UE Project*, Figure B.3.

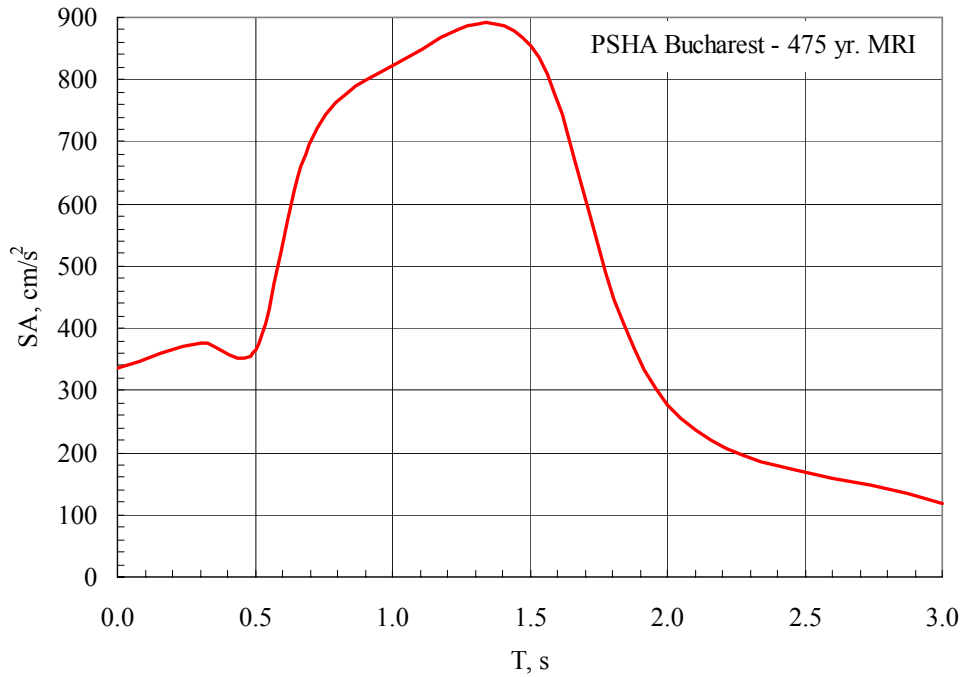


Figure B.3. Elastic acceleration response spectrum, *MRI* = 475 yr.

The spectrum was converted into *ADRS* format, Figure B.4.

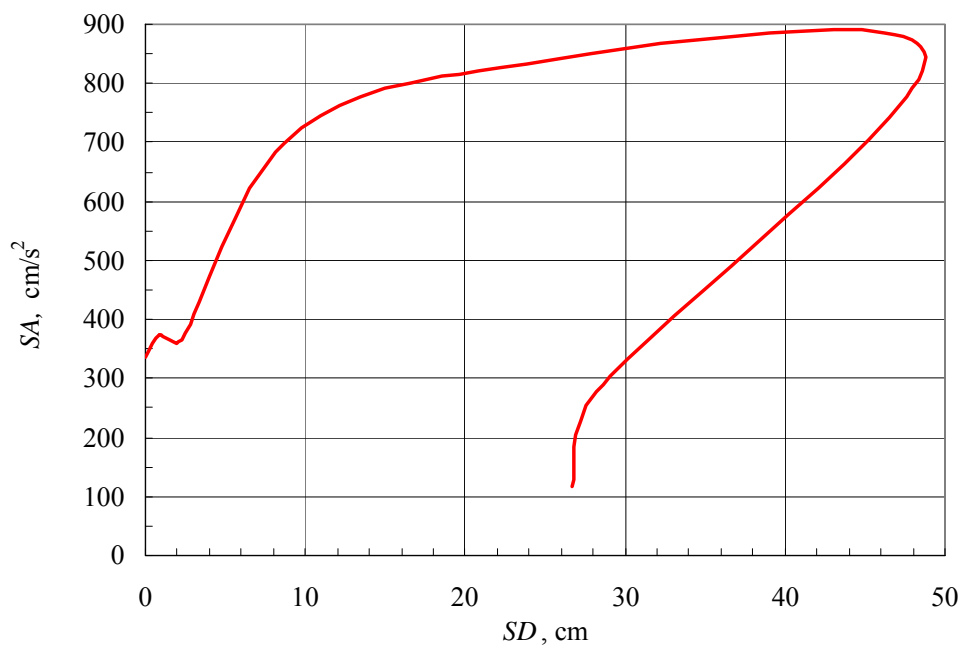


Figure B.4. *ADRS* format for seismic action



The acceleration spectrum was reduced for inelastic effects, Figure B.5 using strength reduction factors and converted back to ADRS format, Figure B.6.

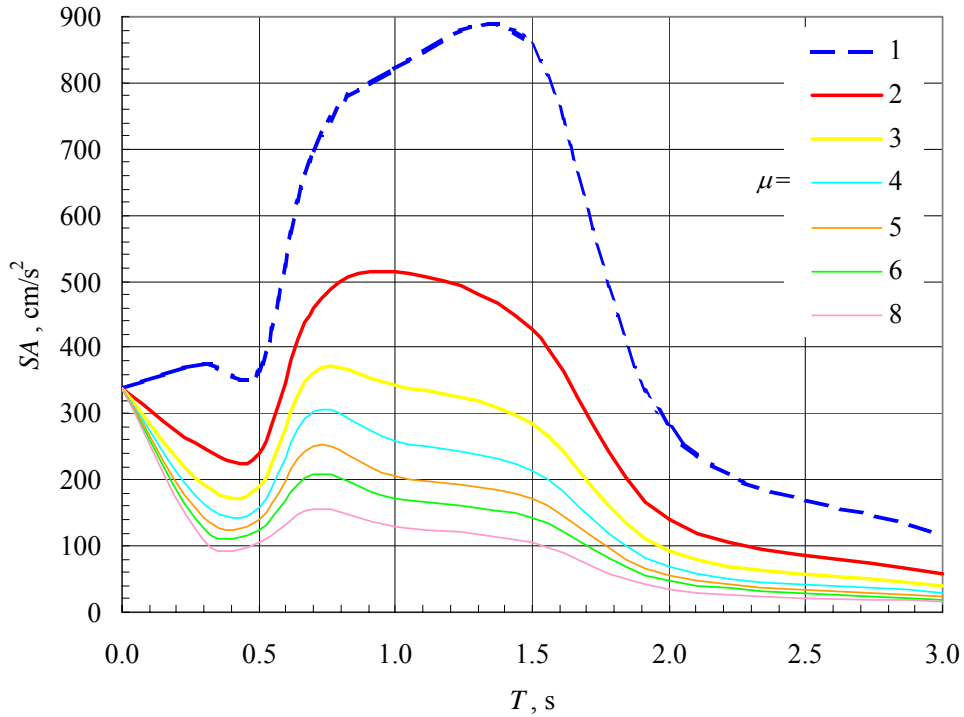


Figure B.5. Inelastic acceleration response spectrum

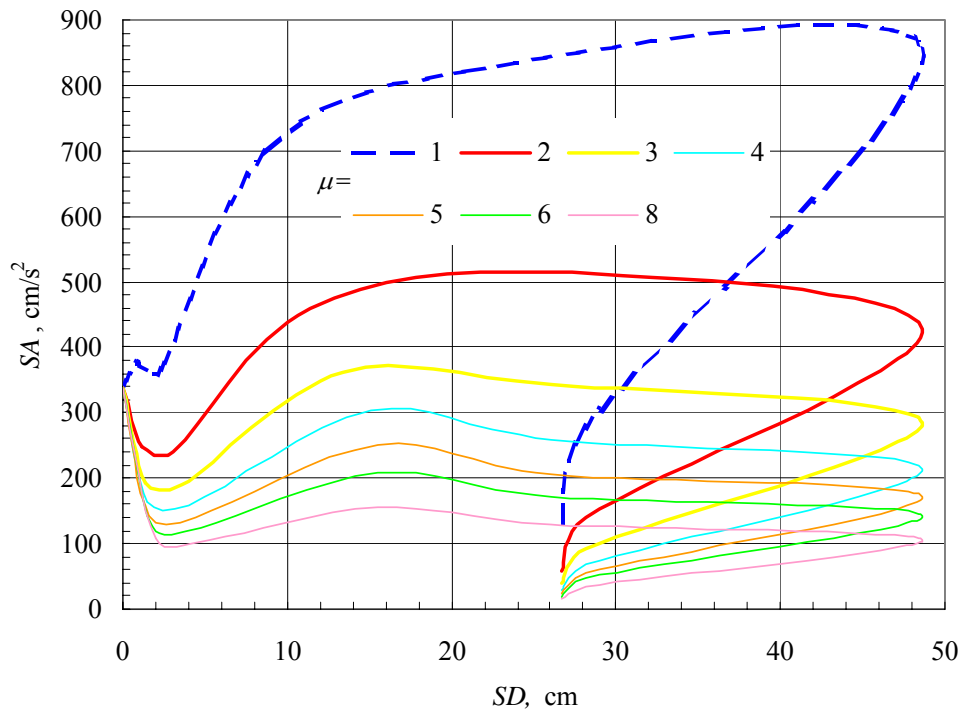


Figure B.6. Elastic and inelastic ADRS



Direct physical losses

Capacity spectrum method was applied to get the expected response of building types (Figure B.7, Figure B.9, Figure B.11 and Figure B.13) and fragility functions (Figure B.8, Figure B.10, Figure B.12 and Figure B.14) were derived.

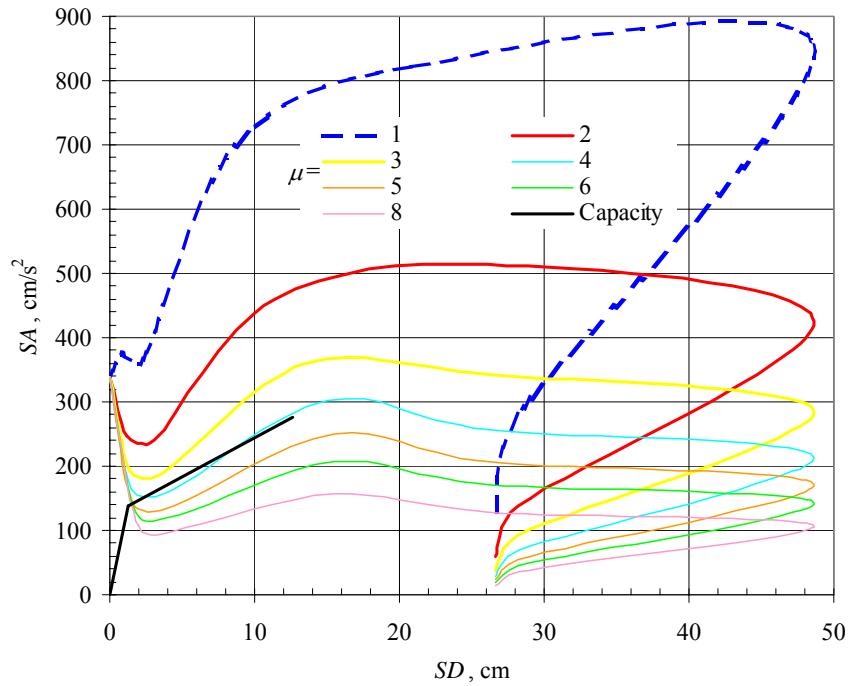


Figure B.7. Expected response of *RCIM* building type

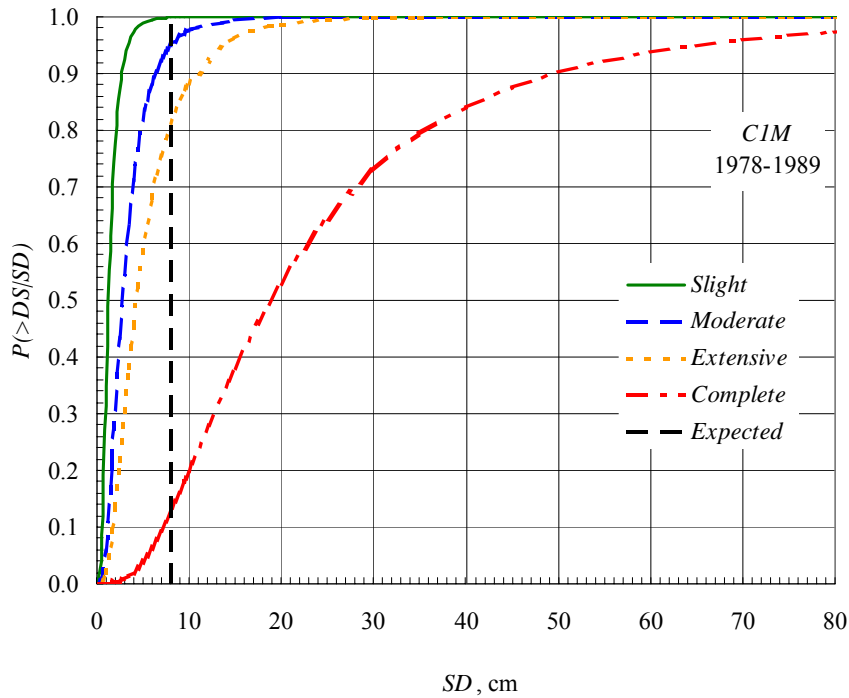


Figure B.8. Fragility functions of *RCIM* building type

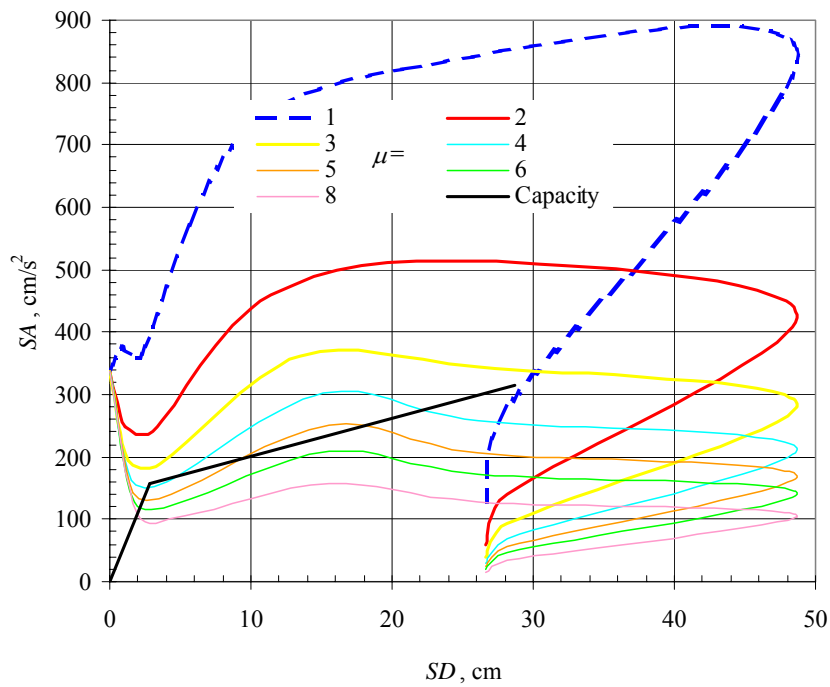


Figure B.9. Expected response of *RC1H* building type

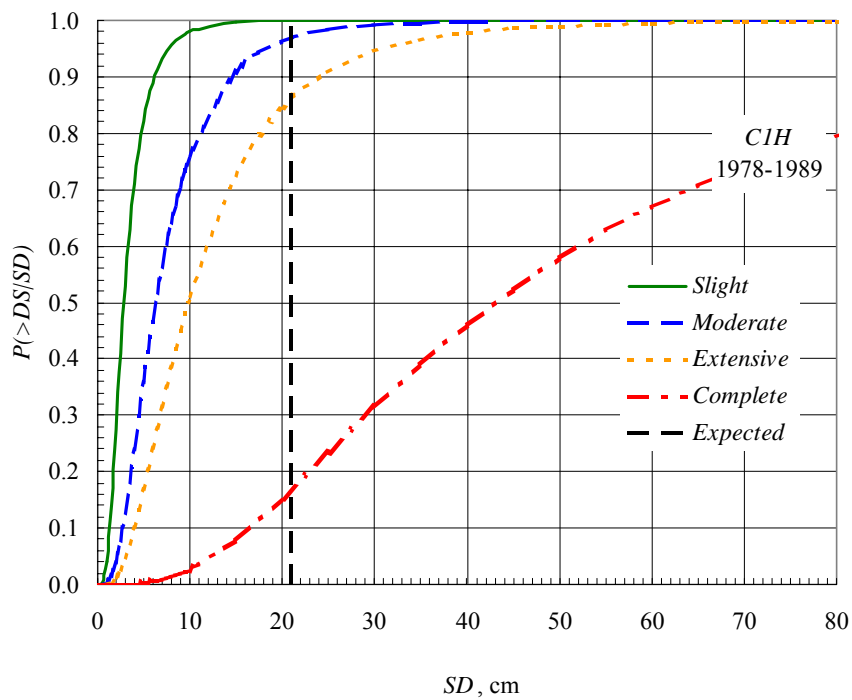


Figure B.10. Fragility functions of *RC1H* building type

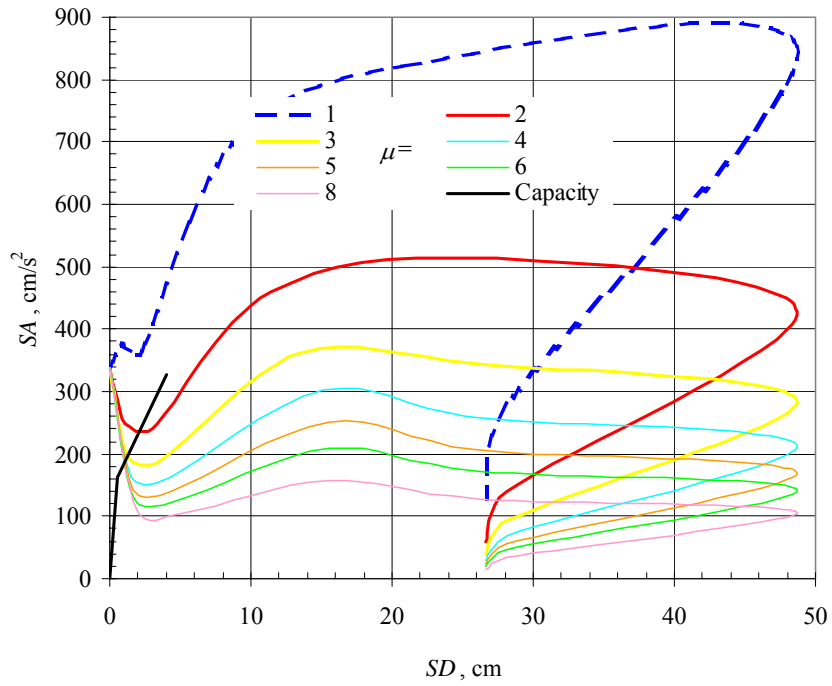


Figure B.11. Expected response of RC2M building type

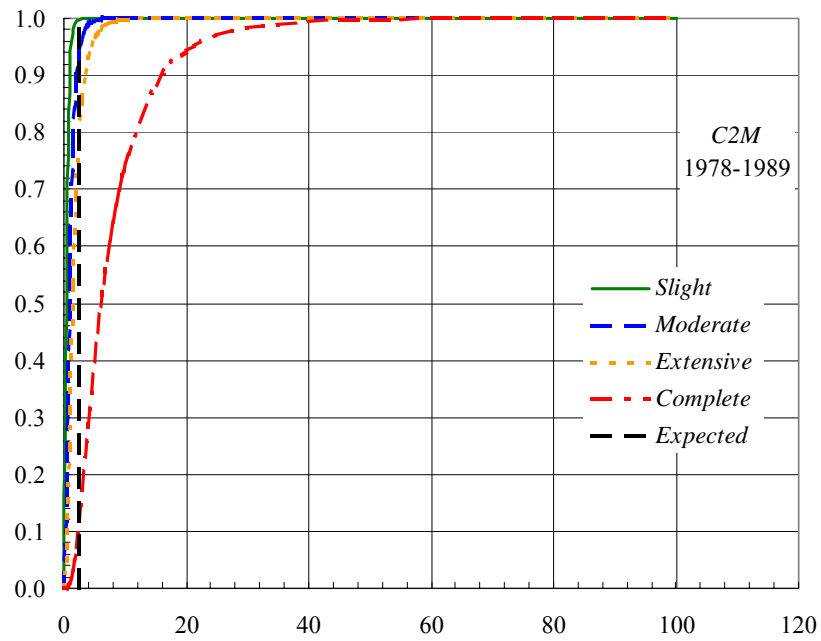


Figure B.12. Fragility functions of RC2M building type

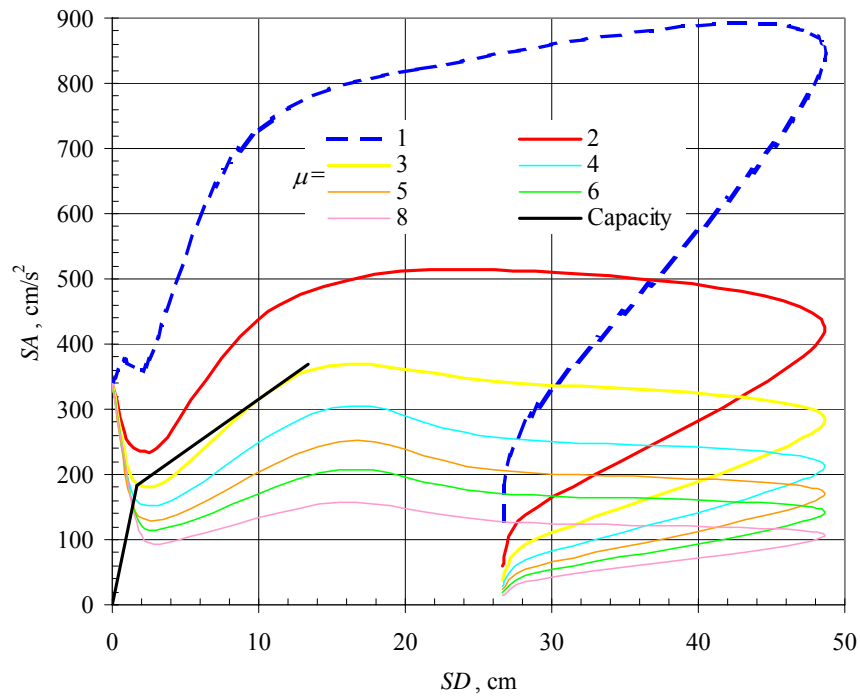


Figure B.13. Expected response of RC2H building type

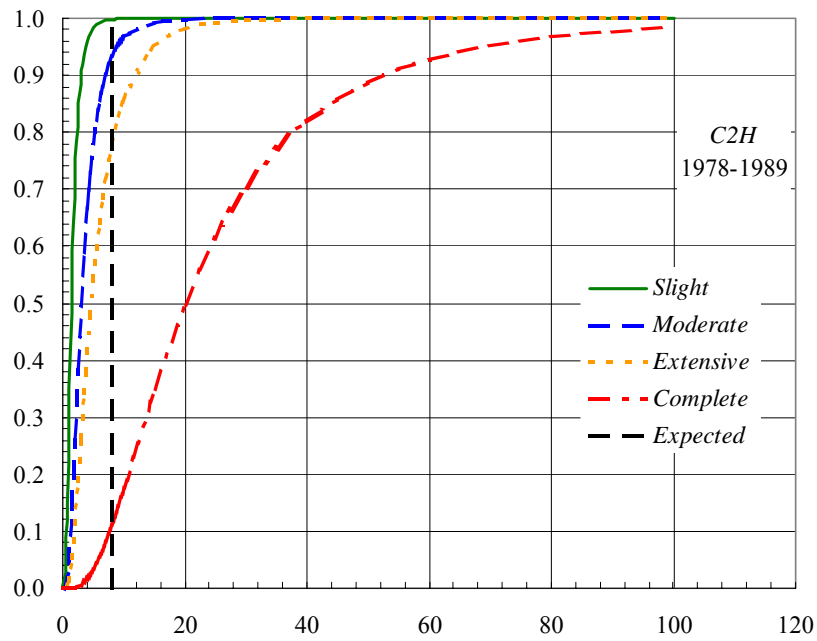


Figure B.14. Fragility functions of RC2H building type



Given the expected response and the fragility functions, the following damage probability matrix was obtained for the analysed building typologies, Table 1.1.

Table B.1. Damage probability matrix

| <i>ds</i> | <i>P(ds/Sd)</i> | | | |
|-----------|-----------------|-------------|-------------|-------------|
| | <i>RC1M</i> | <i>RC1H</i> | <i>RC2M</i> | <i>RC2H</i> |
| <i>N</i> | 0.001 | 0.001 | 0.002 | 0.002 |
| <i>S</i> | 0.052 | 0.038 | 0.060 | 0.066 |
| <i>M</i> | 0.137 | 0.116 | 0.145 | 0.152 |
| <i>E</i> | 0.686 | 0.692 | 0.676 | 0.671 |
| <i>C</i> | 0.125 | 0.153 | 0.118 | 0.109 |

The building stock in Bucharest built in between 1977 and 1990 corresponding to the analyzed building types is expressed in millions of m² of floor area as follows in Table B.2:

Table B.2. Total floor area, in millions of m²

| <i>RC1M</i> | <i>RC1H</i> | <i>RC2M</i> | <i>RC2H</i> |
|-------------|-------------|-------------|-------------|
| 0.43 | 2.225236 | 0.3 | 5.1922182 |

Assuming a ratio of 0.05 persons/m² one gets the number of people living in each building type, Table B.3.

Table B.3. Number of inhabitants in each building type

| <i>RC1M</i> | <i>RC1H</i> | <i>RC2M</i> | <i>RC2H</i> |
|-------------|-------------|-------------|-------------|
| 21500 | 111262 | 14333 | 259611 |

Debris

The expected debris fraction for model building type *k* and debris type *i* due to structural damage is given by, HAZUS, 1999:

$$EDF_s(i, k) = \sum_{j=2}^5 P_s(j, k) * DF_s(i, j, k) \quad (B.1)$$

where:

- $EDF_s(i, k)$ - the expected debris fraction of debris type *i* due to structural damage for building type *k*, Table B.5
- $P_s(j, k)$ - the probability of structural damage state *j* for building type *k* at the location being considered, given in Table B.1
- $DF_s(i, j, k)$ - the debris fraction of debris type *i* for building type *k* in structural damage state *j*, given in Table B.4

The expected debris fraction of debris type *i* due to structural damage for building type *k* is given in Table B.5. These values indicate the expected percentage of debris type *i* generated due to structural damage to building type *k*. If one knows the total floor area of each building type and weights of debris of type *i* per 1000 m² of building, then the amount of debris for this particular location can be obtained by multiplying the expected debris fraction of debris type *i* due to structural damage for building type *k*, Table B.5 with the weight of debris type *i*



per 1000 m² of floor area of model building type *k* (From Table B.6) and with the total floor area of each building type, Table B.2 and the summing for all *k* in Table B.8.

Table B.4. Reinforced concrete and wrecked steel generated from damaged structural elements, in percentage of weight

| Building type | Structural damage state | | | |
|---------------|-------------------------|----------|-----------|----------|
| | Slight | Moderate | Extensive | Complete |
| RC1M | 0 | 5 | 33 | 100 |
| RC1H | 0 | 5 | 33 | 100 |
| RC2M | 1 | 8 | 35 | 100 |
| RC2H | 1 | 8 | 35 | 100 |

Table B.5. Expected fraction of debris, in percentage of weight

| | |
|------|-------|
| RC1M | 35.83 |
| RC1H | 38.73 |
| RC2M | 36.66 |
| RC2H | 35.71 |

Table B.6. Unit weight for structural elements, adapted from HAZUS, 1999, in t/1000m²

| Building Type | Reinforced Concrete and Steel |
|---------------|-------------------------------|
| RC1M | 1055 |
| RC1H | 1055 |
| RC2M | 1206 |
| RC2H | 1206 |

Table B.7. Reinforced concrete and wrecked steel generated from damaged structural elements, in t/1000m²

| | |
|------|--------|
| RC1M | 377.98 |
| RC1H | 408.56 |
| RC2M | 442.11 |
| RC2H | 430.61 |

Table B.8. Reinforced concrete and wrecked steel generated from damaged structural, in t

| | |
|------|---------|
| RC1M | 162533 |
| RC1H | 909147 |
| RC2M | 126737 |
| RC2H | 2235809 |

The total amount of debris is 3,434,225 tons.

Casualties

The number of casualties due to collapse of buildings can be expressed as, Coburn and Spence, 2002:



$$K_s = C \times [M1 \times M2 \times M3 \times (M4 + M5 \times (1 - M4))] \quad (B.2)$$

where C is total number (or floor area) of collapsed buildings in that typology class. C is given in Table B.9 and is obtained multiplying the floor area of each building type, Table B.2 by the corresponding complete damage state probability in Table B.1.

Table B.9. Floor area of collapsed buildings, in m²

| <i>RC1M</i> | <i>RC1H</i> | <i>RC2M</i> | <i>RC2H</i> |
|-------------|-------------|-------------|-------------|
| 53837 | 340620 | 33733 | 567566 |

M1 is the occupancy rate (number of people/built m²) and it is assumed to be 0.05 for Bucharest.

M2 is the occupancy at time of earthquake; in this scenario it is considered the earthquake strikes at 6 AM and the assumed value of *M2* is 0.65.

M3 represents the percentage of occupants trapped by collapse; assumed value of *M3* = 0.50.

M4 gives the injury distribution at collapse according to Table B.10.

Table B.10. Injury distribution at collapse

| <i>Triage injury category</i> | <i>M4</i> |
|-------------------------------|-----------|
| dead | 0.4 |
| life threatening | 0.1 |
| injured - required hospit | 0.4 |
| lightly injured | 0.1 |

M5 represents the mortality post-collapse – assumed in this scenario to be 0.70.

The casualties, expressed in number of persons, in the case of this scenario are given in Table B.11. Table B.12 gives the breakdown of casualties in percentages.

Table B.11. Breakdown of casualties for buildings typology

| <i>Human casualties, no.</i> | <i>RC1M</i> | <i>RC1H</i> | <i>RC2M</i> | <i>RC2H</i> |
|------------------------------|-------------|-------------|-------------|-------------|
| Dead | 717 | 4539 | 449 | 7563 |
| life threatening | 639 | 4041 | 400 | 6733 |
| injured - required hospit | 717 | 4539 | 449 | 7563 |
| lightly injured | 639 | 4041 | 400 | 6733 |
| Uninjured | 18788 | 94103 | 12634 | 231020 |

Table B.12. Breakdown of casualties in percentage

| <i>Human casualties, %</i> | <i>RC1M</i> | <i>RC1H</i> | <i>RC2M</i> | <i>RC2H</i> |
|----------------------------|-------------|-------------|-------------|-------------|
| dead | 3.33 | 4.08 | 3.14 | 2.92 |
| life threatening | 2.97 | 3.63 | 2.79 | 2.59 |
| injured - required hospit | 3.34 | 4.08 | 3.14 | 2.91 |
| lightly injured | 2.97 | 3.63 | 2.79 | 2.59 |
| uninjured | 87.39 | 84.58 | 88.14 | 88.99 |

Homeless estimation

The total floor area of uninhabitable dwelling units (#*UNU*) is the output of this portion of the model.



The following inputs are required to compute the number of uninhabitable dwelling units and the number of displaced households, HAZUS, 1999:

- ✓ Total Number of Dwelling Units (#MFU)
- ✓ Damage state probability for moderate structural damage state in the building type (%MFM).
- ✓ Damage state probability for extensive structural damage state in the building type (%MFE).
- ✓ Damage state probability for complete structural damage state in the building type (%MFC).

The probabilities %SFM, %SFE, %SFC, %MFM, %MFE, and %MFC are provided in Table B.1.

The number of uninhabitable dwelling units due to structural damage is determined by combining a) the number of uninhabitable dwelling units due to actual structural damage, and b) the number of damaged units that are perceived to be uninhabitable by their occupants. Based on comparisons with previous work (Perkins, 1992), the methodology considers all dwelling units located in buildings that are in the complete damage state to be uninhabitable. In addition, dwelling units that are in moderately and extensively damaged multi-family structures are also considered to be uninhabitable due to the fact that renters perceive some moderately damaged rental property as uninhabitable. Therefore, the total floor area of uninhabitable units (#UNU_{SD}) due to structural damage is calculated by the following relationship, HAZUS, 1999:

$$\begin{aligned} \%MF &= w_{MFM} \times \%MFM + w_{MFE} \times \%MFE + w_{MFC} \times \%MFC \\ \#UNU_{SD} &= \#MFU \times \%MF \end{aligned} \tag{B.3}$$

The values of weighting factors are provided in Table B.13.

Table B.13. Default Values for Damage State Probabilities

| Weight Factor | Default Value |
|---------------|---------------|
| w_{MFM} | 0.0 |
| w_{MFE} | 0.9 |
| w_{MFC} | 1.0 |

The percentage of uninhabitable units is given in Table B.14 and the total floor of uninhabitable dwelling units is given in Table B.15.

Table B.14. Percentage of uninhabitable units

| | |
|------|------|
| RC1M | 0.74 |
| RC1H | 0.78 |
| RC2M | 0.73 |
| RC2H | 0.71 |

Table B.15 Total floor are of uninhabitable dwelling units, 1000 m²

| | |
|------|---------|
| RC1M | 319.16 |
| RC1H | 1726.65 |
| RC2M | 208.25 |
| RC2H | 3704.38 |

The total floor area of uninhabitable units amounts at 5,958.44 thousands of sq.m.

Direct economical losses

For building related items, methods for calculating the following monetary losses are provided for:

- ✓ Building Repair and Replacement Costs
- ✓ Building Contents Losses.

Building Repair and Replacement Costs

To establish monetary loss estimates, the damage state probabilities are converted to monetary loss equivalents. For a given occupancy and damage state, building repair and replacement costs are estimated as the product of the floor area of each building type within the given occupancy, the probability of the building type being in the given damage state, and repair costs of the building type per square meter for the given damage state, summed over all building types within the occupancy.

For structural damage, losses are calculated as follows, HAZUS, 1999:

$$CS_{ds} = \sum_j FA_j \times PMBTSTR_{ds,j} \times RCS_{ds,j} \quad (B.4)$$

$$CS = \sum_{ds=2}^5 CS_{ds} \quad (B.5)$$

where:

| | |
|------------------|---|
| CS_{ds} | cost of structural damage (repair and replacement costs) for damage state ds |
| CS | cost of structural damage (repair and replacement costs) |
| FA_j | floor area of building type j (in m^2), based on the total floor area and the distribution of floor area between building types, Table B.2 |
| $PMBTSTR_{ds,j}$ | probability of building type j being in structural damage state ds , Table B.1 |
| $RCS_{ds,j}$ | structural repair and replacement costs (per m^2) for building type j in damage state ds |

Note that damage state "None" ($ds = 1$) does not contribute to the calculation of the cost of structural damage and thus the summation in Equation B.3 is from $ds = 2$ to $ds = 5$.

The cost of damage is expressed as a percentage of the complete damage state. The assumed relationship between damage states and repair/replacement costs, for both structural and non-structural components, is as follows, ATC 13, 1985:

| | |
|-------------------|-----------------|
| Slight damage: | 2% of complete |
| Moderate damage: | 10% of complete |
| Extensive damage: | 50% of complete |

Structural repair costs for complete damage is considered 300 Euro/ m^2 .



The direct economic losses from buildings repair and replacement costs are given in Table B.16.

Table B.16. Building Repair and Replacement Costs, Euro

| Monetary losses, Euro | RC1M | RC1H | RC2M | RC2H |
|------------------------------|-------------------|--------------------|-------------------|--------------------|
| <i>N</i> | 0 | 0 | 0 | 0 |
| <i>S</i> | 132,974 | 508,888 | 102,731 | 2,048,190 |
| <i>M</i> | 1,762,418 | 7,752,412 | 1,243,442 | 23,644,605 |
| <i>E</i> | 44,220,524 | 231,004,651 | 29,086,539 | 522,802,448 |
| <i>C</i> | 16,151,066 | 102,185,939 | 10,119,863 | 170,269,821 |
| Total monetary losses | 62,266,982 | 341,451,889 | 40,552,575 | 718,765,064 |

Total monetary losses due to building repair and replacement costs are in excess of 1.16 billion Euros.

Building Content Losses

Building content is defined as the furniture, equipment that is not integral with the structure, computers and other supplies. From Table 4.11 of *ATC-13*, 1985 it is assumed that for residential buildings contents value represent 50 percent of building replacement value.

Thus, the building content loss is half of the building repair and replacement cost rising up to more than 581 million Euros.

Overall, the direct economic losses are in excess of 1.74 billion Euros.



3. Full Probabilistic Risk Assessment of Current Buildings

3.1 Introduction

Seismic risk represents the expectancy of damage or losses (expressed in probabilistic terms) in relation to the performance of a definite built system, as a function of duration.

The risk analysis recognizes basically the impossibility of deterministic prediction of events of interest, like future earthquakes, exposure of elements at risk, or chain effects occurring as a consequence of the earthquake-induced damage. Since the expectancy of losses represents the outcome of a more or less explicit and accurate predictive analysis, a prediction must be made somehow in probabilistic terms, by extrapolating or projecting into the future the present experience. A probability-based prediction relies on two major premises:

1. the conceptual and methodological framework of the theory of probabilities;
2. the assumption that there exists some intrinsic stability and stationarity of objective processes determining the input and outcome of phenomena and events dealt with (Sandi, 1986).

The general relation for the determination of the total risk can be expressed as (Whitman & Cornell, 1976):

$$P[R_i] = \sum_j P[R_i/S_j] \cdot P[S_j] \quad (3.1)$$

in which $P[]$ signifies the probability of the event indicated within the brackets, R_i denotes the event that the state of system is i , S_j means that the seismic input experienced is level j , and $P[R_i/S_j]$ states the probability that the state of the system will be R_i given that the seismic input S_j takes place.

The probabilistic risk assessment is not a straightforward matter and involves a high computational effort. The probabilistic risk assessment is aiming at computing the annual probability of exceedance of various damage states for a given structural system. The consistent probabilistic approach is based on the idea of (Cornell & Krawinkler, 2000) using the total probability formula applied in a form that suits the specific needs:

$$P(\geq d_s) = \int_{PGA} \int_{Sd} \Phi(\geq d_s | Sd) \cdot f(Sd/PGA) \cdot f(PGA) d(Sd) d(PGA) \quad (3.2)$$

where:

- $P(\geq d_s)$ – annual probability of exceedance of damage state d_s
- $\Phi(\geq d_s | Sd)$ – standard normal cumulative distribution function of damage state d_s conditional upon spectral displacement Sd
- $f(Sd / PGA)$ - probability density function of spectral displacement Sd given the occurrence of peak ground acceleration PGA
- $f(PGA)$ – probability density function of peak ground acceleration PGA

One can change Eq. (3.2) to solve for the mean annual rate of exceedance of various damage states for a given structural system:

$$\lambda(\geq d_s) = \sum_{PGA} \sum_{Sd} P(\geq d_s/Sd) \cdot P(Sd/PGA) \cdot \lambda(PGA) \quad (3.3)$$



where:

- $\lambda(\geq d_s)$ – mean annual rate of exceedance of damage state d_s
- $P(\geq d_s / Sd)$ – probability of exceedance of damage state d_s conditional upon spectral displacement Sd
- $P(Sd / PGA)$ - probability of reaching spectral displacement Sd given the occurrence peak ground acceleration PGA
- $\lambda(PGA)$ – mean annual rate of occurrence of peak ground acceleration PGA .

Consequently, the probabilistic assessment of seismic risk involves the:

1. probabilistic seismic hazard assessment, $\lambda(PGA)$
2. probabilistic assessment of seismic structural response, $P(Sd / PGA)$
3. probabilistic assessment of seismic structural vulnerability, $P(\geq d_s / Sd)$

Equations (3.2) and (3.3) are disaggregating the seismic risk assessment problem into three probabilistic analysis of: hazard, structural response and vulnerability. Then it aggregates the risk via summation (or integration) over all levels of the variables of interest.

3.2 Probabilistic seismic hazard assessment

According to the 20th century seismicity, the epicentral Vrancea area is confined to a rectangle of 40x80km² having the long axis oriented N45E and being centered at about 45.6° Lat.N and 26.6° Long. E.

The average number per year of Vrancea subcrustal earthquakes with moment magnitude equal to and greater than M_w is (Lungu et.al., 2000, Lungu et. al. 1999):

$$\log n(\geq M_w) = 3.76 - 0.73 M_w \quad (3.4)$$

The values of surface rupture area (SRA) and surface rupture length (SRL) from Wells and Coppersmith (1994) equations for "thrust" rupture were used to estimate maximum credible Vrancea magnitude, (Lungu et. al. 1997). According to Romanian geologists Sandulescu & Dinu, in Vrancea subduction zone: $SRL \leq 150 \div 200$ km, $SRA \leq 8000$ km². Based on this estimation, one gets:

$$M_{w,max} = 8.1. \quad (3.5)$$

If the source magnitude is limited by an upper bound magnitude $M_{w,max}$, the recurrence relationship can be modified in order to satisfy the property of a probability distribution (McGuire & Arabasz, 1990):

$$n(\geq M_w) = e^{\alpha - \beta M_w} \frac{1 - e^{-\beta(M_{w,max} - M_w)}}{1 - e^{-\beta(M_{w,max} - M_{w0})}} \quad (3.6)$$

and, in the case of Vrancea source (Elnashai and Lungu 1995):

$$n(\geq M_w) = e^{8.654 - 1.687 M_w} \frac{1 - e^{-1.687(8.1 - M_w)}}{1 - e^{-1.687(8.1 - 6.3)}} \quad (3.7)$$

In Eq.(3.5), the threshold lower magnitude is $M_{w0}=6.3$, the maximum credible magnitude of the source is $M_{w,max}=8.1$, and $\alpha = 3.76 \ln 10 = 8.654$, $\beta = 0.73 \ln 10 = 1.687$.



The depth of the Vrancea foci has a great influence on the experienced seismic intensity. The damage intensity of the Vrancea strong earthquakes is the combined result of both magnitude and location of the focus inside the earth.

The relationship between the magnitude of a destructive Vrancea earthquake ($M_w \geq 6.3$) and the corresponding focal depth shows that higher the magnitude, deeper the focus (Lungu et.al., 2000, Lungu et. al., 1999):

$$\ln h = -0.866 + 2.846 \ln M_w - 0.18 \quad (3.8)$$

where P is a binary variable: $P=0$ for the mean relationship and $P=1.0$ for mean minus one standard deviation relationship.

The following model was selected for the analysis of attenuation (Mollas & Yamazaki, 1995):

$$\ln PGA = c_0 + c_1 M_w + c_2 \ln R + c_3 R + c_4 h + \varepsilon \quad (3.9)$$

where: PGA is peak ground acceleration at the site, M_w - moment magnitude, R - hypocentral distance to the site, h - focal depth, c_0, c_1, c_2, c_3, c_4 - data dependent coefficients and ε - random variable with zero mean and standard deviation $\sigma_\varepsilon = \sigma_{\ln PGA}$, Table 3.1. Details are given elsewhere (Lungu et.al., 2000, Lungu et. al. 2001).

Table 3.1. Regression coefficients inferred for horizontal components of peak ground acceleration during Vrancea subcrustal earthquakes, Equation (3.9)

| c_0 | c_1 | c_2 | c_3 | c_4 | $\sigma_{\ln PGA}$ |
|-------|-------|--------|---------|--------|--------------------|
| 3.098 | 1.053 | -1.000 | -0.0005 | -0.006 | 0.502 |

For a given earthquake recurrence, the probability of exceeding a particular value of peak ground acceleration, PGA^* , is calculated using the total probability formula (Cornell, 1968, Kramer, 1996):

$$\lambda(PGA > PGA^*) = \iint P(PGA > PGA^* / m, r) \cdot f(m) \cdot f(r) dm dr \quad (3.10)$$

where:

- $\lambda(PGA > PGA^*)$ – mean annual rate of exceedance of PGA^* ;
- $P(PGA > PGA^* / m, r)$ – probability of exceedance of PGA^* given the occurrence of an earthquake of magnitude m at source to site distance r . This probability is obtained from attenuation relationship (3.9) assuming log-normal distribution for PGA ;
- $f(m)$ – probability density function for magnitude;
- $f(r)$ – probability density function for source to site distance.

The probability density function for magnitude is obtained from Eq. (3.6) (McGuire & Arabasz, 1990). The probability density function for source to site distance is considered, for the sake of simplicity, uniform over the rectangle of $40 \times 80 \text{ km}^2$ having the long axis oriented N45E and being centered at about 45.6° Lat.N and 26.6° Long. E.

The mean annual rate of exceedance of PGA – the hazard curve - for Bucharest site and Vrancea seismic source is represented in Figure 3.1.

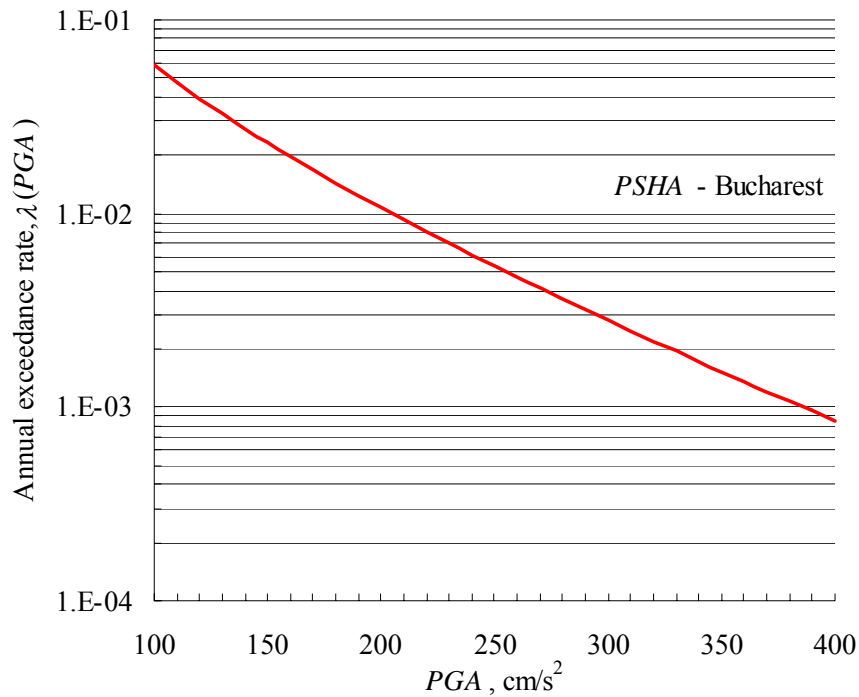


Figure 3.1. Hazard curve for Bucharest from Vrancea seismic source

The hazard curve can be approximated by the form $H = k_o \cdot a_g^{-k}$ (Fajfar et al, 1994), where a_g is peak ground acceleration, and k_o and k are constants depending on the site (in this case $k_o=1.176E-05$, $k=3.0865$).

3.3 Probabilistic assessment of seismic structural response

3.3.1 The structural model

The building analyzed has a reinforced concrete moment resisting frame structure and it was erected in early '70's. It is a thirteen-storey building, the first two storeys being of 3.60 m, all the rest of 2.75 m height. The building has two spans of 6.00 m each in the transversal direction and five spans of 6.00 m each in the longitudinal direction. The concrete is of class Bc 20 and the steel is of quality PC 52. Some details regarding the structural members are given in Table 3.2. Further details can be found elsewhere (Vacareanu, 1998).

Table 3.2. Description of the structural members

| Storey # | Columns (BxD) | Overall reinforcement ratio | Hoop bar diameter | Hoop bar spacing | Beams (BxD) | Bottom reinforcement ratio | Top reinforcement ratio | Stirrup diameter | Stirrup spacing |
|----------|---------------|-----------------------------|-------------------|------------------|-------------|----------------------------|-------------------------|------------------|-----------------|
| | (mm) | (%) | (mm) | (mm) | (mm) | (%) | (%) | (mm) | (mm) |
| 1,2 | 700 x 900 | 1.75 | 8 | 150 | 350 x 700 | 0.30 | 0.70 | 6 | 200 |
| 3-5 | 700 x 750 | 1.70 | 8 | 200 | 350 x 700 | 0.32 | 0.75 | 6 | 200 |
| 6 – 9 | 600 x 750 | 1.40 | | 200 | 300 x 700 | 0.32 | 0.60 | 6 | 250 |
| 10 – 13 | 600 x 600 | 1.00 | 6 | 200 | 300 x 600 | 0.30 | 0.50 | 6 | 250 |

3.3.2 Ground motions

In this paper, the seismic motion intensity is quantified by peak ground acceleration (*PGA*). The seismic motions used in the analyses consist of seven classes of random processes comprising ten samples each. Elastic acceleration spectra are used to simulate samples. The input seismic motions are simulated using a stationary Gaussian model based on elastic acceleration spectra (Shingal & Kiremidjian, 1997). The time histories are generated such as to fit the given response spectrum. The probability distributions of the dynamic amplification factors are used to obtain an ensemble of response spectra corresponding to a given level of seismic motion (Vacareanu, 2000).

For parametric analysis purpose, the accelerograms are simulated at predefined values of *PGA*, as follows: 0.10g, 0.15g, 0.20g, 0.25g, 0.30g, 0.35g, 0.40g (g – acceleration of gravity).

3.3.3 Non-linear dynamic analyses

The structural model in the transversal direction consists of six - two spans - reinforced concrete moment resisting frames acting together due to the action of horizontal diaphragms located at each storey. The computer program *IDARC 2D* (Valles et. al., 1996) is used for performing inelastic dynamic analyses.

To trace the hysteretic response of structural elements, the piece-wise linear three-parameter model that included stiffness degradation, strength deterioration and slip is used to model the response of reinforced concrete structural elements. The trilinear hysteretic model relies on four parameters that scale the main characteristics represented in the model: stiffness degradation, strength deterioration and pinching. In this paper, for analysis purpose, the default values ($HC = 2.0$; $HBD = 0.0$; $HBE = 0.10$; $HS = 1.0$) are used, these values allowing for nominal stiffness degradation and strength deterioration and no pinching effects.

Nonlinear dynamic analyses are performed for 10 simulated ground motions generated at each value of *PGA*. An integration time step of 0.002s is used in the analyses. The accelerograms last for 20 s and the total duration of the analysis is 21 s. The damping coefficient is 5 % of the critical damping and the structural damping is assumed to be mass proportional.

In damage analysis, the uncertainties associated with seismic demands and structural capacities need to be modelled. The Monte-Carlo technique involves the selection of samples of the random structural parameters and seismic excitations required for nonlinear analyses, the performance of nonlinear analyses and the computation of the structural response.

In brief, the Monte-Carlo simulation technique implies the following steps:

- simulation of structural parameters and seismic excitations;
- random permutations of structural parameters and of excitations;
- performing nonlinear analyses using generated samples;
- sample statistics of results of analyses.

The direct Monte-Carlo technique requires a large number of simulation cycles to achieve an acceptable level of confidence in the estimated probabilities. The Latin hypercube technique might be used to reduce the number of simulation cycles. Using the Latin hypercube



technique for selecting values of the input variables, the estimators from the simulation are close to the real values of the quantities being estimated. The Latin hypercube technique uses stratified sampling of the input variables, which usually results in a significant decrease in the variance of the estimators (Rubinstein, 1981).

The compressive strength of concrete and the yield strength of steel are the only parameters treated as structural random variables in this paper. Following Galambos et al. (1982), normal probability distribution for concrete strength and lognormal probability distribution for steel strength are used in this research. Concrete strength has a mean of 25 MPa and a coefficient of variation of 15%. Steel strength has a mean of 397 MPa and a coefficient of variation of 7%. For simulation purposes 10 values for concrete and reinforcement strengths are randomly generated and used for each *PGA* value considered within the analysis. Latin hypercube technique is used for randomly combine the generated strength variables and accelerations.

Spectral displacements are calculated using nonlinear dynamic analyses. Data regarding the randomness of the seismic response of the structural system are obtained. The statistic indicators of the spectral displacement obtained at each *PGA* value are used to get the parameters of a lognormal distribution function for that level of intensity of ground motion. The computed mean and standard deviation of the spectral displacements are reported in Table 3.3.

Table 3.3 Mean and standard deviation of DI

| <i>PGA</i> , 'g | $\mu_{Sd PGA}$ | $\sigma_{Sd PGA}$ |
|-----------------|----------------|-------------------|
| 0.1 | 13.1 | 2.2 |
| 0.15 | 22.8 | 3.3 |
| 0.2 | 30.0 | 4.0 |
| 0.25 | 39.5 | 3.8 |
| 0.3 | 49.8 | 5.3 |
| 0.35 | 59.0 | 6.4 |
| 0.4 | 68.7 | 6.9 |

Finally, the lognormal probability density function of spectral displacement conditional upon *PGA* is evaluated:

$$f(Sd | PGA) = \frac{1}{\sqrt{2\pi}} \cdot \frac{1}{Sd} \cdot \frac{1}{\sigma_{\ln(Sd|PGA)}} \cdot e^{-\frac{1}{2} \left(\frac{\ln(Sd) - \mu_{\ln(Sd|PGA)}}{\sigma_{\ln(Sd|PGA)}} \right)^2} \quad (3.11)$$

Examples of lognormal probability density functions of *Sd* conditional upon *PGA*= 0.1g, 0.2g and 0.3g are presented in Figure 3.2. Using the density functions one obtains probability of reaching spectral displacement *Sd* given the occurrence of peak ground acceleration, *PGA*, $P(Sd | PGA)$.

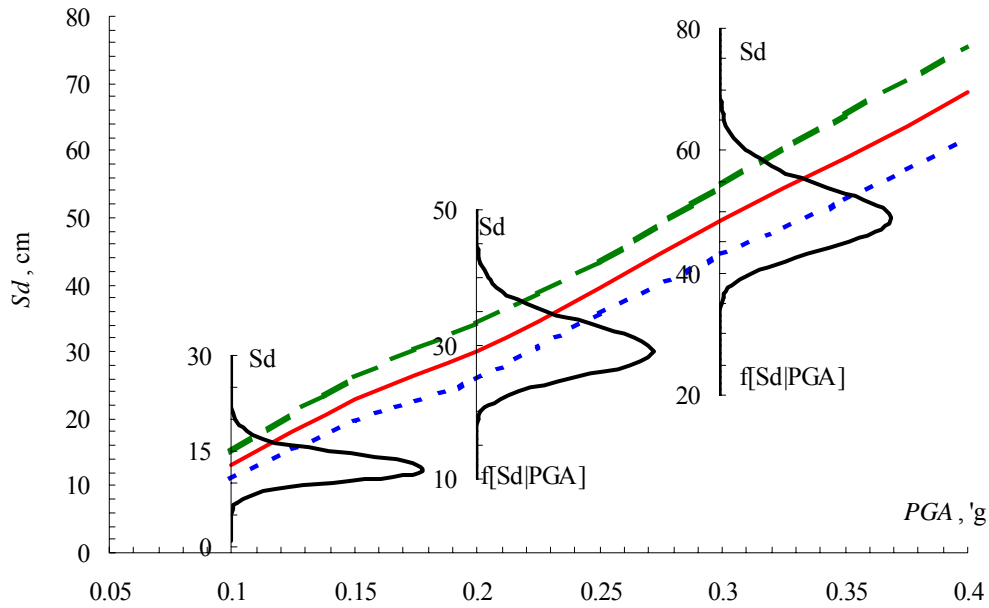


Figure 3.2. Mean and standard deviation of the spectral displacement

3.3.4 Probabilistic assessment of seismic structural vulnerability

The probabilistic assessment of seismic structural vulnerability involves the determination of the building vulnerability functions. These functions describe the conditional probability of being in, or exceeding, a particular damage state, d_s , given the spectral displacement, S_d , and is defined as HAZUS (1997) :

$$P[d_s|S_d] = \Phi \left[\frac{1}{\beta_{d_s}} \ln \left(\frac{S_d}{\bar{S}_{d,d_s}} \right) \right] \quad (3.12)$$

where:

- \bar{S}_{d,d_s} is the median value of spectral displacement at which the building reaches the threshold of the damage state, d_s ,
- β_{d_s} is the standard deviation of the natural logarithm of spectral displacement for damage state d_s , and
- Φ is the standard normal cumulative distribution function.

For the spectral (maximum) displacement, S_d , expected for the demand earthquake, one determines the structural damage state probabilities using vulnerability functions (Eq. 3.12). HAZUS (1997) includes the vulnerability function parameters, \bar{S}_{d,d_s} and β_{d_s} appropriate for each type of building corresponding to USA practice of design and construction. In order to calibrate the vulnerability function parameters appropriate for structural systems which are different from USA practice, the Monte-Carlo simulation technique can be used. For simulation purposes 10 values for concrete and for reinforcement strengths are randomly generated and randomly combined for each push-over analysis.

The outcome of the pushover analyses is a family of capacity curves, which can be described as mean and mean plus/minus one standard deviation capacity curves, Figure 3.3 (Vacareanu et. al., 2001).

For calibration of vulnerability function parameters it is necessary to establish a correlation between Park&Ang (1985) damage index and interstory drift ratio at threshold of damage state. The more recent slightly modified version of Park&Ang index, in which the recoverable deformation is removed from the first term might be used:

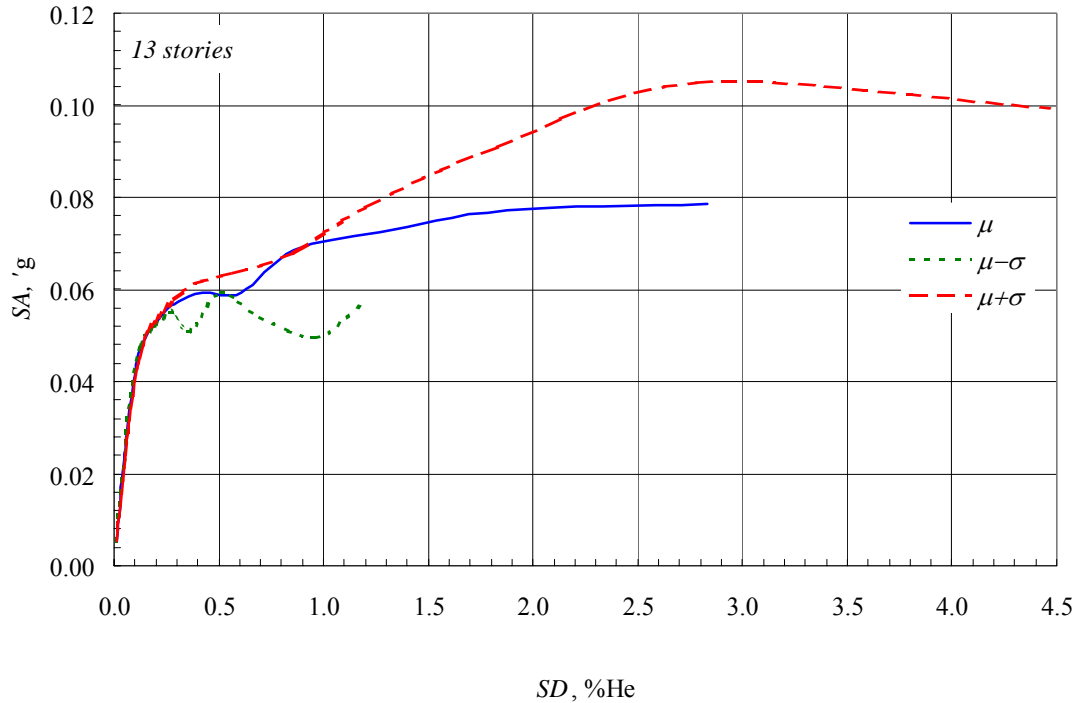


Figure 3.3. Capacity curve, Monte-Carlo simulation

$$D = \frac{D_m - D_y}{D_u - D_y} + \beta_e \cdot \frac{\int dE}{F_y \cdot D_u} \quad (3.13)$$

where D_m = maximum displacement; D_u = ultimate displacement; D_y = yielding displacement; β_e = strength deterioration parameter; F_y = yielding force and E = dissipated hysteretic energy. The correlation between Park&Ang damage index and damage state is given in Table 3.4 (Williams & Sexsmith, 1995):

Using the definition of Park&Ang damage index (Eq. 3.13) and the structural behavior described by the capacity curve, one can determine the correlation between Park&Ang damage index and mean (± 1 standard deviation) interstory drift ratio values, Figure 3.4 (Vacareanu et. al., 2001).

Table 3.4. Relations between damage index and damage state

| Range of damage index | Damage state |
|-----------------------|--------------|
| $D \leq 0.1$ | None |
| $0.1 < D \leq 0.25$ | Slight |
| $0.25 < D \leq 0.40$ | Moderate |
| $0.40 < D \leq 1.00$ | Extensive |
| $D > 1.00$ | Complete |

Making vertical sections in Figure 3.4 for the threshold values of Park&Ang damage index given in Table 3.4 one can identify the mean and standard deviation values of interstory drift at threshold of damage state, Table 3.5, Figure 3.5. The median value of spectral displacement at which the building reaches the threshold of the damage state, $S_{d,ds}$ is obtained by multiplying the interstory drift by the height of the building and by the fraction of the building height at the location of push-over mode displacement, Table 3.6. The standard deviation of the natural logarithm of spectral displacement for damage state ds , β_{ds} is obtained using the standard deviation of structural displacement.

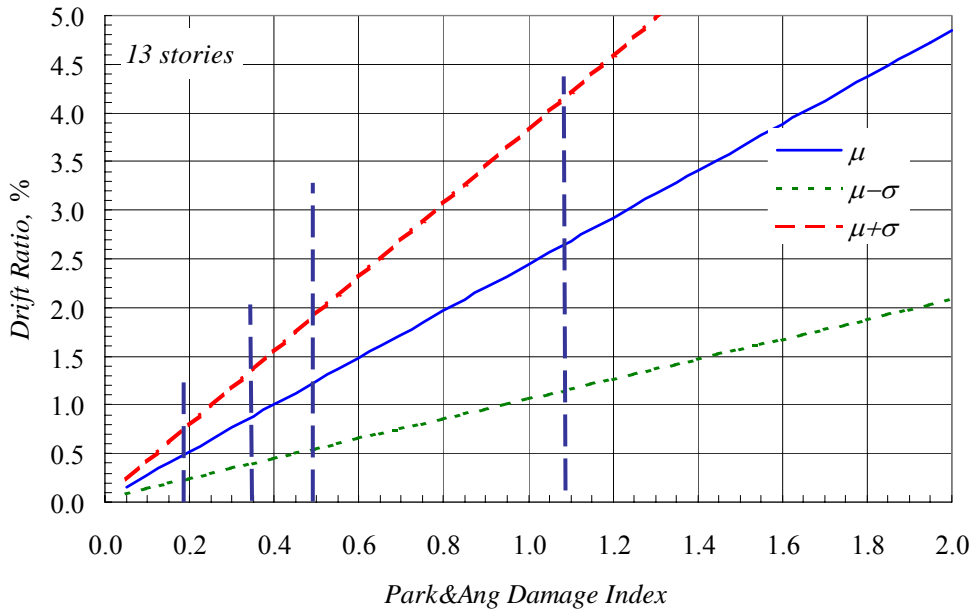


Figure 3.4. Correlation between Park&Ang damage index and interstory drift ratio

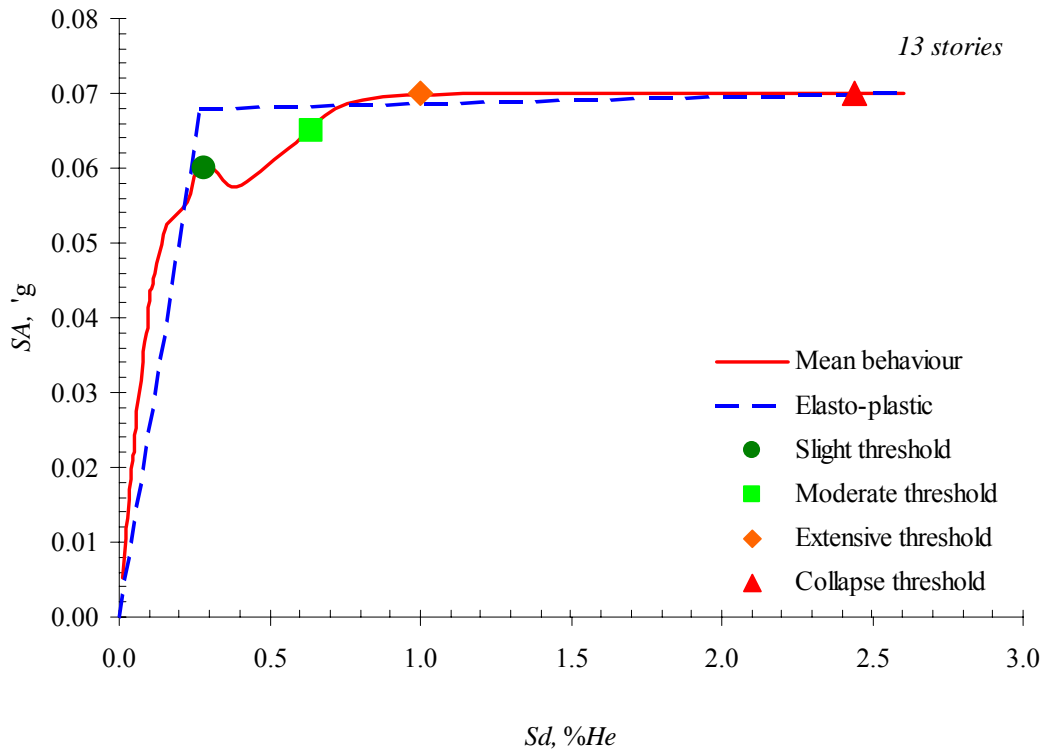


Figure 3.5. Median capacity curve and thresholds of damage states

One can notice from Figure 3.5 that the complete damage state corresponds to the collapse prevention limit state and the extensive damage state corresponds roughly to the life safety limit state.

Once the parameters of vulnerability function, $S_{d,ds}$ and β_{ds} , are obtained one can compute and plot the functions using Eq. 3.12, Figure 3.6.

Table 3.5. Mean interstory drift ratio at threshold of damage state

| Mean interstory drift ratio; Monte-Carlo Simulation | | | |
|---|----------|-----------|----------|
| Slight | Moderate | Extensive | Complete |
| 0.0028 | 0.0064 | 0.0100 | 0.0244 |

Table 3.6. Vulnerability function parameters (Monte-Carlo Simulation)

| Damage state | | | | | | | |
|-----------------|--------------|-----------------|--------------|-----------------|--------------|-----------------|--------------|
| Slight | | Moderate | | Extensive | | Complete | |
| $S_{d,ds}$, cm | β_{ds} |
| 7.82 | 0.66 | 17.88 | 0.66 | 27.94 | 0.76 | 68.16 | 0.91 |

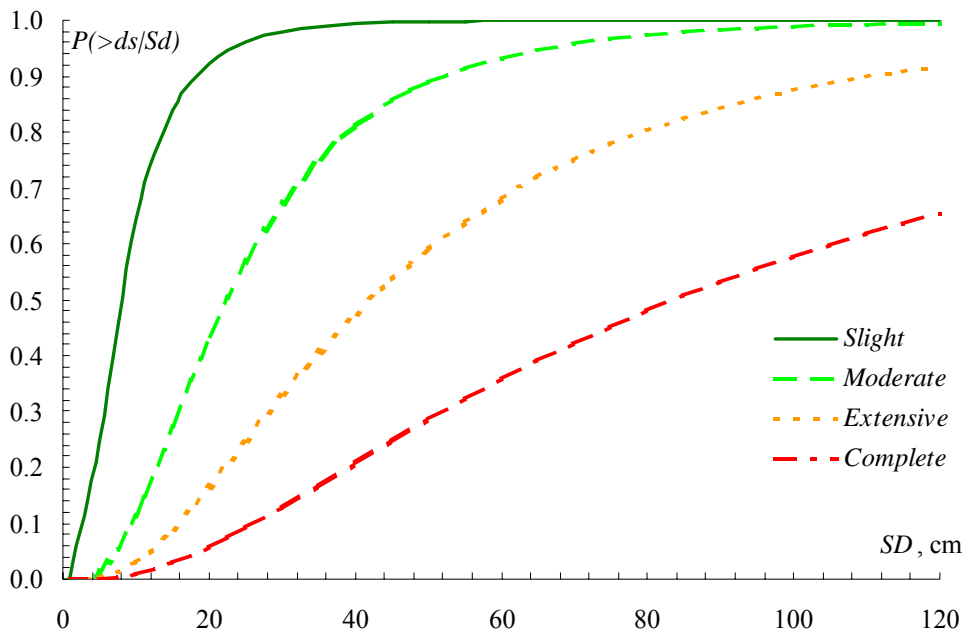


Figure 3.6. Vulnerability functions, Monte-Carlo simulation

3.3.5 Risk analysis

Given the results of the probabilistic seismic hazard assessment, $\lambda(PGA)$, the probabilistic assessment of seismic structural response, $P(Sd / PGA)$, and the probabilistic assessment of seismic structural vulnerability, $P(\geq d_s / Sd)$ one can aggregate the risk via summation (or integration) over all levels of the variables of interest using Equation 3.3. The results on risk are presented as mean annual rate of exceedance of damage state d_s , $\lambda(\geq d_s)$, in Table 3.7. Also, in Table 3.7 is presented the exceedance probability of various damage states in 1 year, 50 years and 100 years assuming that the damage states follows a Poisson distribution:



$$P_{exc}(d_s, T) = 1 - e^{-\lambda(\geq d_s)T} \quad (3.14)$$

where:

- $P_{exc}(d_s, T)$ - exceedance probability of damage state d_s in time T .

Table 3.7. Results of seismic risk analysis

| Damage state - d_s | Annual exceedance rate, $\lambda(\geq d_s)$ | Exceedance prob., $P_{exc}(d_s, T)$ in: | | |
|----------------------|---|---|------------|-------------|
| | | T=1 year | T=50 years | T=100 years |
| Slight | 5.1E-02 | 5.0E-02 | 9.2E-01 | 9.9E-01 |
| Moderate | 2.6E-02 | 2.6E-02 | 7.3E-01 | 9.3E-01 |
| Extensive | 1.2E-02 | 1.2E-02 | 4.4E-01 | 6.9E-01 |
| Complete | 4.7E-03 | 4.7E-03 | 2.1E-01 | 3.7E-01 |

One can notice from Table 3.7 the exceedance probability of complete damage state in 1 year of $4.7 \cdot 10^{-3}$ which is much higher than the commonly accepted probabilities of failure of 10^{-4} to 10^{-5} as in the case of non-seismic loads. The main reason for this high probability comes from the design of the building which was accomplished taking into account an inferior code for earthquake resistant design (*P13-70*) combined with the low level of seismic hazard considered in the design process.

3.4 Conclusions

1. The approach used is fully probabilistic and is the only one that incorporates uncertainties and enables quantification of the safety level on a consistent theoretical basis.
2. Interstory drift at threshold of damage states can be analytically evaluated for different structural typologies. The actual values of the interstory drifts could be different with respect to that specified in *HAZUS* for USA design and construction practice.
3. Monte-Carlo simulation is a very powerful tool that can validate and complete the database on seismic behavior and vulnerability of buildings.
4. The unsatisfactory building safety level against seismic actions is put to evidence. The reasons for the un-conservative safety margins against earthquake action are the inferior code (*P13-70*) used for earthquake resistant design of building and the low level of seismic hazard considered in design.
5. The state of the practice in seismic design and seismic assessment of structural performances has to incorporate, in an appropriate and correct manner, the basic concepts of seismic vulnerability and risk.

References Chapter 3

- Cornell, C. A. - Engineering Seismic Risk Analysis. *Bull. SSA*, 56, 1968
- Cornell C.A., Krawinkler H. 2000. Progress and Challenges in Seismic Performance Assessment. *PEER Center News* (4)1:1-3.
- Elnashai A., Lungu D., 1995. Zonation as a tool for retrofit and design of new facilities. Report of the Session A.1.2. *5th International Conference on Seismic Zonation*, Nice, France, Oct. 16-19, Proceedings Vol.3, Ouest Editions, Preses Academiques, p.2057-2082.
- Galambos, T. V., Ellingwood, B., MacGregor, J. G., and Cornell, C. A.. Probability based load criteria: Assessment of current design practice. *Journal of Structural Division*, ASCE, vol. 108, No. ST5, pp. 959-977, 1982
- Fajfar P. et al 1994. Probabilistic assessment of seismic hazard at Krško Nuclear Power Plant. *Revision 1 prepared for Nuclear Power Plant Krško*
- HAZUS – Technical Manual 1997. Earthquake Loss Estimation Methodology*, 3 Vol.



- Kramer, S. L., 1996 – *Geotechnical Earthquake Engineering* – Prentice Hall, Inc., p. 653
- C. Lomnitz, E. Rosenblueth (eds.) - *Seismic Risk and Engineering Decisions*. R. Whitman and C. A. Cornell - *Design, Chapter 9*. Elsevier, Amsterdam - Oxford - New York, 1976
- Lungu, D., Vacareanu, R., Aldea, A., Arion, C., 2000. *Advanced Structural Analysis*, Conspress, UTCB, 177p.
- Lungu, D., Aldea, A., Demetriu, S., Arion, C., (2000) Zonation of seismic hazard for the city of Bucharest – Romania *Technical Report prepared for Association Française du Génie Parasismique*.
- Lungu, D., Arion, C., Aldea, A., Demetriu, S. (1999), Assessment of seismic hazard in Romania based on 25 years of strong ground motion instrumentation, *NATO ARW Conference on strong motion instrumentation for civil engineering structures*, Istanbul, Turkey, June 2-5, 1999.
- Lungu, D., Cornea, T., Aldea, A., Nedelcu, C., Zaicenco, A. (1997). *Seismic microzonation of the city of Bucharest*. Technical Report prepared for Association Française du Génie Parasismique, Vol.1&Vol.2, 91p.+69p.
- McGuire, R. K. & Arabasz, W.J., 1990 – An introduction to probabilistic seismic hazard analysis. In S. H. Ward, ed. *Geotechnical and Environmental Geophysics*, Society of Exploration Geophysicist, Vol. 1, p. 333-353
- Molas, G., Yamazaki, F., 1995. Attenuation of Earthquake Ground Motion in Japan including deep focus events. *Bull.Seis.Soc.Am.*, Vol.85, No.5, p.1343-1358
- Park, Y.-J & Ang, A. H.-S.. Mechanistic seismic damage model for reinforced concrete. *Journal of Structural Engineering*. ASCE vol. 111 (4): 722-739, 1985
- Rubinstein, R. Y. *Simulation and the Monte-Carlo method*. John Wiley & Sons, New York, 1981
- Sandi, H. (convener) - Vulnerability and Risk Analysis for Individual Structures and for Systems. *Report of EAEE WG 5/10 to the 8-th European Conference on Earthquake Engineering*, Lisbon, 1986
- Singhal, A. & Kiremidjian, A. S., 1997 A method for earthquake motion-damage relationships with application to reinforced concrete frames. *Technical Report NCEER-97-0008*. National Center for Earthquake Engineering Research, State University of New York at Buffalo
- Valles R. E., Reinhorn A. M., Kunnath S. K., Li C., Madan A. – IDARC2D Version 4.0: A Computer Program for the Inelastic Damage Analysis of Buildings, *Technical Report NCEER-96-0010*, NCEER, State University of New York at Buffalo, 1996
- Văcăreanu R., 1998 - Seismic Risk Analysis for a High Rise Building - *Proceedings of the 11th European Conference on Earthquake Engineering*, Paris, Abstract Volume pg. 513 and CD-ROM
- Văcăreanu R., 2000 – Monte-Carlo Simulation Technique for Vulnerability Analysis of RC Frames – An Example – *Scientific Bulletin on Technical University of Civil Engineering of Bucharest*, pg. 9-18
- Văcăreanu, R., Aldea, A., Arion C. - Probabilistic Risk Assessment Of Current Buildings - *Bulletin on Technical University of Civil Engineering of Bucharest*, 1/2002, Bucharest
- Văcăreanu R., Cornea T., Lungu D., 2001 - Evaluarea comportării structurale și a vulnerabilității seismice folosind metodologiile HAZUS și ATC-40 modificat (in Romanian) – *Proceedings of the 2nd National Conference on Earthquake Engineering*, Vol. 2, p. 2.16-2.31
- Williams, M. S. & Sexsmith, R. G. 1995. Seismic Damage Indices for Concrete Structures: A State-of-the-Art Review. *Earthquake Spectra*. Vol. 11(2): 319-345, 1997